Identification and characterization of the *Drosophila melanogaster* meiotic MCM complex

Kathryn Patricia Kohl

A dissertation submitted to the faculty of the University of North Carolina at Chapel Hill in partial fulfillment of the requirements for the degree of Doctor of Philosophy in the Curriculum in Genetics and Molecular Biology.

Chapel Hill
2013

Approved by:

Jeff Sekelsky, Ph.D.

Frank Conlon, Ph.D.

Corbin Jones, Ph.D.

Steven Matson, Ph.D.

Patricia Pukkila, Ph.D.

ABSTRACT

KATHRYN PATRICIA KOHL: Identification and characterization of the *Drosophila melanogaster* meiotic MCM complex
(Under the direction of Jeff Sekelsky)

Meiotic recombination increases genetic diversity and aids the proper segregation of homologous chromosomes through the formation of crossovers. Since improper crossing over can lead to non-disjunction and aneuploidy, the formation of crossovers is highly regulated and their distribution is non-random across the genome. My research has investigated the molecular mechanisms by which meiotic recombination occurs and the pathways involved in regulating this recombination. Through the course of my studies, I have used a combination of genetic, biochemical and evolutionary biological techniques to identify a novel complex of meiotic mini-chromosome maintenance proteins (mei-MCMs) that is essential for proper meiotic recombination in *Drosophila melanogaster*. I have found that this complex promotes crossover formation by antagonizing the anti-crossover protein BLM. In this manner, the mei-MCMs fill the functional niche of Msh4-Msh5, a protein complex that is absent in *Drosophila* but is necessary for interfering crossover formation in other organisms. In addition, I have discovered a role for the mei-MCMs in the regulation of crossover formation. In particular, I have shown that the mei-MCMs affect the number and distribution of crossovers. Collectively, these findings have provided insight into the pathways utilized in the regulation and formation of meiotic crossovers and have uncovered new avenues for future research in the meiotic recombination field.

To my parents, John and Patty, and my sister, Kristine,

for their love and support.

TABLE OF CONTENTS

LIST OF TABLES

LIST OF FIGURES

LIST OF ABBREVIATIONS

AAA – ATPases associated with a variety of cellular activities

CO – crossover

DCO – double crossover

dHJ – double Holliday junction

DSB – double-strand break

DSBR – double-strand break repair

hDNA – heteroduplex DNA

HJ – Holliday junction

JM – joint molecule

MCM – mini-chromosome maintenance

NCO – non-crossover

NDJ – non-disjunction

pre-RC – pre-replicative complex

SCO – single crossover

SDSA – synthesis-dependent strand annealing

TCO – triple crossover

CHAPTER 1

INTRODUCTION

Meiosis is essential to maintaining the proper complement of chromosomes in sexually reproducing organisms. By following one round of DNA replication with two rounds of cellular division, meiosis effectively halves the chromosome content of participating cells. Prior to the first meiotic division, homologous chromosomes pair and, in many organisms, undergo recombination. Both crossovers (COs), characterized by the reciprocal exchange of flanking markers, and non-crossovers (NCOs), in which flanking DNA remains unchanged, result from these recombination events. COs can also occur in mitotically proliferating cells during repair of certain types of DNA damage, especially double-strand breaks (DSBs). Meiotic COs likewise are initiated from DSBs, and many of the proteins used in mitotic DSB repair are also used in meiotic recombination. This has led to the suggestion that meiotic recombination evolved from mitotic recombination (Marcon and Moens, 2005). However, several modifications were necessary to give rise to meiotic recombination in its current form (reviewed in Villeneuve and Hillers, 2001). First, a mechanism of generating programmed DSBs to initiate recombination was needed. This was achieved through the use of Spo11, the catalytic subunit of a complex that generates regulated meiotic DSBs (Keeney et al., 1997). Second, whereas COs are avoided in mitotic cells to prevent loss of heterozygosity and chromosome rearrangement, CO formation is emphasized in meiotic recombination to facilitate the

segregation of homologous chromosomes and to increase genetic diversity. Third, the preferred repair template was changed from the sister chromatid in mitotic cells to the homologous chromosome in meiotic cells, since only COs between homologs give the aforementioned benefits. Finally, exquisite CO control mechanisms arose to ensure the optimal number and distribution of COs across the genome and relative to one another. In particular, every chromosome pair receives at least one CO and if additional COs occur, they tend not to occur near one another, a phenomenon called crossover interference (reviewed in Berchowitz and Copenhaver, 2010).

A complication obscuring the relationship between the mitotic and meiotic recombination pathways has been the apparent existence of two meiotic CO pathways – one pathway that produces COs subject to interference and another that produces non-interfering COs. Recent studies suggest that the interfering CO pathway fits the scenario described above - i.e., it is a derivative of the mitotic DSB repair pathway that contains numerous meiosis-specific embellishments. The non-interfering pathway, however, shares striking similarities to mitotic DSB repair in its original form. Additional discoveries reveal functions that are essential for generating meiotic COs can be carried out by different proteins in different species. These findings provide a new framework through which meiotic recombination pathways can be viewed and allow organisms previously thought to use disparate CO pathways to be brought under the same umbrella.

COs and NCOs in meiotic recombination models

In 1964, Holliday proposed a novel molecular model to explain how meiotic recombination could produce both COs and NCOs (Holliday, 1964). The central

intermediate in his model is a structure in which strands from two homologous duplexes swap pairing partners across a short region, yielding a four-stranded intermediate now known as the Holliday junction (HJ). Holliday proposed that these junctions are cleaved by DNA repair enzymes, now known as resolvases, to reestablish two separate duplexes. Depending on which strands are nicked, this process, now called resolution, could result in CO or NCO products. The equally likely outcomes of resolution fit with fungal recombination studies that suggested that COs and NCOs occur in equal numbers.

In Holliday's model, meiotic recombination is initiated by symmetric nicks on homologous chromosomes, but this mechanism did not fit with subsequent observations (reviewed in Stahl, 1994). To accommodate the new data, Szostak *et al.* (Szostak et al., 1983) proposed that meiotic recombination is initiated by a DSB on one chromatid. In the DSB repair (DSBR) model they proposed (Figure 1A), based largely on observations of double-strand gap repair in mitotic cells, the pre-CO intermediate has two HJs. Each junction in this double-HJ (dHJ) intermediate is proposed to be resolved independently, but the outcome is similar to Holliday's model: COs and NCOs are produced in equal numbers. Strong support for the DSBR model came from physical studies of meiotic recombination intermediates and products in *Saccharomyces cerevisiae*. These studies identified joint molecules (JMs) that form between homologous chromosomes (Collins and Newlon, 1994; Schwacha and Kleckner, 1994). These JMs have many of the properties expected of dHJs, the key intermediate in the DSBR model (Schwacha and Kleckner, 1995), and are widely considered to be dHJs. In this review, we use JM to refer to the molecule detected in experiments, and dHJ to refer to the intermediate predicted in models.

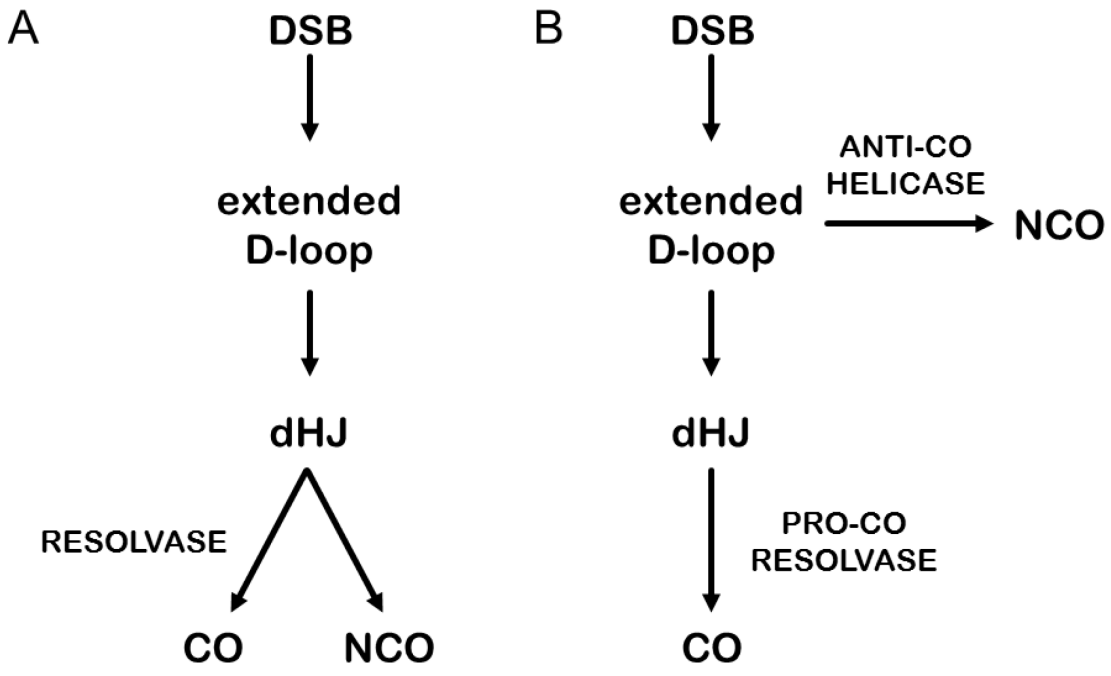

Figure 1. Models of meiotic double-strand break repair. (A) In the Szostak *et al*. (Szostak et al., 1983) model recombination initiates with a double-strand break (DSB) that is processed into an extended displacement loop (D-loop) and then a double Holliday junction (dHJ) structure. The dHJ is resolved into either a crossover (CO) or non-crossover (NCO) with equal probability. (B) In the revised model of Allers and Lichten (Allers and Lichten, 2001), some extended D-loops are unwound by an anti-CO helicase to produce NCOs, and dHJs are resolved by a pro-CO resolvase into COs.

Subsequent studies of JMs also led to a major challenge to the DSBR model. Allers and Lichten (Allers and Lichten, 2001) discovered that NCOs arose at the same time as JMs and prior to COs, a finding incompatible with the Szostak *et al.* DSBR model. In light of this finding, Allers and Lichten suggested that NCOs do not come from dHJs, as in the DSBR model, but from an earlier intermediate in the pathway, the extended D-loop (Figure 1B). A D-loop is formed when a single-stranded DNA end invades a homologous duplex, annealing to one strand and displacing the other. Allers and Lichten suggested that meiotic NCOs arise via synthesis dependent strand annealing (SDSA), a process proposed to be a major mechanism through which COs are avoided in

mitotic DSB repair (reviewed in Pâques and Haber, 1999). In SDSA, after the invading strand is extended by DNA synthesis, helicases can disrupt the D-loop, freeing the nascent strand to anneal to the other end of the DSB.

Allers and Lichten noted another departure from the original DSBR model: Most JMs are processed into COs (Allers and Lichten, 2001) (Figure 1B). Although this discovery opposes the notion that resolution of a dHJ can produce a CO or a NCO with equal probability, it more readily accommodates the finding that NCOs outnumber COs, sometimes by a factor of ten or more (reviewed in Cole et al., 2012). Thus, in the revised model of Allers and Lichten, the backone of the original DSBR model is intact, but dHJs are now preferentially repaired as COs, and NCOs arise via SDSA instead of dHJ resolution. In this revised model, helicases that promote SDSA act as anti-CO factors and HJ resolvases become pro-CO factors rather than proteins that produce both COs and NCOs.

Rise of the two-pathway paradigm

Another major impact on meiotic recombination models came from studies of the *S. cerevisiae* ZMM (Zip1-Zip4, Msh4–Msh5, Mer3) proteins. Msh4 and Msh5 are two widely-conserved ZMM proteins that form a meiosis-specific complex (Pochart et al., 1997). Notably, loss of Msh4 or Msh5, like loss of other ZMM proteins, does not eliminate COs, but merely reduces them by ~50-70% (Hollingsworth et al., 1995; Ross-Macdonald and Roeder, 1994). In *Caenorhabditis elegans*, however, Msh4 and Msh5 seem to be essential for all meiotic COs (Kelly et al., 2000; Zalevsky et al., 1999). To reconcile these organismal differences and explain the remaining COs in *S. cerevisiae msh4* and *msh5* mutants, Zalevsky *et al.* (Zalevsky et al., 1999) proposed that there are

two different pathways for meiotic CO formation (Table 1). The first pathway, which requires Msh4–Msh5, is responsible for a majority of COs in *S. cerevisiae* and all COs in *C. elegans*; the second, independent of Msh4–Msh5, produces the remaining COs in *S. cerevisiae msh4* and *msh5* mutants.

Class	Type of CO	Defining Proteins	Percentage of COs				
			Sc	*Sp*	*Ce*	*At*	*Dm*
I	interfering	Msh4–Msh5	50-70	0	100	75-85	0
II	non-interfering	Mus81–Mms4	30-50	100	0	9-12	<10

Table 1. Percentage of crossovers attributed to each pathway in the early two-pathway paradigm. Organism abbreviations: Sc, *Saccharomyces cerevisiae;* Sp, *Schizosaccharomyces pombe;* Ce, *Caenorhabditis elegans;* At, *Arabidopsis thaliana;* Dm, *Drosophila melanogaster.* See text for references.

The idea of two meiotic CO pathways helped explain additional seemingly disparate findings in other organisms. The fission yeast *Schizosaccharomyces pombe* lacks orthologs of Msh4 and Msh5 (Villeneuve and Hillers, 2001). Instead, most or all COs are dependent on the Mus81–Mms4 resolvase (the ortholog of Mms4 is called Eme1 in *S. pombe* and many other organisms; for simplicity, we use the *S. cerevisiae* protein name here) (Boddy et al., 2001; Smith et al., 2003). In budding yeast, loss of Mus81–Mms4 causes only ~30-50% reduction in meiotic COs (de los Santos et al., 2001). In light of the two-pathway paradigm, these results suggested that Mus81–Mms4 functions in one of the two meiotic CO pathways, and that this pathway is responsible for all meiotic COs in *S. pombe* but only a subset of COs in *S. cerevisiae*. This begged the question of whether Mus81–Mms4 and Msh4–Msh5 function in the same meiotic CO pathway or in two different pathways. In both *S. cerevisiae* and *Arabidopsis thaliana,*

double mutants that lack both the Msh4–Msh5 and Mus81–Mms4 complexes have more severely reduced CO levels than mutants lacking either one, strongly supporting the existence of two pathways – one dependent on Msh4–Msh5 (Class I) and another on Mus81–Mms4 (Class II) (Berchowitz et al., 2007; de los Santos et al., 2003).

The nature of the COs produced by the two pathways was also in question – i.e., if there are two meiotic CO pathways, do the COs produced by them have different properties? A clue to the answer came from mathematical modeling of crossover interference. Copenhaver *et al.* (Copenhaver et al., 2002) were able to fit *Arabidopsis* data to a counting model for interference (Foss et al., 1993) if they assumed two types of COs, some that participate in interference and some that do not. Consistent with this prediction, experimental studies demonstrated that the residual COs in *Arabidopsis* and budding yeast *msh4* and *msh5* mutants do not display interference (Argueso et al., 2004; Higgins et al., 2004; Lu et al., 2008; Novak et al., 2001). Conversely, Mus81–Mms4-independent COs in *S. cerevisiae* and *Arabidopsis* do exhibit interference (Berchowitz et al., 2007; de los Santos et al., 2003). These results suggested that the Msh4–Msh5-dependent pathway produces COs subject to interference, whereas the Mus81–Mms4-dependent pathway produces non-interfering COs (Table 1). This formulation explains the finding that COs are non-interfering in *S. pombe* (Munz, 1994), as these COs are produced from the Mus81–Mms4 pathway, and the strong interference of all COs in *C. elegans* (Meneely et al., 2002), as these are all produced by the Msh4–Msh5 pathway.

Although the paradigm of two meiotic CO pathways helped to explain many observations, this model also had some weaknesses. First, not all meiotic COs fit into these two pathways. *S. cerevisiae* mutants lacking both Msh4–Msh5 and Mus81–Mms4

still have some residual COs (de los Santos et al., 2003). In addition, though mathematical models of recombination in *Drosophila* fit best if most or all COs are interfering (Copenhaver et al., 2002), the *Drosophila* genome lacks Msh4 and Msh5 (Sekelsky et al., 2000), suggesting that another pathway produces interfering COs in this species.

Another shortcoming of the two-pathway paradigm is that the proteins used to define these pathways have very different functions: Mus81–Mms4 is an HJ resolvase whose activity presumably directly produces CO products (Boddy et al., 2001) (i.e., it is a pro-CO resolvase). Msh4–Msh5, however, does not directly produce COs, but instead blocks anti-CO helicases (i.e., it is an anti-anti-CO complex; see discussion below). Notably, the pro-CO resolvase that acts in the Msh4–Msh5-dependent pathway was unknown. Furthermore, the relationship between these pathways and the revised model for meiotic COs was unclear. Does the model fit both Class I and Class II pathways, with different proteins used for each, or is a second model necessary? These apparent weaknesses in the two-pathway paradigm for meiotic COs have largely been solved in the past year, as studies in a number of laboratories using different model organisms have clarified the roles and identities of pro-CO resolvases, anti-CO helicases, and anti-anti-CO complexes.

Anti-CO and pro-CO activities of Sgs1

Studies of anti-CO helicases have been particularly illuminating. COs are a beneficial product of meiotic recombination, but they are avoided during mitotic recombination because they can cause genome instability. DSBs in non-meiotic cells are

preferentially repaired into NCOs, largely through the action of anti-CO helicases. One key anti-CO protein is the Bloom syndrome helicase BLM (reviewed in Andersen and Sekelsky, 2010). Although BLM likely has many anti-CO functions, two activities are relevant to DSB repair. First, studies in *Drosophila* suggested that BLM promotes SDSA, probably by disrupting D-loops after repair DNA synthesis (Adams et al., 2003; McVey et al., 2004). Second, *in vitro* studies demonstrated that BLM, together with topoisomerase IIIα and other proteins, can catalyze dHJ dissolution, a process in which the two HJs are migrated toward one another and then decatenated (Wu and Hickson, 2003). Unlike resolution of dHJs, dissolution generates only NCOs.

Genetic studies suggested a similar anti-CO role for the *S. cerevisiae* BLM ortholog Sgs1 in meiosis. COs are reduced in mutants lacking ZMM proteins, including Msh4–Msh5, but, remarkably, COs are restored in double mutants that also lack Sgs1 (Jessop et al., 2006; Oh et al., 2007). An attractive interpretation of these results is that one function of ZMMs is to antagonize the anti-CO activity of Sgs1. Thus, Msh4–Msh5 is an anti-anti-CO protein.

Although these experiments with ZMMs and Sgs1 are consistent with the known mitotic anti-CO functions of Sgs1, *sgs1* mutants have only a modest increase in meiotic COs, much less than would be expected if all DSBs were processed through a pathway in which dHJs were produced and resolved into COs (Jessop et al., 2006; Rockmill et al., 2003). Novel insights into the solution to this apparent paradox came again from physical measurements of recombination intermediates and products. De Muyt *et al.* (De Muyt et al., 2012) found that NCOs are still produced in *sgs1* mutants, but, unlike the case in wild-type cells, these NCOs arise as JMs disappear and COs appear. This

suggests that when Sgs1 is absent, dHJs are resolved into COs and NCOs, as in the original DSBR model.

Additional insights came from physical studies of recombination in mutants lacking the known HJ resolvases. Three proteins, Mus81–Mms4, Yen1, and Slx1–Slx4, possess resolvase activity *in vitro* (Boddy et al., 2001; Fekairi et al., 2009; Ip et al., 2008). Mus81–Mms4 was shown to be important in generating mitotic crossovers, with Yen1 playing a compensatory or partially redundant role (Ho et al., 2010). Experiments by De Muyt *et al.* (De Muyt et al., 2012) and Zakharyevich *et al.* (Zakharyevich et al., 2012) found that single mutants lacking any one of these enzymes were still able to resolve most JMs and produce approximately normal numbers of COs. Even triple mutants lacking all three resolvases showed only a modest reduction in JM resolution and CO formation. These results suggest that the known resolvases collectively process only a small fraction of JMs. If these are JMs from the Class II pathway, then most JMs must be generated in the Class I pathway and be resolved by an unidentified resolvase.

Yet another surprise came when the same experiments were done in the absence of Sgs1. In this case, removing all three resolvases resulted in most JMs being left unresolved. Again, this result indicates that JMs produced in the absence of Sgs1 are different from those produced in the presence of Sgs1. In the absence of Sgs1, JMs are acted on by the known resolvases to produce both COs and NCOs, much like in the original DSBR model. The known resolvases, functioning in the Class II pathway, are therefore neither pro-CO nor anti-CO, since they generate both outcomes. Conversely, JMs produced in the presence of Sgs1 (Class I pathway) are cut by an unknown, pro-CO resolvase to produce exclusively COs.

What is the identity of the pro-CO resolvase that functions in the Class I pathway? It had previously been suggested that the mismatch repair proteins Mlh1–Mlh3 (MutLγ complex) and Exo1 might act in dHJ resolution (Nishant et al., 2008; Zakharyevich et al., 2010). COs are reduced in *mlh3* mutants, but removal of Sgs1 restores COs, suggesting that Mlh3, like ZMMs, functions in the Class I pathway (Oh et al., 2007). Consistent with this hypothesis, Zakharyevich *et al.* (Zakharyevich et al., 2012) found that when all three known resolvases were removed, eliminating Mlh3 resulted in a similar reduction in COs as eliminating Sgs1. A parallel set of experiments suggested that Exo1 functions in a different pathway than Mus81–Mms4, putting Exo1 also in the Class I pathway.

These results are consistent with Sgs1 having the expected anti-CO functions: It promotes SDSA (in wild-type cells) and dHJ dissolution (when the three known resolvases and the putative pro-CO resolvase are all missing). Unexpectedly, the results also reveal a pro-CO role of Sgs1. This pro-CO role may be in influencing pathway choice: In the presence of Sgs1, the ZMM-dependent Class I CO pathway can be used, but in the absence of Sgs1, the alternative Class II pathway gives rise to both COs and NCOs from dHJ resolution.

Extending the two-pathway paradigm

The results discussed above provided substantial support for and clarification of the two-pathway paradigm for meiotic COs in *S. cerevisiae*. Other recent results reveal the applicability of this paradigm to other model organisms. In wild-type *C. elegans* all COs are generated through the Class I pathway (Kelly et al., 2000; Zalevsky et al., 1999). However, when additional COs are induced, either by induction of DSBs through

exposure to ionizing radiation or by removal of RTEL-1 (yet another anti-CO helicase), the additional COs require MUS-81 but not the ZMM protein ZHP-3 (Youds et al., 2010). Crossover interference is reduced, consistent with these extra COs being formed through the Class II pathway. These findings expose the availability of the Class II pathway in *C. elegans*, even though it is normally not used to generate meiotic COs.

Additionally, Crismani *et al.* (Crismani et al., 2012) found that *Arabidopsis* mutants lacking the FANCM helicase had elevated COs. The additional COs were interference-insensitive, arose from a ZMM-independent pathway, and relied on Mus81 for formation. These findings parallel results seen in *S. cerevisiae*, where the absence of Sgs1 leads to COs being formed in an alternative, Mus81-dependent pathway. Furthermore, loss of FANCM rescues the meiotic defects of *Arabidopsis zmm* mutants, just like the removal of Sgs1 in *S. cerevisiae zmm* mutants (Crismani et al., 2012; Knoll et al., 2012). These findings strongly suggest that *Arabidopsis* FANCM functions as a meiotic anti-CO protein in a role that is antagonized by the ZMM proteins, similar to the role of Sgs1 in budding yeast. Thus, it appears that organisms can exchange proteins that occupy the same functional niche (in this case, swapping two anti-CO helicases) and still follow the framework of the two-pathway paradigm.

Meiotic and mitotic DSB repair in meiosis

These recent findings have added much to our understanding of the two CO pathways used in meiosis, and suggest a unified model that describes the relationship between the two pathways (Figure 2). By understanding that organisms use each pathway to varying degrees and use different proteins to accomplish the same tasks, this

unified model appears to be applicable to a more diverse set of model organisms than previously recognized. Furthermore, it is now apparent that the Class II pathway is strikingly similar to mitotic DSB repair in many respects. First, NCOs – not COs – are the predominant product. This outcome is achieved through SDSA, mediated by one or more anti-CO helicases. In instances where SDSA does not occur and a dHJ is generated, this intermediate can be resolved in an unbiased manner by "mitotic" resolvases to give either an NCO or a CO, but these COs are non-interfering. Despite these similarities, it should be noted that there are features of the Class II pathway that are unique to meiosis. For example, DSBs are generated by meiosis-specific Spo11 complexes, and engagement of DNA strands from the broken chromosome to the homologous chromosome is mediated in most species by meiosis-specific strand exchange proteins like Dmc1 (reviewed in Neale and Keeney, 2006). These events, however, may occur prior to the split between the Class I and Class II pathways (Figure 2).

While the Class II pathway is similar to mitotic DSB repair, the Class I pathway is a meiosis-specific DSB repair mechanism with embellishments to favor the formation of interfering COs. To ensure that dHJs are generated, anti-CO activities of helicases are blocked by meiosis-specific anti-anti-CO proteins. These dHJs are resolved mostly or exclusively into CO products by a pro-CO, possibly meiosis-specific, resolvase. Finally, Class I COs exert and are sensitive to CO interference, perhaps as a consequence of functional connections between this pathway and structural components of meiotic chromosomes, including the synaptonemal complex and meiosis-specific cohesins (de Boer and Heyting, 2006; Zickler and Kleckner, 1999).

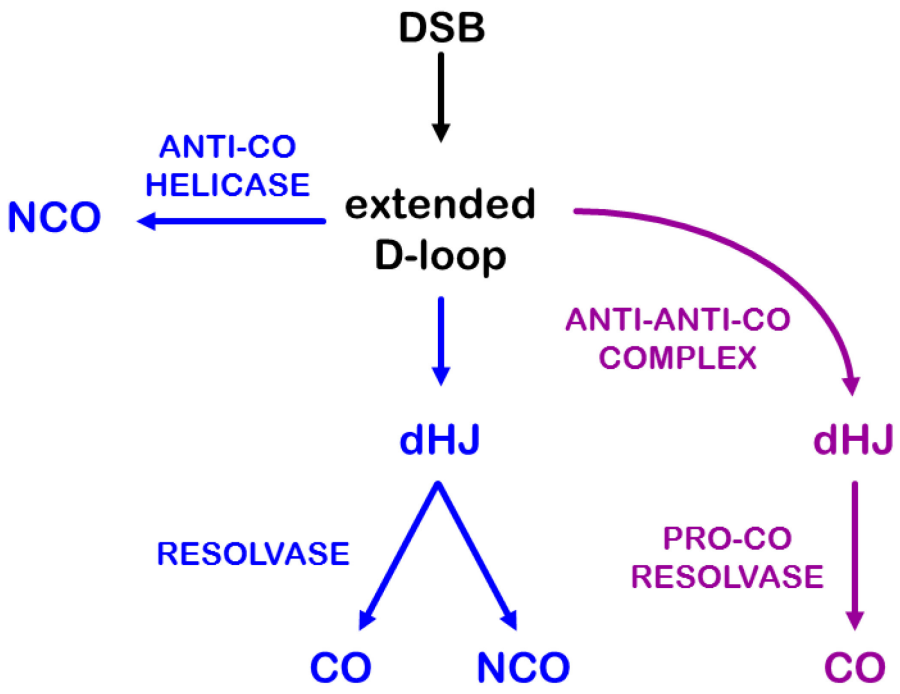

Figure 2. Two meiotic crossover pathways. In this unified model, a DSB is processed into an extended D-loop. In the "mitotic-like" pathway (blue, Class II), the extended D-loop can be unwound by an anti-CO helicase to produce NCOs. In some cases a dHJ is generated and then resolved by an unbiased resolvase into either a CO or NCO product. In the meiosis-specific CO pathway (purple, Class I), an anti-anti-CO complex blocks the action of anti-CO helicases to promote formation of a dHJ intermediate, which is then acted upon by a pro-CO resolvase to form exclusively CO products. A dHJ is presented as a key intermediate to fit the original models and the detection of joint molecules (JMs) with properties of dHJs in physical assays. However, there are other models which posit additional/alternative intermediates, including single HJs and multi-chromatid JMs. Variations on the two-pathway model can accommodate these other intermediates and less-common fates of DSBs.

The findings described above provide new insights into the evolution of meiotic recombination. Meiosis has long been thought to have evolved from mitosis (Cavalier-Smith, 1981; Wilkins and Holliday, 2009), and the evolution of meiotic DSB repair from mitotic DSB repair has been suggested previously (Marcon and Moens, 2005). We hypothesize that early in the evolution of meiosis, meiotic recombination occurred only through the Class II pathway, a method of DSB repair already in use in somatic cells.

Over time, the Class I pathway evolved to place additional constraints on meiotic recombination to promote the optimal placement of COs. To ensure CO formation, additional regulation of anti-CO helicases active during mitotic DSB repair was developed. This functional niche was filled by meiosis-specific anti-anti-CO proteins like Msh4–Msh5. The Class I pathway also evolved so that dHJs are resolved in a biased way to produce COs but not NCOs. The Class II pathway remained available, perhaps as a failsafe to ensure that all DSBs are repaired.

Many questions about meiotic recombination remain unsolved. One key question is how the CO/NCO decision (i.e., whether a given DSB is repaired as a CO or an NCO) is made. Studies in *S. cerevisiae* suggest that this decision is made early in the recombination process (reviewed in Bishop and Zickler, 2004). In light of the two-pathway paradigm, the CO/NCO decision must be enforced at or prior to divergence of the Class I and Class II pathways. Since Sgs1 appears to control pathway choice (De Muyt et al., 2012; Zakharyevich et al., 2012), it stands to reason that this protein may play a role in the CO/NCO decision. The CO/NCO decision must also be intertwined with the mechanism that mediates crossover interference. In the two-pathway model presented in Fig. 2, interference could be mediated by crossovers themselves or by any pre-CO intermediate specific to the Class I pathway, such as D-loops or dHJs loaded with the anti-anti-CO complex. Feedback from these pre-CO intermediates or Class I COs would have to impact the CO/NCO decision of nearby DSB repair events to ensure they go down the NCO pathway. How the CO/NCO decision is made, how Sgs1 mediates this decision, and how crossover interference works are important areas for future research in

the meiotic recombination field. The unified view of recombination pathways depicted in Figure 2 may help to guide some of these studies.

Drosophila melanogaster as a meiotic model system

The *Drosophila* model system is excellent for studying meiotic recombination. The long history of *Drosophila* meiotic research (Hawley, 1993), coupled with the absence of meiotic recombination in males (Morgan, 1912) (thus allowing the study of recombination events derived from a single parent only), the ability of *Drosophila* to tolerate high (0.5%) heterology (to aid in mapping recombination events) (Hilliker et al., 1991), and the increased likelihood of recovering non-disjunction (NDJ) progeny (some aneuplodies involving both the first and fourth chromosomes are viable) (Ashburner, 1989), all make *Drosophila* an ideal system for studying meiotic recombination.

Historically, two classes of *Drosophila* meiotic recombination mutants have been described: exchange and precondition mutants (Carpenter and Sandler, 1974; Sandler et al., 1968). The exchange class of mutants is characterized by a uniform decrease in COs across a chromosome arm. Precondition mutants have a non-uniform decrease in crossing over such that the frequency of exchange in intervals distal to the centromere are the most greatly decreased, while the frequency of exchange in proximal intervals is approximately wild-type or even increased. The first class was so named because these mutants were believed to be involved in the actual meiotic recombination exchange reaction, while the precondition mutants were believed to be necessary for establishing the preconditions of exchange.

The exchange class of meiotic recombination mutants contains four proteins hypothesized to form a complex necessary for HJ resolution: MEI-9, ERCC1, MUS312 and HDM (Joyce et al., 2009; Radford et al., 2005; Sekelsky et al., 1995; Yildiz et al., 2002). The precondition class genes include: *mei-217, mei-218, recombination defective* (*rec*) and *Mcm5* (Baker and Carpenter, 1972; Blanton et al., 2005; Lake et al., 2007; Liu et al., 2000). Single mutants with null mutations in *mei-217, mei-218* or *rec* exhibit identical phenotypes – a severe reduction in crossing over with residual COs showing the abnormal precondition distribution, high NDJ, normal synaptonemal complex formation, and no hypersensitivity to DNA damaging agents (Baker et al., 1976; Baker and Carpenter, 1972; Blanton et al., 2005; Carpenter, 1979; Grell, 1984; Liu et al., 2000). Epistasis experiments suggest that these precondition proteins function at an intermediate step in the meiotic recombination pathway (Blanton et al., 2005; Liu et al., 2000; Sekelsky et al., 1995). Likewise, a separation-of-function allele in *Mcm5*, called $Mcm5^{A7}$, shows these same precondition mutant phenotypes (Lake et al., 2007).

Mini-chromosome maintenance proteins

Two of the *Drosophila* precondition proteins are members of the mini-chromosome maintenance (MCM) protein family: REC, the *Drosophila* ortholog of MCM8, and MCM5. The eukaryotic MCM protein family is comprised of MCM2-9 (Bochman and Schwacha, 2009). The MCM proteins are characterized by a highly conserved ATPase domain located within a larger "MCM domain" (Bochman and Schwacha, 2009). At the core of this ATPase domain are Walker A and Walker B ATPase motifs (Walker et al., 1982). The Walker A motif interacts with the β- and γ-

phosphates of ATP (Lindegren, 1955), while residues in the Walker B motif bind Mg^{2+} necessary for ATP catalysis (Schulz, 1992). MCM proteins are members of the AAA+ (ATPases Associated with a variety of cellular Activities) ATPase family (Koonin, 1993; Wu et al., 2007), which typically form toroidal, hexameric complexes (Hanson and Whiteheart, 2005).

MCM2-7 are found in all eukaryotes and form a heterohexameric complex that is a component of the pre-replicative complex (pre-RC) (Bell and Dutta, 2002). The formation of the pre-RC is one of many steps required to couple DNA replication with the cell cycle. Once DNA replication is initiated, the MCM2-7 complex becomes the replicative helicase responsible for unwinding the DNA duplex ahead of the replication machinery (Bochman and Schwacha, 2009). It is the binding and hydrolysis of ATP that provides the energy necessary for the MCM helicase to unwind DNA (Bochman and Schwacha, 2009). The MCM2-7 proteins likely have additional roles in cellular processes beyond replication, potentially explaining the excess of MCM proteins that do not localize to replication forks (the "MCM paradox") (Laskey and Madine, 2003). These processes include transcription, chromatin remodeling and checkpoint responses (Forsburg, 2004). Additionally, an examination of the meiotic transcriptional profiles of three fungi – *S. cerevisiae, S. pombe* and *Coprinus cinereus* – found that one MCM protein (MCM2 in *C. cinereus*, MCM5 in *S. cerevisiae* and MCM6 in *S. pombe*) was up-regulated separately from the remaining MCM2-7 complex members (Burns et al., 2010) – an intriguing finding as a meiotic role for *Drosophila* MCM5 has also been discovered (Lake et al., 2007). These results suggest a specialized role for (at least) one MCM protein per organism in meiosis.

While MCM2-7 are found in all eukaryotes, MCM8 and MCM9 are absent in some lineages (Blanton et al., 2005), and less is known about their cellular function. Early experiments with MCM8 produced contradictory results, as one report found that MCM8 interacted with the MCM4,6,7 complex (Johnson et al., 2003), while three other groups failed to show this interaction (Gozuacik et al., 2003; Maiorano et al., 2005; Volkening and Hoffmann, 2005). Furthermore, while one group provided evidence that MCM8 was required for loading the pre-RC (Volkening and Hoffmann, 2005), another group suggested MCM8 was required for DNA synthesis (Maiorano et al., 2005). More recently, data from two studies has shown that MCM8 and MCM9 form a complex involved in homologous recombination-mediated DNA repair (Lutzmann et al., 2012; Nishimura et al., 2012). In particular, Lutzmann *et al.* found that male and female $MCM8^{-/-}$ mice and $MCM9^{-/-}$ female mice are sterile, showing a role for the MCM8-MCM9 complex in gametogenesis (Lutzmann et al., 2012). Finally, the *Drosophila* ortholog of MCM8, REC, is required for normal meiotic CO formation (Blanton et al., 2005). Interestingly, whereas all other organisms possessing MCM8 also have MCM9, the *Drosophila* genome only encodes MCM8/REC (Blanton et al., 2005).

Investigations into the role of the *Drosophila* precondition proteins

At the outset of this work, more questions than answers surrounded the *Drosophila* precondition proteins: REC, MEI-217, MEI-218 and MCM5. Two of the precondition proteins were readily recognizable as members of the MCM family (MCM8/REC and MCM5), and MEI-218 had been suggested to have a weak, MCM-like domain at its C-terminus (Lake et al., 2007). At first glance, this suggested the

precondition proteins might have some connection to the MCM family. MEI-217, however, was an orphan protein, lacking identifiable homology to any known protein. In this work, I investigated the possible connection between the MCM family and the precondition proteins. Additionally, by definition, all precondition mutants had the same abnormal meiotic CO distribution. It was unknown whether this phenotype was the result of a common function for the precondition proteins, or was merely a coincidence of the four proteins having varied roles in the meiotic recombination pathway. To this end, I sought to identify the role of the precondition proteins and to determine whether the proteins functioned together. Finally, I hoped to discover why *Drosophila* meiotic recombination did not fit into the two-pathway paradigm unlike so many other model systems. For example, how was *Drosophila,* the organism in which meiotic recombination and interference were discovered (Morgan, 1911; Sturtevant, 1913), able to create interfering meiotic COs without key pathway members Msh4 and Msh5? By utilizing genetic, biochemical and evolutionary biological techniques I was able to answer these fundamental questions and discover new avenues for future research.

CHAPTER 2

EVOLUTION OF AN MCM COMPLEX IN FLIES THAT PROMOTES MEIOTIC CROSSOVERS BY BLOCKING BLM HELICASE[1]

Crossovers (COs) between homologous chromosomes can be beneficial or detrimental, depending on their context (Andersen and Sekelsky, 2010). Meiotic COs increase genetic diversity and promote accurate chromosome segregation, whereas mitotic COs can lead to loss of heterozygosity, potentially triggering tumorigenesis. Mitotic COs are prevented by "anti-CO" proteins. A key anti-CO protein is the Bloom syndrome helicase BLM, which generates non-CO products by unwinding recombination intermediates that might otherwise be processed into COs (Chu and Hickson, 2009). In meiosis, CO formation is encouraged through inhibition of anti-CO proteins. The budding yeast Msh4-Msh5 heterodimer antagonizes the BLM ortholog Sgs1 (Jessop et al., 2006). Msh4 and Msh5 are found in all metazoans for which sequence is available, except *Drosophila* species and their fellow schizophoran *Glossina morsitans*, the tsetse fly (Figures 3 and 4). The lack of recognizable orthologs of these proteins suggests that these species evolved another protein or complex to block the anti-CO activity of BLM.

[1] This chapter was previously published as *Evolution of an MCM Complex in Flies That Promotes Meiotic Crossovers by Blocking BLM Helicase*. Kohl KP, Jones CD and Sekelsky J. *Science.* 2012. 338: 1363-1365. Molecular evolutionary analysis was conducted by Corbin Jones and all authors contributed to writing the manuscript.

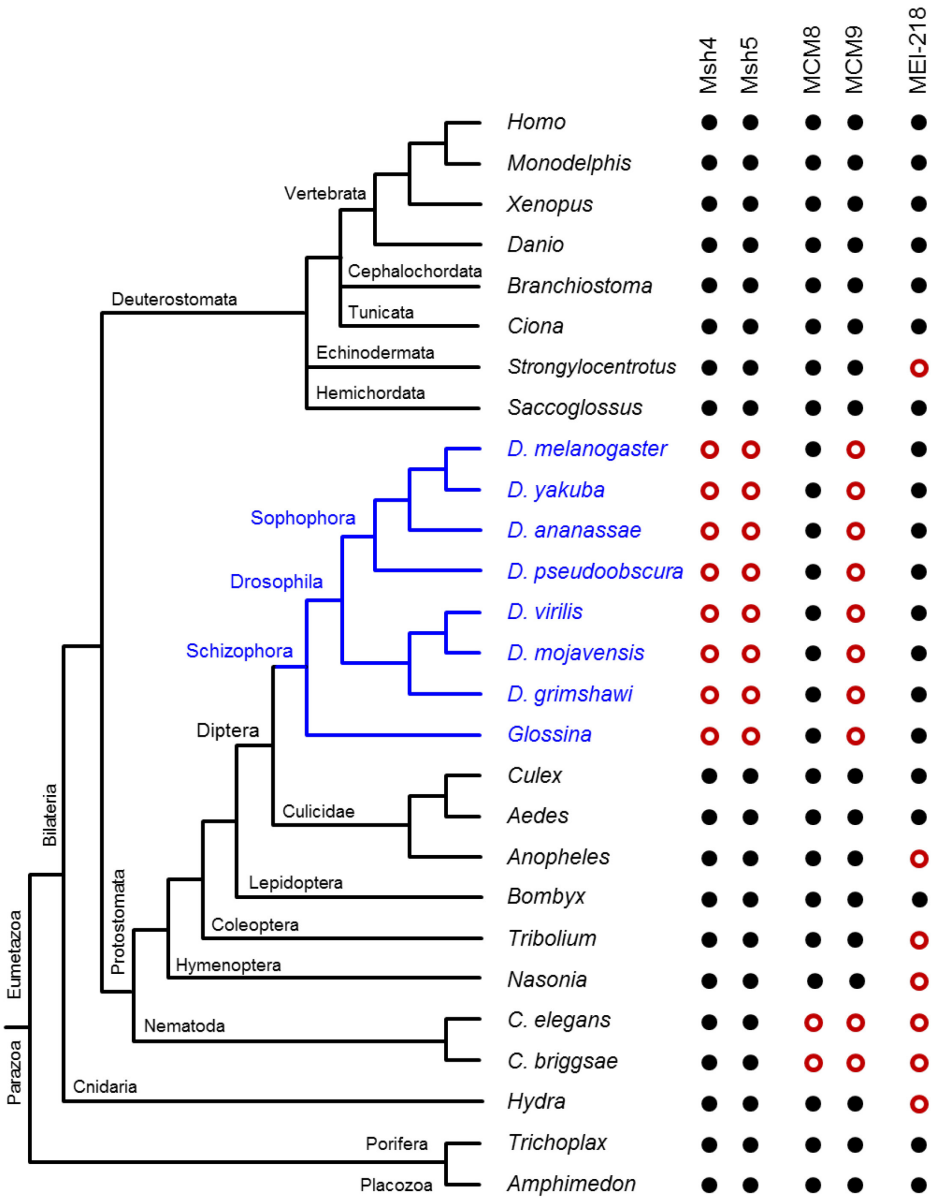

Figure 3. *Drosophila* and *Glossina* uniquely lack MSH4, MSH5, and MCM9. The presence (filled black circles) or absence (open red circles) of MSH4, MSH5, MCM8, MCM9, and MEI-218 orthologs within representative genera spanning the metazoa is indicated. The topology of phylogenetic relationships was created from an alignment of DNA polymerase alpha catalytic subunit (this protein was not present in the *Saccoglossus kovalevski* sequences, so this species was inserted into its consensus location). Protein absence was assumed when an ortholog could not be identified following multiple rounds of BLAST searches against several databases (see Materials and Methods).

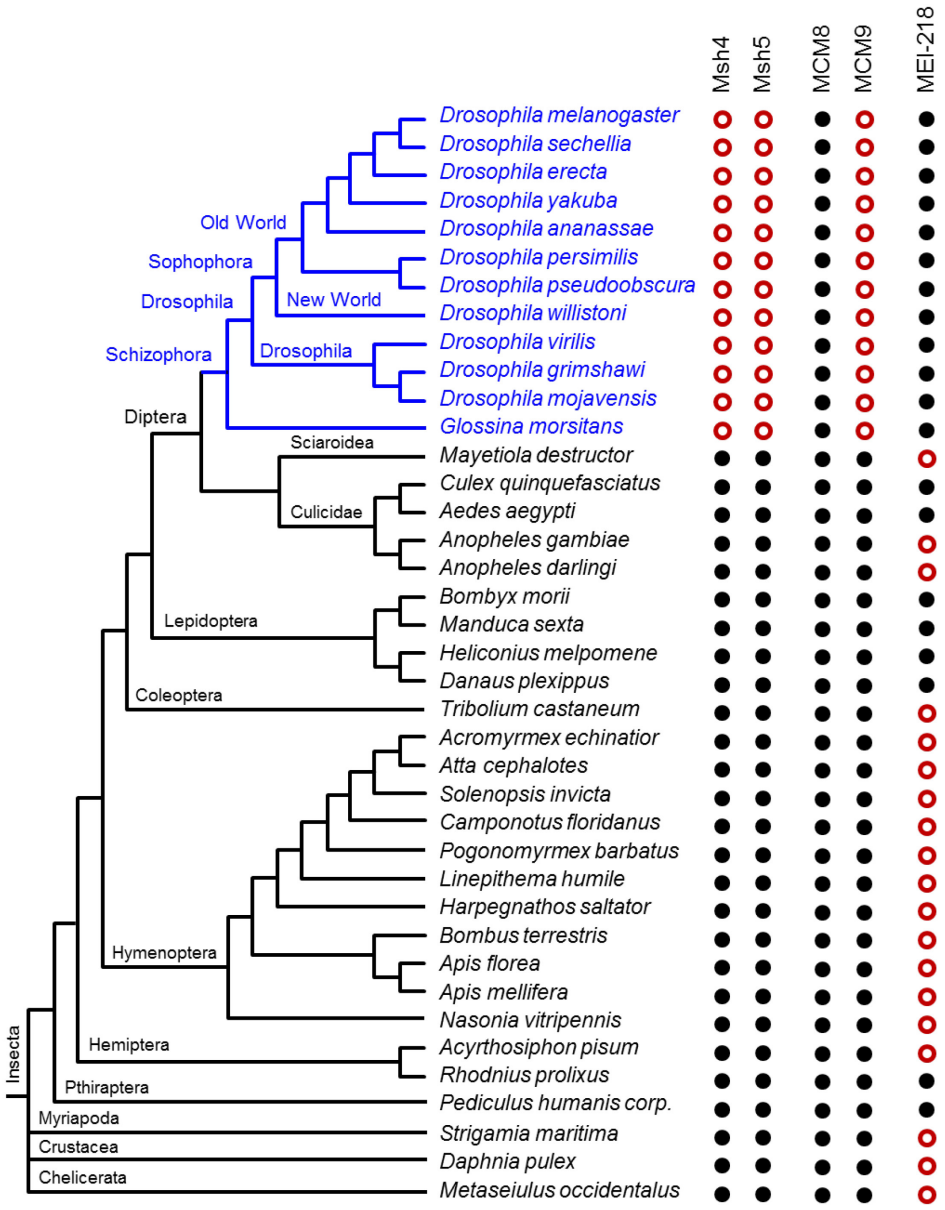

Figure 4. *Drosophila* and *Glossina* uniquely lack MSH4, MSH5, and MCM9. This figure is similar to Figure 3, but includes only arthropods. See Figure 3 for details.

Like *Saccharomyces cerevisiae Msh4* and *Msh5* mutants, the only defects in *Drosophila rec*, *mei-217*, and *mei-218* mutants are in meiotic recombination (Baker and Carpenter, 1972; Blanton et al., 2005; Hollingsworth et al., 1995; Liu et al., 2000; Manheim et al., 2002; Ross-Macdonald and Roeder, 1994). REC is orthologous to

MCM8 (Blanton et al., 2005); MCMs have properties reminiscent of Msh4-Msh5. MCM2 through MCM7, which are essential for replication in eukaryotes, form a heterohexamer that encircles DNA (Remus et al., 2009). Similarly, Msh4-Msh5 is thought to encircle recombination intermediates (Snowden et al., 2004). In both cases, this activity is regulated by adenosine triphosphate (ATP) binding and hydrolysis (Remus et al., 2009; Snowden et al., 2004).

MEI-217 initially appeared to be novel, because BLAST searches failed to identify homologs outside dipterans, and searches of the Conserved Domain Database (CDD) (Marchler-Bauer et al., 2011) did not detect any domains. BLAST searches with MEI-218 identified a single putative ortholog in metazoans (Figures 3 and 4). A CDD search returned a hit to the MCM domain in the C terminus of MEI-218, but the score was low and the match covered only one-third of the domain (Figure 5A). To verify the presence of this domain, we conducted structure-based searches with PHYRE (Figure 6A) (Kelley and Sternberg, 2009). This analysis revealed that the C terminus of MEI-218 has a structure similar to that of the AAA adenosine triphosphatase (ATPase) domain of MCMs (Figure 5B). Canonical MCMs have both an N-terminal MCM domain and a C-terminal ATPase domain. The N-terminal domain is present in vertebrate MEI-218 but not in *Drosophila* MEI-218. However, PHYRE with MEI-217 shows that its predicted structure is similar to the MCM N-terminal domain. Because MEI-217 and MEI-218 are encoded by overlapping open reading frames on the same transcript (Liu et al., 2000), we infer that they evolved from an MCM-like protein represented by a single polypeptide in other metazoans.

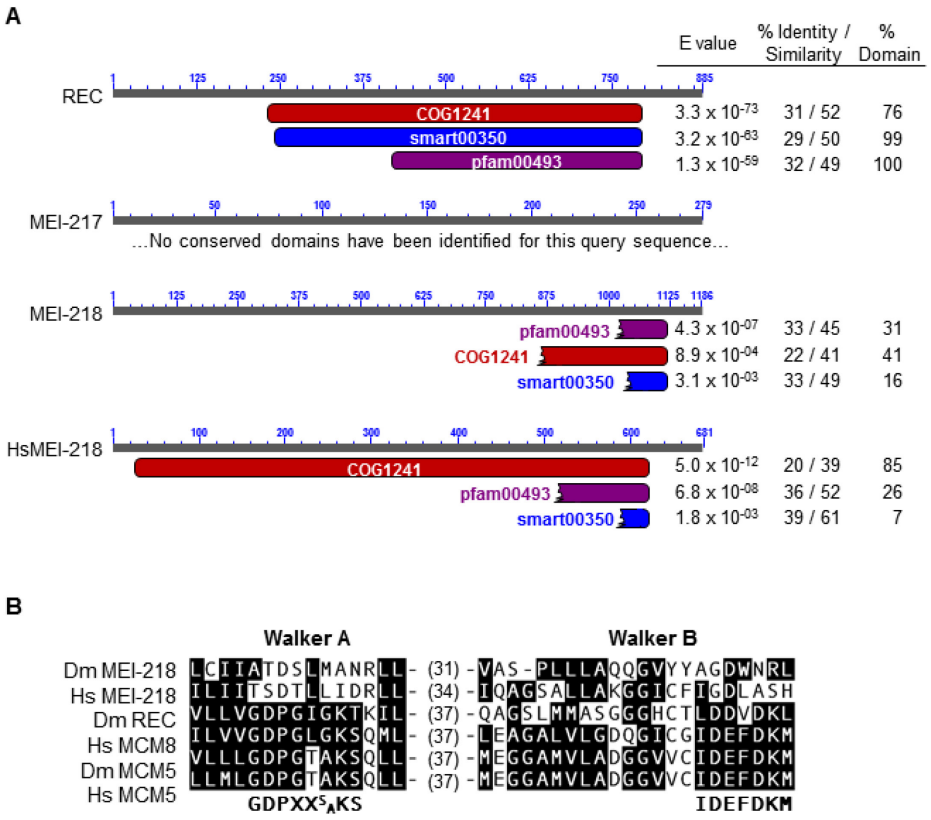

Figure 5. Domains identified by a search of the Conserved Domain Database in *Drosophila melanogaster* REC, MEI-217, MEI-218 and human MEI-218. (A) In database descriptions COG1241 is "MCM2", while smart00350 and pfam00493 are both listed as "MCM". To the right of each domain is the E value, percent identity/percent similarity between the domain and input sequences, and the percentage of the domain definition that the alignment spans. For REC only the top three domain hits are shown. (B) Alignment of the Walker A and B motifs in human and *Drosophila melanogaster* MCM5, MCM8/REC, and MEI-218. These motifs are involved in ATP binding and hydrolysis. Identical or conserved residues have a black background. Numbers in parentheses denote number of amino acids between motifs. The consensus sequences are given below the alignment. The changes in both *Drosophila* and human MEI-218 suggest that this protein does not bind or hydrolyze ATP.

The shared phenotypes and MCM domains suggest that REC, MEI-217, and MEI-218 function together in meiotic recombination. To distinguish them from the replicative MCMs, we refer to REC, MEI-217, and MEI-218 as "mei-MCMs." Because MCM2 through MCM7 function together as a heterohexamer, we investigated whether the mei-MCMs form a complex. MEI-217 interacted strongly with both the C-terminal third of

MEI-218 and REC (Figure 6B and C), which suggests that the mei-MCMs form a complex. This complex likely also contains one or more replicative MCMs. A meiosis-specific mutation in *Mcm5* causes the same phenotypes as *mei-MCM* mutants (Lake et al., 2007), making MCM5 a strong candidate to be a component of the complex.

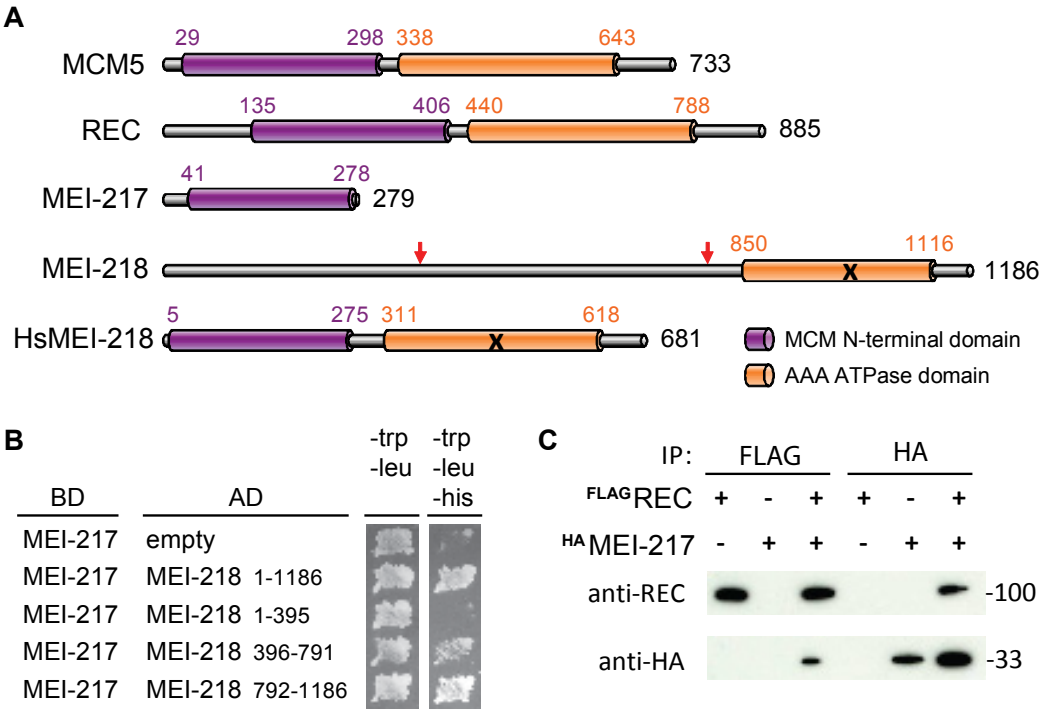

Figure 6. mei-MCM complex. (A) Structural domains identified through PHYRE. "MCM N-terminal domain" corresponds to Protein Data Bank fold 3f9v and "AAA ATPase domain" to fold ID 3f8t. The "x" on *Drosophila* and human (Hs) MEI-218 symbolizes changes in the ATP binding and hydrolysis motifs predicted to abolish ATPase activity (Figure 5). Red arrows on MEI-218 indicate segments used in yeast two-hybrid analysis. (B) Yeast two-hybrid interactions between MEI-217 and MEI-218. Cells expressing the indicated fusions to the GAL4 DNA binding domain (BD) or activating domain (AD) were streaked onto selective media. Growth on –trp –leu –his indicates an interaction. (C) Co-immunoprecipitation of REC and MEI-217. Epitope-tagged mei-MCMs were co-expressed in insect cells, immunoprecipitated with antibodies to the indicated epitope tags, blotted and probed with antibodies to REC and to the hemagglutinin (HA) tag.

Noting the genetic and biochemical similarities between mei-MCMs and Msh4-Msh5, we hypothesized that the mei-MCMs antagonize *Drosophila melanogaster* BLM (DmBLM) in lieu of Msh4-Msh5. This hypothesis predicts that removing DmBLM should compensate for *mei-MCM* mutations; in budding yeast, the CO defect in *msh4* mutants is suppressed by removing Sgs1 (Jessop et al., 2006). Few COs were made in *rec* and *mei-218* single mutants, resulting in high nondisjunction (NDJ) of meiotic chromosomes (Figure 7A). In contrast, mutations in *mus309*, which encodes DmBLM, caused only a mild reduction in COs and correspondingly low levels of NDJ. Strikingly, *mus309* mutations suppressed the high-NDJ phenotype of *rec* and *mei-218* mutants (Figure 7A). Furthermore, the low CO rate in *rec* mutants returned to an approximately wild-type rate in *mus309 rec* double mutants (Figures 7B and 8, and Table 2); this finding indicates that mei-MCMs are not essential for generating meiotic COs if DmBLM is absent, thereby supporting our hypothesis that mei-MCMs oppose the known anti-CO activities of DmBLM (Adams et al., 2003; McVey et al., 2007).

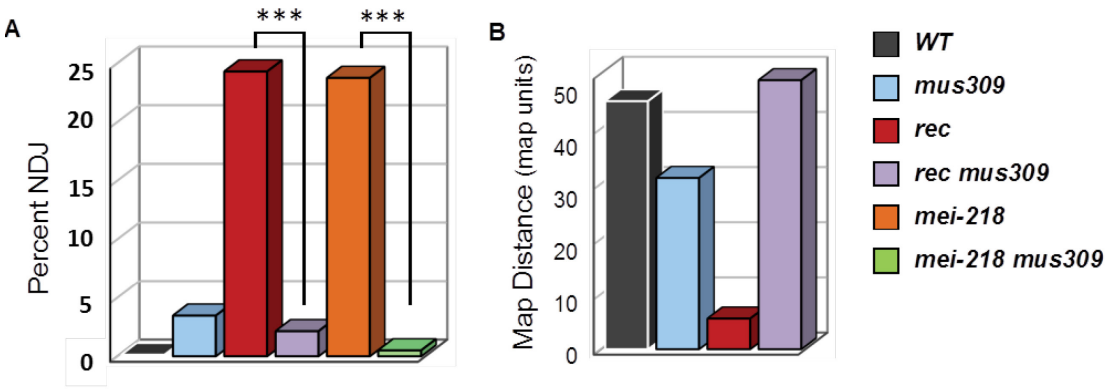

Figure 7. mei-MCMs antagonize DmBLM. (A) *X* chromosome non-disjunction (NDJ) across more than 1500 individuals for each genotype except *mei-218*; *mus309* (n=383). ***, $P < 0.0001$. (B) This graph shows the summed map distance in map units (m.u., equivalent to centiMorgans) across five intervals spanning ~20% of the genome for over 1000 individuals for each genotype. $P < 0.0001$ for all comparisons except *WT* versus *mus309 rec*, $P = 0.0674$.

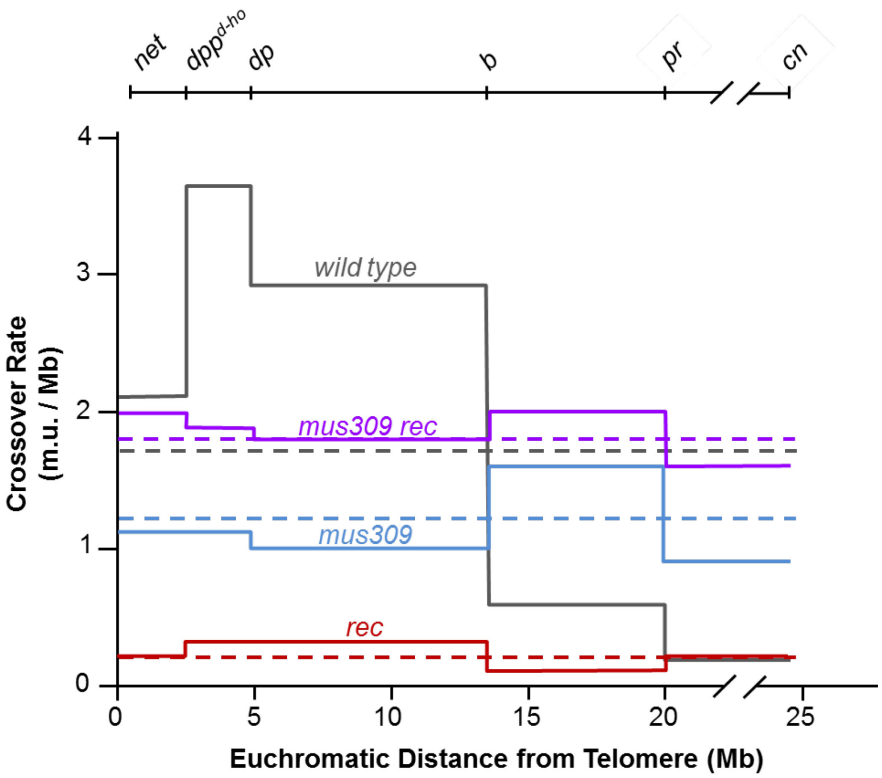

Figure 8. Crossovers in *rec* and *mus309* mutants. Crossover distribution across five intervals on chromosome *2L* and proximal *2R* is shown. The markers used in mapping are shown above the graph. Hash marks between *pr* and *cn* indicate the position of the centromere. Solid lines depict the number of map units (m.u.) per megabase pair (Mb) in each interval for wild-type, *rec*, *mus309*, and *mus309 rec* for more than 1000 individuals for each genotype. Dashed lines indicate the mean CO rate across the entire region. Determining the cause of the increased COs in *mus309 rec* compared to *mus309* is difficult, since we cannot distinguish between true meiotic COs and pre-meiotic mitotic COs occurring in the *mus309* mutant background. The occurrence of pre-meiotic mitotic crossovers also complicates efforts to determine whether crossover interference is altered in *mus309* genotypes (McVey et al., 2007); however, there are significantly more double crossover (DCO) and triple crossover (TCO) progeny in *mus309 rec* compared to *mus309* (Table 2) ($P < 0.0001$ for DCO, $P = 0.046$ for TCO, Fisher's exact test) and to wild-type ($P < 0.0001$ for DCO, $P = 0.0002$ for TCO, Fisher's exact test), suggesting that interference is disrupted in *rec* mutants even in the absence of DmBLM. Recent studies suggest that Sgs1 has, in addition to its anti-CO functions, a pro-CO role in meiosis, perhaps directing recombination into the Msh4–Msh5 pathway (De Muyt et al., 2012; Zakharyevich et al., 2012). If true in *Drosophila*, the COs in *mus309 rec* mutants may arise from a mei-MCM-independent CO pathway rather than the lack of need to block DmBLM anti-CO activities. However, this scenario cannot explain the finding that REC regulates CO distribution even in the absence of DmBLM.

Genotype	non-CO (NCO)	Single Crossovers (SCOs)								Double Crossovers (DCOs)										Triple Crossovers (TCOs)
		I		II		III		IV		V												
	net ho dp b pr cn / + + + + + +	+ ho dp b pr cn	net + + + + +	+ + dp b pr cn	net ho + + + +	+ + b pr cn	net ho dp + + +	+ + + pr cn	net ho dp b + +	+ + + + cn	net ho dp b pr +	DCO flies	TCO flies	**Total flies**	I and II	I and III	I and IV	I and V	II and III	II and IV	II and V	III and IV	III and V	IV and V	
wild-type	1323	106		163		602		65		16		44	1	2320	0	7	3	2	5	2	5	9	10	1	III,IV,V
rec	1923	10		14		51		13		25		0	0	2036	0	0	0	0	0	0	0	0	0	0	
mus309	844	23		22		89		104		61		33	0	1176	1	4	2	1	1	2	2	11	7	2	
mus309 rec	705	31		29		136		103		87		80	10	1181	0	11	5	2	5	7	2	19	21	8	I,III,V (3)
																									I,II,IV (3)
																									II,IV,V (2)
																									I,III,IV (2)

Table 2. Crossover distribution. Each row lists the number of non-crossover (NCO), single crossover (SCO), double crossover (DCO), and triple crossover (TCO) progeny for each indicated genotype. For NCO and SCO, the + symbol indicates wild-type for a marker, while the gene name indicates mutant for a marker, in the order along the chromosome (*net ho dp b pr cn*). Intervals for DCOs and TCOs are given in the columns on the right, with interval I being *net* to *ho*, etc. Numbers in parentheses denote number of times that particular TCO combination was observed in that genotype.

mei-MCMs appear to functionally replace Msh4-Msh5 in Schizophora, and presumably evolved to do so in response to natural selection. Several evolutionary scenarios could lead to this result (Figure 9), but most predict that there would be evidence of adaptive divergence of *mei-MCM* genes in Schizophora. REC was previously noted to be highly diverged in *Drosophila* (Blanton et al., 2005; Liu et al., 2009); we found that *Glossina* MCM8/REC is similarly divergent (Figure 10). The presence or absence of MCM8 correlates with that of its functional partner MCM9 throughout eukaryotes, except in *Drosophila* and *Glossina*, which retained MCM8/REC while losing MCM9 (Figures 3 and 4). The loss of MCM9 suggests that MCM8 evolved a novel function in an ancestor to Schizophora.

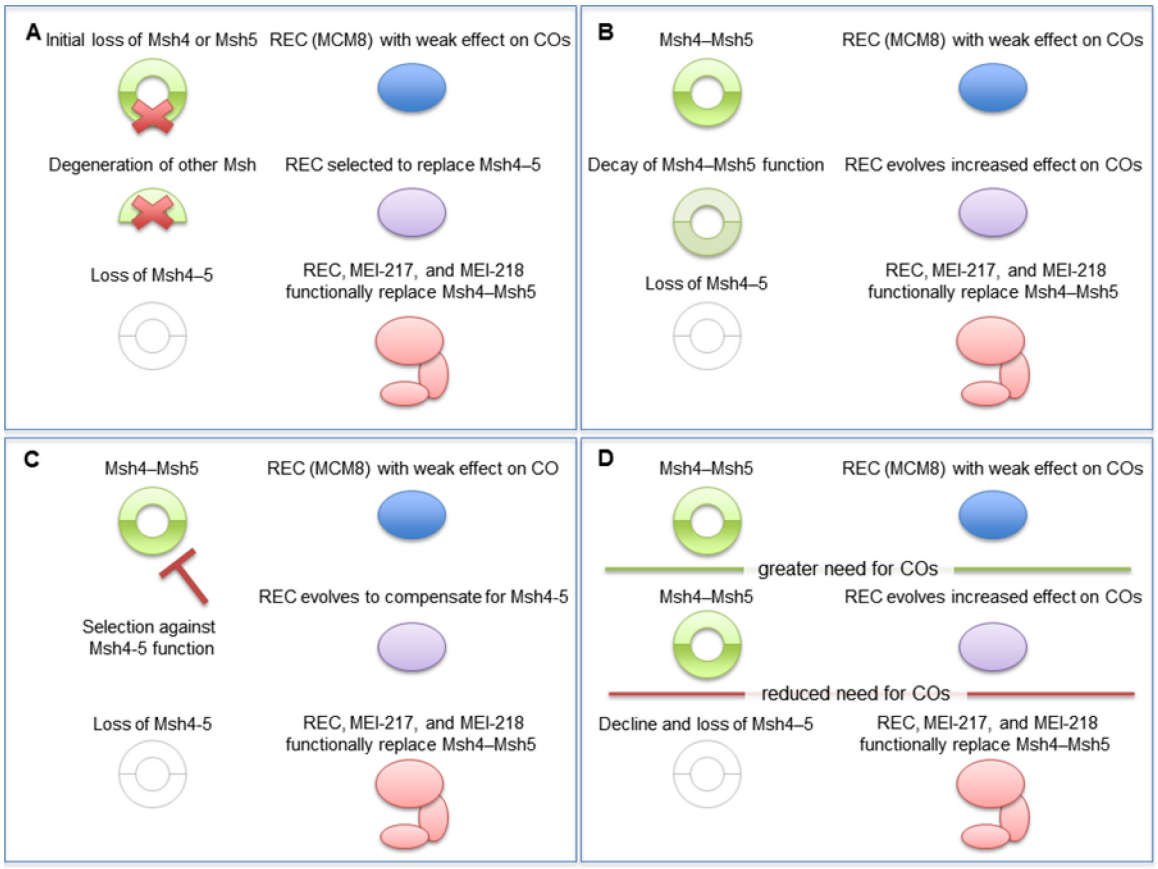

Figure 9. Possible evolutionary scenarios for the loss of Msh4–Msh5 in *Drosophila* and the evolution of mei-MCM complex. Across metazoans Msh4–Msh5 antagonize the anti-CO activity of BLM to promote meiotic COs. Given the presumed evolutionary stability of this interaction over hundreds of millions of years, loss of Msh4–Msh5 and its replacement by mei-MCMs in the higher Dipterans is surprising. A range of evolutionary scenarios could explain this pattern. The four scenarios presented here depict archetypes of these possibilities (within a panel, top to bottom represents past to present). (A) Sudden loss of Msh4–Msh5 (green), followed by recruitment and evolution of mei-MCMs (red). This scenario would provide the strong signature of selection observed at REC (shift from blue, to purple, to red), as it would be needed to restore antagonism of BLM and promote the formation of crossovers. However, this scenario seems unlikely, as a sudden loss of Msh4–Msh5 would lead to meiotic chromosome instability and could likely occur only in small populations with substantial genetic drift. (B) Gradual recruitment and replacement of Msh4–Msh5 by mei-MCMs. MCM8 and MCM9 have a role in meiotic recombination and other DNA repair processes (Lutzmann et al., 2012; Nishimura et al., 2012). This may have been as a nascent BLM antagonist with a minor recombination role that gradually expanded and eventually supplanted that of Msh4–Msh5. This scenario also seems unlikely as it does not necessarily result in a strong signature of selection. The strong signature of selection we observed suggests that extensive evolution was needed in REC to replace Msh4–Msh5, but this also seems implausible given the evolutionary stability of Msh4–Msh5 in all other metazoans. (C) Selection against Msh4–Msh5 results in the repurposing and remodeling of REC from an ancestral MCM. Either an endogenous force (*e.g.*, transposon, driving chromosome, or other selfish element) or exogenous force (*e.g.*, viruses integrating at breaks, highly consistent environment) selected for reduced crossover activity during meiosis. This could result in a

gradual diminishing of Msh4–Msh5 activity. Dollo's law of irreversibility suggests that once a trait is lost, it never re-evolves exactly as before (Collin and Cipriani, 2003; Collin and Miglietta, 2008). It may have been evolutionarily simpler to evolve the mei-MCMs than to restore Msh4–Msh5 activity (and potentially face the same evolutionary pressure that drove this activity down). (D) Positive selection for increased CO activity or antagonism of BLM drives evolution of mei-MCMs. CO rates are genetically labile and increased recombination rate is thought to facilitate adaptation (Adams et al., 2000). Schizophora represents a recent rapid radiation of lineages that may have diversified along with flowering plants in an anciently tropical world (Grimaldi and Engel, 2005; Wiegmann et al., 2011). Selection for increased crossover rate may have resulted in the repurposing of REC and its elevated rate of evolution. Once these new niches were filled, the need for elevated crossing over may have reduced. As Blanton *et al.* (Blanton et al., 2005) suggested, REC may promote repair synthesis to generate more stable intermediates that are refractory to unwinding by DmBLM. Thus, in this reduced CO scenario selection would act to preserve REC at the cost of Msh4–Msh5.

It is likely that the actual events encompassed elements of one or more of these scenarios. In three of these scenarios, the strong pressure to find a means to segregate chromosomes accurately may have driven the development of recombination-independent segregation in male *Drosophila* and *Glossina* (Gooding and Rolseth, 1995; Morgan, 1912). Consistent with this speculative hypothesis, male recombination is retained in mosquitoes (Gilchrist and Haldane, 1947; McClelland, 1966; Zheng et al., 1996), which also have conserved Msh4–Msh5 (Figures 3 and 4).

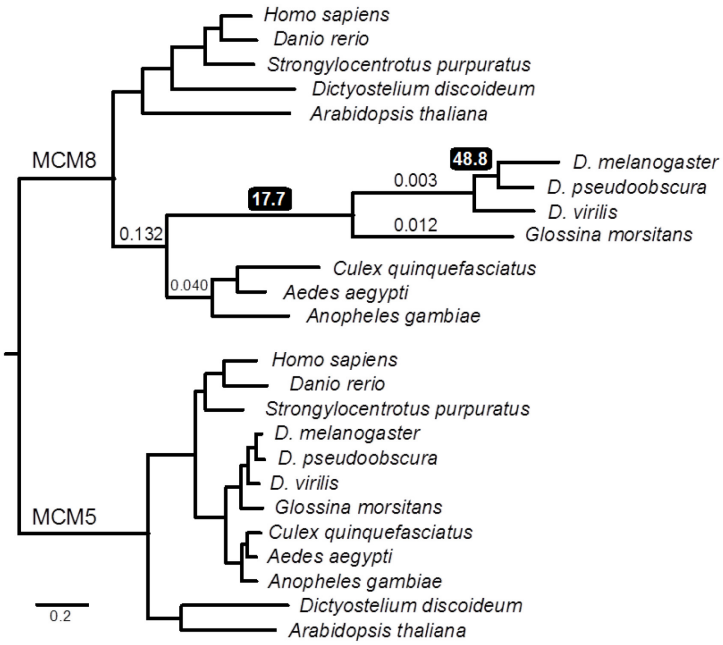

Figure 10. Divergence of MCM8 in *Drosophila*. Maximum-likelihood tree from an alignment of the conserved MCM domains of MCM8/REC and MCM5 from diverse taxa. Branch lengths indicate the number of substitutions per site (see scale). Numbers above branches show dN/dS estimates for selected branches; those with black background highlight branches with dN/dS estimates greater than one, suggesting positive selection.

Divergence in *rec* and loss of MCM9 occurred after the split between mosquitos and higher flies 200 to 250 million years ago, but prior to the emergence of the Schizophora 65 million years ago. To test whether patterns of sequence evolution were consistent with positive selection leading to the divergence of *rec*, we estimated the ratio between the rate of base pair substitutions at nonsynonymous sites (dN) and the rate at synonymous sites (dS) among dipterans in *MCM8/rec*. We compared 15 evolutionary models, ranging from conservation of dN/dS ratios across all taxa surveyed to allowing free evolution of dN/dS ratios along all branches, and including models testing specific hypotheses about the evolution of *rec* along different branches of the insect phylogeny. The best-fitting model ($P = 0.0002$ versus the next best model) supports the hypothesis that rapid protein-coding divergence was driven by positive selection prior to the split of tsetse flies from fruit flies (Figures 10 and 11, and Table 3). Thus, we infer that natural selection likely drove the repurposing of REC into its new role as an antagonist of DmBLM. Recent evolution of *rec* shows much lower levels of nonsynonymous changes, suggesting subsequent functional constraint (Figure 11). MEI-217 and MEI-218 have also diverged substantially from the ancestral MCM structure: They split into two polypeptides, and MEI-218 acquired an N-terminal extension (Figures 12 and 13).

Our data show that flies evolved a novel MCM complex to antagonize the anti-CO functions of BLM during meiosis—a role held by Msh4-Msh5 in other organisms. Although we do not know what evolutionary forces ultimately drove the loss of Msh4-Msh5 and the repurposing of mei-MCMs, it is tempting to speculate that these forces also led to another fundamental meiotic difference in *Drosophila* and *Glossina* relative to mosquitoes: the absence of recombination in males, which was first noted

in *Drosophila* by Morgan 100 years ago (Figure 9) (Morgan, 1912). Resolving the conundrum of why the mei-MCMs supplanted Msh4-Msh5 will require a deeper understanding of both the evolutionary origins of the mei-MCMs and the functional differences between mei-MCMs and Msh4-Msh5.

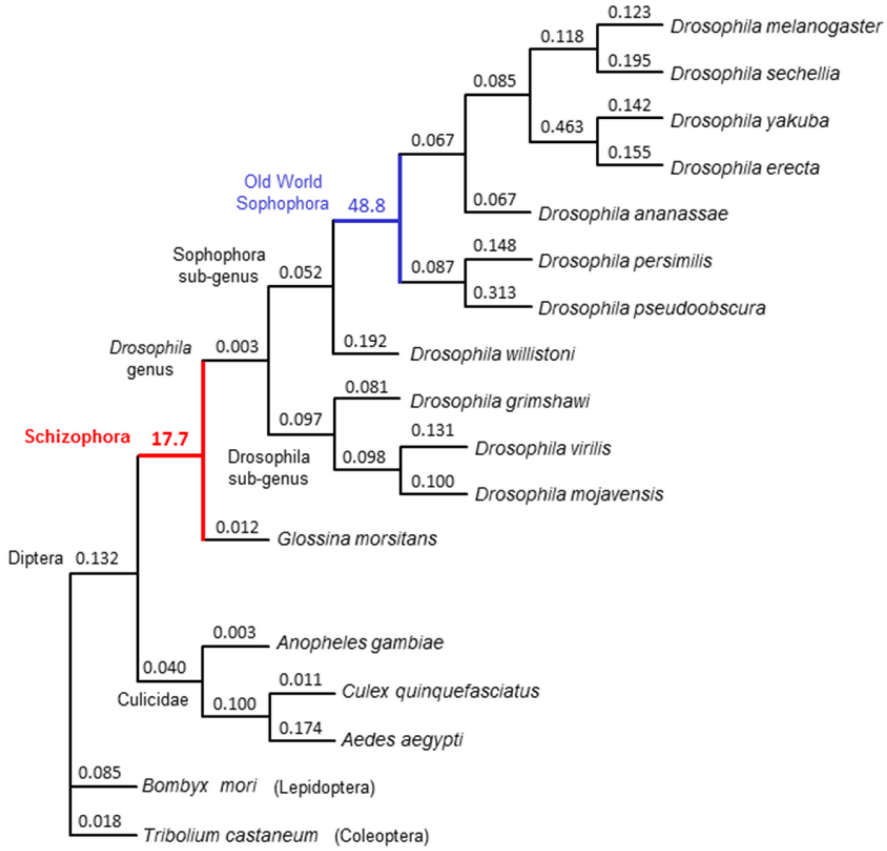

Figure 11. Rates of evolution of REC/MCM8 in Dipteran insects and select outgroups. The tree represents a topology of phylogenetic relationships among the insect species shown. Branch lengths are proportional for ease of reading and do not reflect divergence, which is shown in Figure 10. dN/dS ratios along each branch for the best fitting model (Model 15) are shown. Values less than one suggest purifying selection, whereas values greater than one suggest positive selection along that branch. Consistent with our prediction of rapid evolution of REC before the emergence of Schizophora, the branch leading to *Glossina* and *Drosophila* has a high positive value (red). The biological significance of the other high positive value, on the branch leading to Old World Sophophora (blue), is unknown, since our data do not suggest any hypotheses concerning evolution of REC along this branch.

Model	Type[1]	Para-meters	Log-Likelihood	Description
1	0	33	-29353.66955	One dN/dS rate for all taxa
2	2	34	-29353.13881	One rate for *D. melanogaster*; one rate for all other taxa
3	2	34	-29352.42575	One rate for mosquitoes; one rate for all other taxa
4	2	34	-29348.27369	One rate for Old World Sophophora; one rate for all other taxa
5	2	34	-29340.13854	One rate for Sophophora; one rate for all other taxa
6	2	34	-29322.82126	One rate for higher flies one rate for all other taxa
7	2	34	-29313.19077	One rate for *Drosophila*; one rate for all other taxa
8	2	35	-29341.74626	One rate for *Drosophila*; one rate for *Glossina*; one rate for all other taxa
9	2	35	-29313.18287	One rate for ancestor to higher flies; one rate for *Drosophila*; one rate for all other taxa
10	2	35	-29313.15944	One rate for ancestor to higher flies; one rate for Sophophora; one rate for all other taxa
11	2	36	-29313.15172	One rate for ancestor to higher flies; one rate for *Drosophila*; one rate for *Glossina*; one rate for all other taxa
12	2	36	-29310.98226	One rate for ancestor to higher flies; one rate for *Drosophila*; one rate for Sophophora; one rate for all other taxa
13	2	37	-29310.95229	One rate for ancestor to higher flies; one rate for *Drosophila*; one rate for Sophophora; one rate for *Glossina*; one rate for all other taxa
14	2	51	-29300.10477	dN/dS rate varies for all higher flies
15	1	63	-29280.42216	dN/dS rate varies for all taxa

Table 3. Models for the evolution of *MCM8/rec* in Diptera. [1]Model-type: 0, common rate all lineages; 1, lineage-specific rates; 2, two or more rates assigned to different lineages (detailed in description).

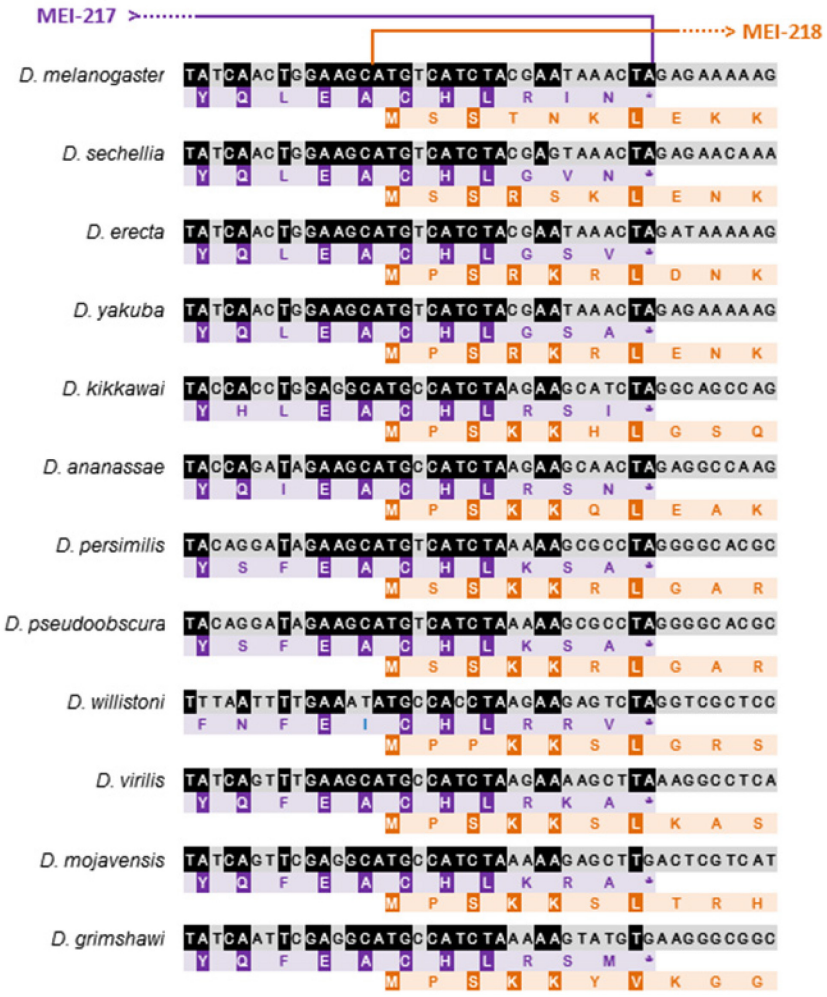

Figure 12. Conservation of MEI-217 and MEI-218 as separate polypeptides throughout *Drosophila*. *D. melanogaster* MEI-217 and MEI-218 are predicted to be separate polypeptides encoded on a single transcript (Liu et al., 2000). This figure shows an alignment of the sequence coding for the C-terminus of MEI-217 (purple) and the N-terminus of MEI-218 (orange) based on TBLASTN searches with *D. melanogaster* MEI-217. Positions that are identical (or similar, for amino acid residues) in at least nine of the twelve species shown are in white text on a dark background. This pattern is also seen in *D. similans*, *D. elegans*, *D. rhopaloa*, *D. ficusphila*, *D. takahashii*, *D. biarmipes*, and *D. bipectinata*. Apparent conservation at the C-terminus of MEI-217 suggests that the coding sequences are accurately represented here. Notably, the ATG predicted to begin the MEI-218 coding sequence is absolutely conserved, even though the A could have mutated to any other base without affecting the MEI-217 sequence. These findings strongly support the conclusion that MEI-217 and MEI-218 are separate polypeptides and that there has been selection to maintain this configuration. We could not detect conservation in this region in *Glossina morsitans*, so that sequence cannot be aligned to these sequences.

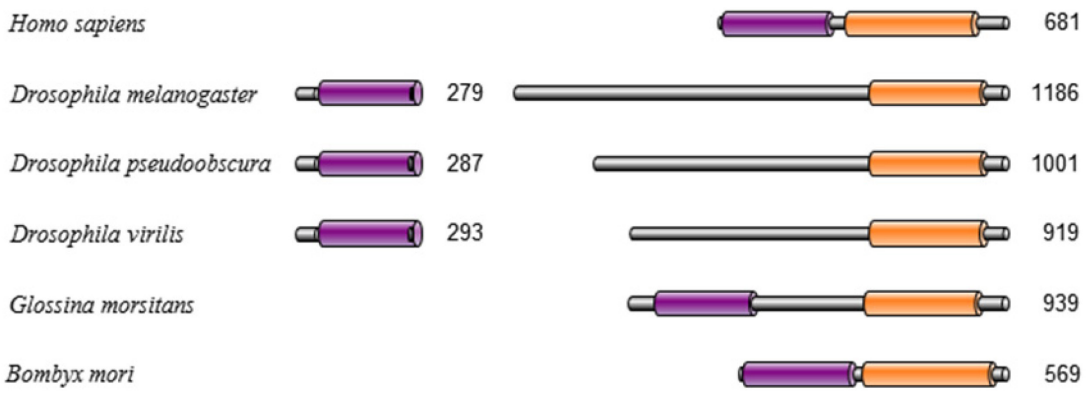

Figure 13. Structural changes in MEI-218. These schematics illustrate the structures of MEI-218 orthologs from humans and several insects. Purple cylinder represents the N-terminal MCM domain, orange the C-terminal AAA ATPase-like domain. The human and *Bombyx mori* orthologs are similar in structure (as are other vertebrates and arthropods other than *Drosophila* and *Glossina*) to canonical MCMs, whereas *Drosophila* and *Glossina* are substantially longer. In *Drosophila* the two domains are found on separate polypeptides.

Materials and Methods

Drosophila stocks and genetics

Flies were maintained on standard medium at 25˚C. All experimental flies were heteroallelic for null mutations that have been described previously: rec^{1} and rec^{2} (Blanton et al., 2005); $mus309^{N1}$ and $mus309^{D2}$ (Boyd et al., 1981; McVey et al., 2007); $mei\text{-}218^{1}$ and $mei\text{-}218^{6}$ (Baker and Carpenter, 1972; McKim et al., 1996). *mus309* mutant females produce few viable progeny due to a requirement for DmBLM in the early embryo (McVey et al., 2007). To overcome this maternal-effect lethality, the *mus309* coding sequence was cloned into the *P{UASp}* (Rørth, 1998) vector, creating *P{UASp-mus309}*. This transgene was injected using standard P-element transformation procedures (Best Gene Inc., Chino Hills, CA). $mus309^{N1}$ *P{UASp-mus309}* / $mus309^{D2}$ *P{matα4-GAL4::VP16}* females express DmBLM during later stages of oocyte development, after meiotic recombination has taken place, thereby creating a *mus309*

meiotic null. This genotype was used in all assays with *mus309* mutants. Nondisjunction was scored by crossing mutant females to *y cv v f / T(1:Y)B*^{S} males. The number of exceptional progeny indicative of nondisjunction (Bar-eyed females and wild-type-eyed males) was multiplied by two to account for triplo-*X* and nullo-*X* progeny, which do not survive to adulthood. This number was divided by the total number of progeny and expressed as a percentage. Crossovers were scored by crossing *net dpp*$^{d\text{-}ho}$ *dp b pr cn* /+ virgin females of various genetic backgrounds to *net dpp*$^{d\text{-}ho}$ *dp b pr cn* males.

Identification of orthologs

Orthologs were found through searches of public databases. The amino acid sequence of the human protein was used in BLASTP searches of refseq_protein at NCBI (http://blast.ncbi.nlm.nih.gov/Blast.cgi), using the default parameters. In cases where orthologs were not immediately identified, searches were repeated using sequence from a more closely related species and searching the nr database. If this was unsuccessful, TBLASTN was done using the nr database. Finally, species-specific databases were searched, either from the NCBI genomic BLAST page (http://www.ncbi.nlm.nih.gov/mapview/) or from species-specific websites. Additionally, a sequence for *rec* from *D. pseudoobscura* was obtained from (McGaugh and Noor, 2012).

Drosophila melanogaster mei-217 and *mei-218* are well-annotated based on experimental data (cDNA sequences and RNA-seq data), but annotations for other species have less support. To generate better predictions of the amino acid sequences of MEI-217 and MEI-218 in other species, we used *D. melanogaster* sequences in

TBLASTN searches. Apparent conservation of MEI-217 allowed high-confidence CDS (coding sequence) predictions, but divergence of MEI-218 made predictions for this gene less reliable.

Sequence alignments and phylogenetic analysis

Protein sequences were aligned in MEGA5 (Tamura et al., 2011) using the MUSCLE algorithm (Edgar, 2004). Maximum-likelihood trees were generated in MEGA5 using the method based on the Whelan and Goldman model (Whelan and Goldman, 2001). Initial trees for the heuristic search were obtained automatically. When the number of common sites was <100 or less than one fourth of the total number of sites, the maximum parsimony method was used; otherwise BIONJ method with MCL distance matrix was used. A discrete Gamma distribution was used to model evolutionary rate differences among sites (5 categories (+G, parameter = 2.8099)). The rate variation model allowed for some sites to be evolutionarily invariable ([+I], 0.0000% sites).

Molecular evolutionary analysis

We compared a suite of molecular evolutionary models of the evolution of *rec* using PAML, which provides a set of maximum likelihood-based tools for combining DNA sequence and phylogenetic data to test molecular evolutionary hypotheses (Yang, 2007). We used a phylogeny based on DNA polymerase alpha catalytic subunit and published trees of insects to identify good outgroups (Grimaldi and Engel, 2005). We limited our analysis of *rec* to the region 3' of position 135 (Figure 6) as this section was clearly homologous across taxa. There are three major steps to using PAML: (i) choice

of appropriate model, (ii) parameterization of that model, and (iii) sequential comparison using log-likelihood ratio tests of simpler to more complex models to evaluate whether a more complex model provides a significantly better fit to the data. In several cases, convergence to maximum likelihood estimates was verified by changing the "small difference" parameter see (Grimaldi and Engel, 2005), p. 19. Evolution of protein-coding regions of *rec* was analyzed independently using the codon model CODEML (Goldman and Yang, 1994; Yang, 1997). The difference in the log likelihood (Δlnl), for the relevant degrees of freedom, was used to infer a *P*-value. Unless noted otherwise, model comparisons involving multiple tests remained significant after Bonferroni corrections. The estimated codon table fit the *rec* data the best. When appropriate, κ, ω, and α fit the data had the best log-likelihood when estimated (Yang, 1997). For the analyses discussed, we *a priori* hypothesized that the lineage prior to the split of *Glossina* from *Drosophila rec* underwent more rapid protein coding evolution because *rec* was under strong selective pressure to functionally compensate for the loss of the Msh4–Msh5. As shown in Table 2-5, we tested a variety of simple and complex models motivated by our understanding of the evolutionary history of flies. Model 1 is the most conservative as it assumes a single evolutionary rate for all branches. Models 2 and 3 are controls that test the hypothesis that *rec* is "special" in *D. melanogaster* (Model 2) and that the patterns observed are specific to higher flies, not just any clade of the tree (Model 3). As expected neither of these models is different from Model 1. The remaining models grow increasingly complex as they step through a variety of evolutionary scenarios (*e.g.*, *Drosophila* differ from others; Sophophora, which have reported evidence of male recombination in *D. willistoni* and *D. ananassae*, differ; Old World Sophophora differ,

etc.). All fit the data better than Models 1-3 and generally improve the fit as their complexity grows. However, Model 15, which allows for dN/dS ratio to vary freely among all branches, has the best fit to the data and is a significantly better than any alternative. This model suggests strong adaptive evolution prior to the divergence of the Schizophora and prior to the radiation of the Old World Sophophora. Simpler models (*e.g.*, 4-14) similarly support that the dN/dS rate of *rec* in higher flies is different compared to the other Dipteran and our outgroups.

Immunoprecipitation

rec was cloned into pFastBac with an N-terminal FLAG tag. *mei-217* and *mei-218* were cloned into pFastBacDual with N-terminal HA and Strep-II tags, respectively. As per the Bac-to-Bac Baculovirus System (Invitrogen, Carlsbad, CA) protocol, constructs were transformed into DH10Bac cells. Sf9 cells were transfected with bacmid DNA extracted from transformed DH10Bac cells. Following two rounds of viral amplification in Sf9 cells, High Five cells were infected with either a single virus or with both viruses. Cells were harvested 2.5 days after infection and were stored at -80˚C until needed. Pellets were resuspended in lysis buffer (50mM Tris-HCl pH 7.5, 150mM NaCl, 1mM EDTA, 1% Triton X-100), sonicated using a Bioruptor (Diagenode, Denville, NJ) on highest setting with 30s on/30s off cycles for 20min at 4˚C. Cell suspension was pelleted with centrifugation at 14k rpm for 5min. Clarified supernatant containing ^{FLAG}REC and ^{HA}MEI-217 was added to either anti-HA agarose (Sigma, St. Louis, MO) or anti-FLAG M2 agarose (Sigma) for 2h. Strep-MEI-218 was co-expressed with these two proteins but was insoluble and therefore not in the clarified lysate from which

immunoprecipitation was carried out. Beads were washed in a cellulose acetate filter spin column (Pierce, Rockford, IL) with either TBS (FLAG purification) or PBS (HA purification) prior to boiling in SDS-PAGE sample buffer. Samples were run on a 4-15% SDS-PAGE gel, transferred to PVDF membrane, and probed with appropriate antibodies: anti-HA (Sigma) 1:20,000; anti-REC-C (raised to amino acids 875-885; Pacific Immunology, San Diego, CA) 1:20,000; HRP-conjugated anti-rabbit secondary (Santa Cruz Biotechnology, Santa Cruz, CA) 1:20,000. SuperSignal West Pico Chemiluminescent Substrate (Pierce) was used to detect proteins.

Yeast two-hybrid assay

mei-217 was cloned into pGBD-DEST, a Gateway-compatible derivative of pGBD-C1 (James et al., 1996) constructed with the Gateway Vector Conversion System (Life Technologies, Carlsbad, CA). Full-length or truncated *mei-218* was cloned into pACT2.2gtwy (Addgene plasmid 11346 deposited by Guy Caldwell), a Gateway-compatible derivative of pACT2.2. Constructs were transformed into *Saccharomyces cerevisiae* strain PJ69-4A (James et al., 1996). Co-transformants were selected on plates of SD minimal medium containing dropout supplements lacking leucine (-leu) and tryptophan (-trp) for 3 days at 30˚C. Single colonies were streaked onto fresh –trp –leu plates and grown for 3 days at 30˚. Colonies were then streaked onto –trp –leu –histidine plates containing 3mM 3AT. Interaction between proteins was scored 3 days later.

CHAPTER 3

MEI-MCMS AFFECT MEIOTIC CROSSOVER DISTRIBUTION

Introduction

Meiotic recombination initiates via a programmed double-strand break (DSB) created by the archaeal topoisomerase VI-like protein Spo11 in all organisms thus far examined (Keeney et al., 1997). This step appears to be a hallmark of meiosis, and as such, the presence of a Spo11 homolog within a genome is used as part of a "meiosis detection toolkit" to identify organisms that undergo meiosis (Malik et al., 2008). Not all breaks are created equal, however, as some DSBs are repaired into crossovers (COs), while others will form non-crossovers (NCOs) instead.

It is currently unknown how a given DSB is chosen to be repaired as either a CO or a NCO. However, it is believed that this decision is made prior to the formation of the first stable strand exchange intermediates (Bishop and Zickler, 2004). In a phenomenon called CO homeostasis, COs are formed at the expense of NCOs so that the organismal-appropriate number of COs can be formed even if fewer DSBs are made than normal (Martini et al., 2006). Additional levels of CO regulation appear to go into the CO/NCO decision, as COs are distributed non-randomly across the genome. Most chromosomes receive at least one CO (the obligate CO) (Jones, 1984), and these COs tend to be located in regions optimal for aiding chromosome segregation – i.e., away from the centromere

and telomeres (Hassold and Hunt, 2007). Also, when more than one CO occurs on a chromosome, they tend to be more widely-spaced than expected by random chance, a phenomenon called CO interference (Berchowitz and Copenhaver, 2010).

Interference was first described in *Drosophila melanogaster (*Sturtevant*,* 1913*)*, and has since been found to operate in many model systems including *Arabidopsis thaliana, Caenorhabditis elegans* and *Saccharomyces cerevisiae* (Copenhaver et al., 2002; Fogel and Hurst, 1967; Meneely et al. 2002). Notably, COs in the fission yeast *Schizosaccharomyces pombe* do not exhibit interference (Munz, 1994). Although it is unknown how interference works, several models hypothesize how CO interference operates. In the "polymerization model", a CO produces some signal that is perpetuated along a chromosome, thus discouraging the formation of COs nearby (King and Mortimer, 1990). The "stress relief model" invokes mechanical stress along chromosomes that is alleviated at CO sites, thus inhibiting nearby COs (Borner et al., 2004). Finally, a "counting model" suggests that an organismal-specific number of NCOs must separate COs (Foss et al., 1993).

The *Drosophila* meiotic mini-chromosome maintenance (mei-MCM) proteins are members of the "precondition class" of *Drosophila* meiotic recombination mutants (Kohl et al., 2012), so named because they appear to be unable to complete the preconditions necessary for proper CO formation (Carpenter and Sandler, 1974; Sandler et al., 1968). The abnormal CO distribution characteristic of precondition mutants suggests that the precondition proteins play a role in CO designation. In an assay scoring the selection of the pro-oocyte in the *Drosophila* germarium, the precondition genes were epistatic to genes necessary for strand invasion and exchange/CO formation (Joyce and McKim,

2009). These results led to the suggestion that the mei-MCMs have an early role in committing some DSBs to the CO pathway (Joyce and McKim, 2009). However, other epistasis experiments have placed RECOMBINATION DEFECTIVE (REC) at an intermediate step in the meiotic recombination pathway, downstream of strand invasion but upstream of exchange/CO formation (Blanton et al., 2005).

To investigate and tease apart the potential early and late roles of the mei-MCMs in CO formation, I created separation-of-function alleles of *rec*. I used a non-disjunction (NDJ) assay to test the ability of these alleles to segregate chromosomes and a CO assay to study their effect on CO number and CO distribution. I created a truncation mutant of another mei-MCM, MEI-218, to investigate the function of this protein's conserved C-terminus. Similar to the *rec* separation-of-function alleles, I assayed this "*mini-MEI*" allele for NDJ, CO number and CO distribution.

Results

REC ATPase mutants differentially affect NDJ and COs

Previous studies of AAA+ proteins have identified mutations within key residues of the Walker A and Walker B motifs that differentially affect ATP binding and hydrolysis. In particular, mutation of the conserved lysine residue in the Walker A motif prevents ATP binding, while mutation of the glutamate residue in the Walker B motif abolishes ATP hydrolysis but does not prevent ATP binding (Hanson and Whiteheart, 2005). As a member of the MCM family, REC has conserved Walker A and Walker B motifs containing these key residues (Figure 14).

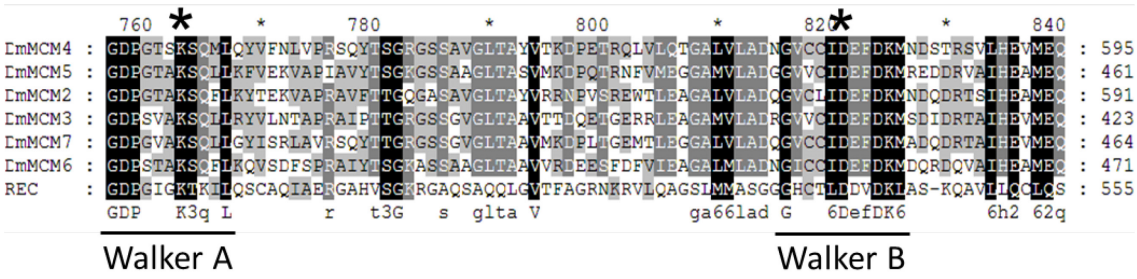

Figure 14. MCM Walker A/B alignment. Protein sequence alignment of *D. melanogaster* MCM2-MCM8 (REC). Positions that have identical or conserved residues in all proteins have a black background. Positions with identical or conserved residues in six of the seven proteins have a dark gray background. Positions with identical or conserved residues in four or five of the seven proteins have a light gray background. Walker A and Walker B motifs are indicated. Asterisks mark residues mutated in *{UAS-rec*}* transgenes.

Previous research has shown that mutation of the conserved lysine in the Walker A motif of a replicative MCM protein does not prevent the MCM2-7 complex from loading onto DNA (Ying and Gautier, 2005). This Walker A mutant complex was unable to unwind DNA, however. In other words, the early role of MCM2-7 in the pre-replicative (pre-RC) complex was separable from MCM2-7's later role during DNA replication via one mutation within one replicative MCM's Walker A motif. Similarly, I hypothesized that by creating Walker A and Walker B mutant versions of REC, I would be able to create alleles of *rec* that separated the protein's early role in CO designation from its later role in CO formation. To this end, I created three *{UASp-rec*}* transgenic fly lines – one wild-type copy of *rec,* one Walker A mutant (K479A), and one Walker B mutant (D537A) (Figure 14). Each transgene was inserted into the same genomic location (*99F*) to control for position effects, was placed into an endogenous *rec* null mutant background, and was expressed using either the *nanos-GAL4* or *tubulin-GAL4* driver. The *nanos-GAL4* driver expresses in the germarium (Rørth, 1998), where meiotic recombination takes place, while the *tubulin-GAL4* driver has ubiquitous expression (Lee

and Luo, 1999). Since meiotic COs are important for the proper segregation of homologous chromosomes, transgenes were scored for NDJ as a readout of CO formation (Figure 15).

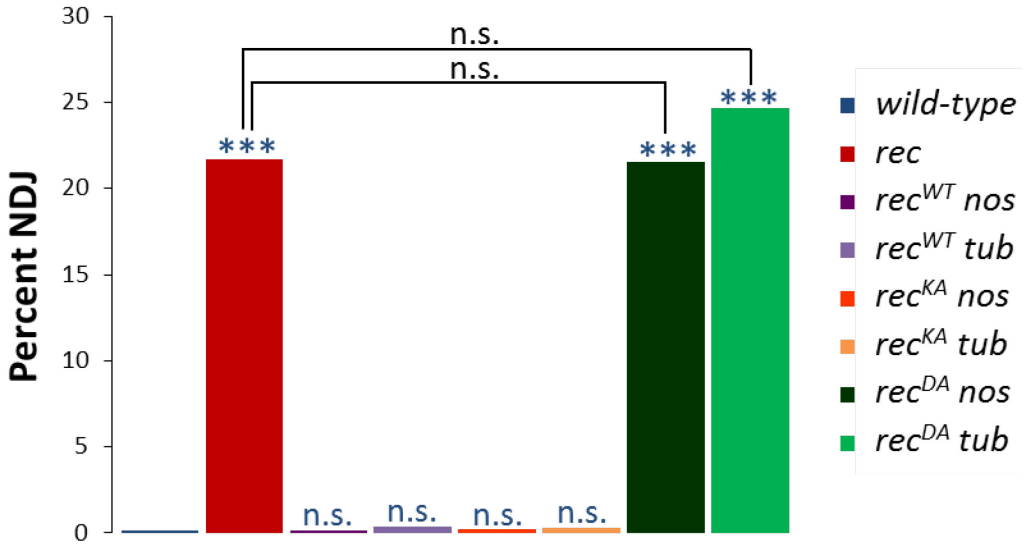

Figure 15. *rec* transgene non-disjunction. Percent non-disjunction (NDJ) was scored in the indicated genotypes. "*KA*" and "*DA*" superscripts denote the Walker A and Walker B mutant alleles of *rec,* respectively, while "WT" superscript denotes the wild-type *rec* gene. "*nos*" and "*tub*" indicate the *rec* transgene was under expression of the *nanos-GAL4* or *tubulin-GAL4* driver, respectively. Over 1000 individuals were scored for each genotype. ***p<0.0001, as compared to *wild-type*. n.s., not statistically significant compared to either *wild-type* (blue lettering) or compared between paired genotypes.

The *{UASp-rec^{WT}}* transgene rescued the high NDJ seen in *rec* mutants when driven by either *GAL4* driver. Therefore, the transgenes are able to be expressed in the *99F* genomic location using either driver. The *{UASp-rec^{KA}}* transgenic (Walker A mutant) also completely rescued the high NDJ characteristic of *rec* mutants, indicating that abolishing REC's ability to bind ATP does not prevent proper meiotic chromosome segregation. Interestingly, the *{UASp-rec^{DA}}* transgenic (Walker B mutant) had NDJ levels similar to *rec* mutants and statistically significantly different (p<0.0001) from

wild-type. This result suggests that allowing REC to bind, but not hydrolyze, ATP prevents proper meiotic chromosome segregation.

To determine if the effects on NDJ paralleled effects on meiotic CO formation, I measured the formation of COs across *2L* (Figure 16). Similar to the results seen in the NDJ assay, the *{UASp-rec^{WT}}* and *{UASp-rec^{KA}}* transgenics had CO distributions very similar to wild-type. At first glance, the *rec* mutant and Walker B mutant CO distributions appeared similar, as both mutants have very low levels of COs. However, as a precondition mutant, *rec* mutants have a polar reduction in crossing over, with a stronger reduction in COs in the center of the chromosome arm as compared to the region closest to the centromere. This phenotype can be easily seen by calculating the ratio between the reduction in crossing-over in the centromere-proximal region to the entire chromosome arm (Blanton et al., 2005). Precondition mutants have a ratio greater than one, whereas wild-type and exchange mutants have a ratio of approximately one. Therefore, to further characterize the CO distribution in our transgenics, I calculated this ratio (Table 4). Notably, while the *rec* mutant value is greater than one (6.6), the Walker B mutant value (2.4) is much closer to one. Although using the strict definition of precondition versus exchange mutants would place the Walker B mutant into the precondition class as its ratio is greater than one, the striking difference in values between the *rec* mutant and the Walker B mutant suggests that the random distribution of residual COs seen in precondition mutants is lost in the *{UASp-rec^{DA}}* transgenic. The actual number of COs observed in the centromere-proximal *pr-cn* interval in *rec* mutants (25 out of 2036 flies scored) compared to those observed in the Walker B mutant (5 out of

2324 flies scored) is statistically significant ($p<0.0001$), further supporting the idea that the Walker B mutant does not have a precondition CO distribution.

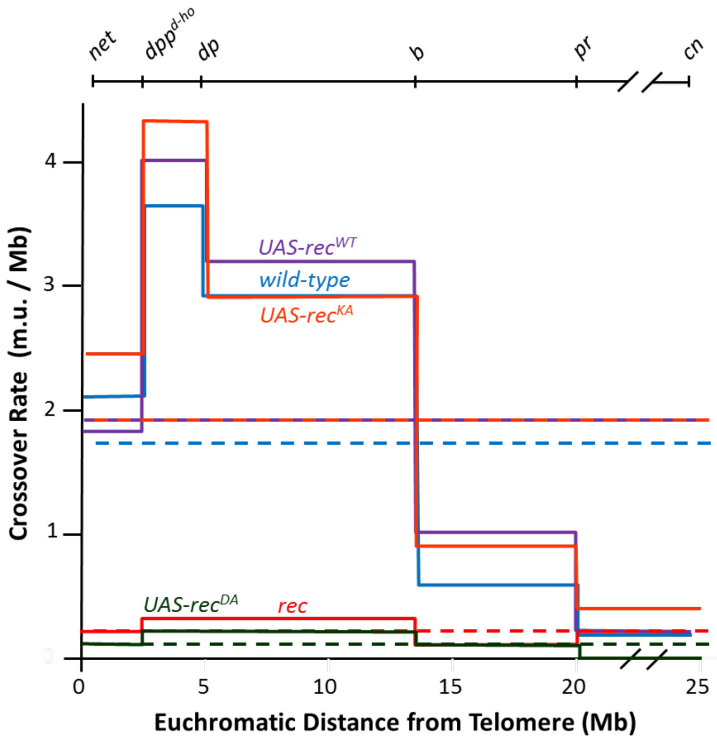

Figure 16. ***rec*** **transgene crossover distribution.** Crossover (CO) distribution across five intervals on chromosome *2L* and proximal *2R* is shown. The markers used in mapping are shown above the graph. Hash marks between *pr* and *cn* indicate the position of the centromere. Solid lines depict the number of map units (m.u.) per megabase pair (Mb) in each interval for more than 2000 individuals for each genotype. Dashed lines indicate the mean CO rate across the entire region. *{UASp-rec*}* transgenes were driven using the *nanos-GAL4* driver.

	net-dpp $^{d\text{-}ho}$	***dpp*** $^{d\text{-}ho}$ ***-dp***	***dp-b***	***b-pr***	***pr-cn***	**total *net-cn***	**ratio *pr-cn* / total***
wild-type	5.09	7.54	27.33	3.49	1.51	44.96	1.0
rec	0.49 (9.6)	0.69 (9.2)	2.5 (9.1)	0.64 (18.3)	1.23 (81.5)	5.55 (12.3)	6.6
UAS-REC ^{WT}	4.40 (86.4)	8.39 (111.2)	29.71 (108.7)	6.00 (171.9)	1.34 (88.7)	49.84 (110.9)	0.8
UAS-REC ^{KA}	5.70 (112.0)	8.99 (119.2)	26.92 (98.5)	5.87 (168.2)	2.32 (153.6)	49.80 (110.8)	1.4
UAS-REC ^{DA}	0.34 (6.7)	0.34 (4.5)	1.42 (5.2)	0.47 (13.5)	0.22 (14.6)	2.80 (6.2)	2.4

Table 4. ***rec*** **transgene recombination frequency.** Recombination frequency is expressed as map units across the intervals shown. Numbers in parentheses denote the percentage of wild-type recombination frequency. *The ratio of the percentage of wild-type recombination frequency across the centromere-proximal interval (*pr-cn*) compared to the percentage of wild-type frequency across the entire chromosome arm.

As expected based on their CO distribution pattern, the wild-type *rec* and Walker A mutant *rec* transgenics had ratios close to one, signifying that the change in CO frequency in the centromere-proximal region was similar to the change across the chromosome arm (Table 4). Interestingly, however, it appeared that most of these intervals had increased recombination frequencies in the Walker A mutant compared to wild-type, even though the CO distribution appeared normal. To investigate this possibility further, I calculated the number of multiple COs observed in these mutants (Table 5). I found that the *{UASp-rec^{WT}}* transgene did not have a significantly different number of single (SCO), double (DCO), or triple (TCO) COs as compared to the wild-type control. In contrast, the *{UASp-rec^{KA}}* transgene had significantly more DCOs than wild-type. The *{UASp-rec^{KA}}* transgene also had significantly more DCOs than the *{UASp-rec^{WT}}* transgene (p=0.0135). Therefore, the difference in COs between the Walker A transgene and wild-type flies is not a consequence of *rec* being expressed off a transgene and instead is a result of the point mutation within the Walker A motif.

	N	SCO	DCO	TCO
wild-type	2320	952	44	1
rec	2036	113^{*}	0^{*}	0^{NS}
UAS-REC^{WT}	3134	1399^{NS}	80^{NS}	1^{NS}
UAS-REC^{KA}	2281	949^{NS}	$86^{\#}$	5^{NS}
UAS-REC^{DA}	2324	65^{*}	0^{*}	0^{NS}

Table 5. *rec* transgene crossover number. Number of single crossover (SCO), double crossover (DCO), and triple crossover (TCO) progeny observed in each genotype out of the total number of progeny (N) scored. *{UASp-rec*}* transgenes were driven using the *nanos-GAL4* driver. $^{\#}$p=0.0002, as compared to *wild-type.* *p<0.0001, as compared to *wild-type*. ^{NS}not statistically significant, as compared to *wild-type.*

Hyperrecombination in a MEI-218 truncation mutant

While the C-terminus of MEI-218 contains a relatively well-conserved AAA ATPase domain, the protein's N-terminus is disordered and much more divergent (Kohl et al., 2012). In particular, the N-terminus is of variable lengths in the various Drosophilids for which genome sequence is available (Kohl et al., 2012), and this region can only be poorly aligned even in closely related Drosophilids (Figure 17). Furthermore, it is through the conserved C-terminus, not the N-terminus, that MEI-218 interacts with MEI-217 (Kohl et al., 2012). To investigate whether this divergent N-terminal sequence was necessary for MEI-218's meiotic function, I created a *{UASp}* transgenic truncation mutant of MEI-218 that eliminates the first 526 amino acids (44%) of the protein, called the "*mini-MEI*" allele (Figure 17). This allele was placed into a *mei-218* null mutant background, and was driven using the same *nanos-GAL4* driver as the *rec* transgenics.

I first assayed NDJ in the *mini-MEI* allele as a readout of CO formation (Figure 18). While *mei-218* mutants have high NDJ, the *mini-MEI* allele rescued this high NDJ to near wild-type levels. There was, however, a slight but statistically significant ($p=0.0202$) increase in NDJ in the *mini-MEI* allele as compared to wild-type. These results suggest that the N-terminus of MEI-218 is mostly dispensable for the protein's role in meiosis, although the slight defect in meiotic chromosome segregation suggests that the N-terminus may play a small part in meiosis. To determine if this role is related to CO formation, I next scored CO distribution across *2L* in the *mini-MEI* allele (Figure 19). The *mini-MEI* CO distribution appeared wild-type, although several of the intervals had an increased CO rate. I investigated whether this increased CO rate was due to an

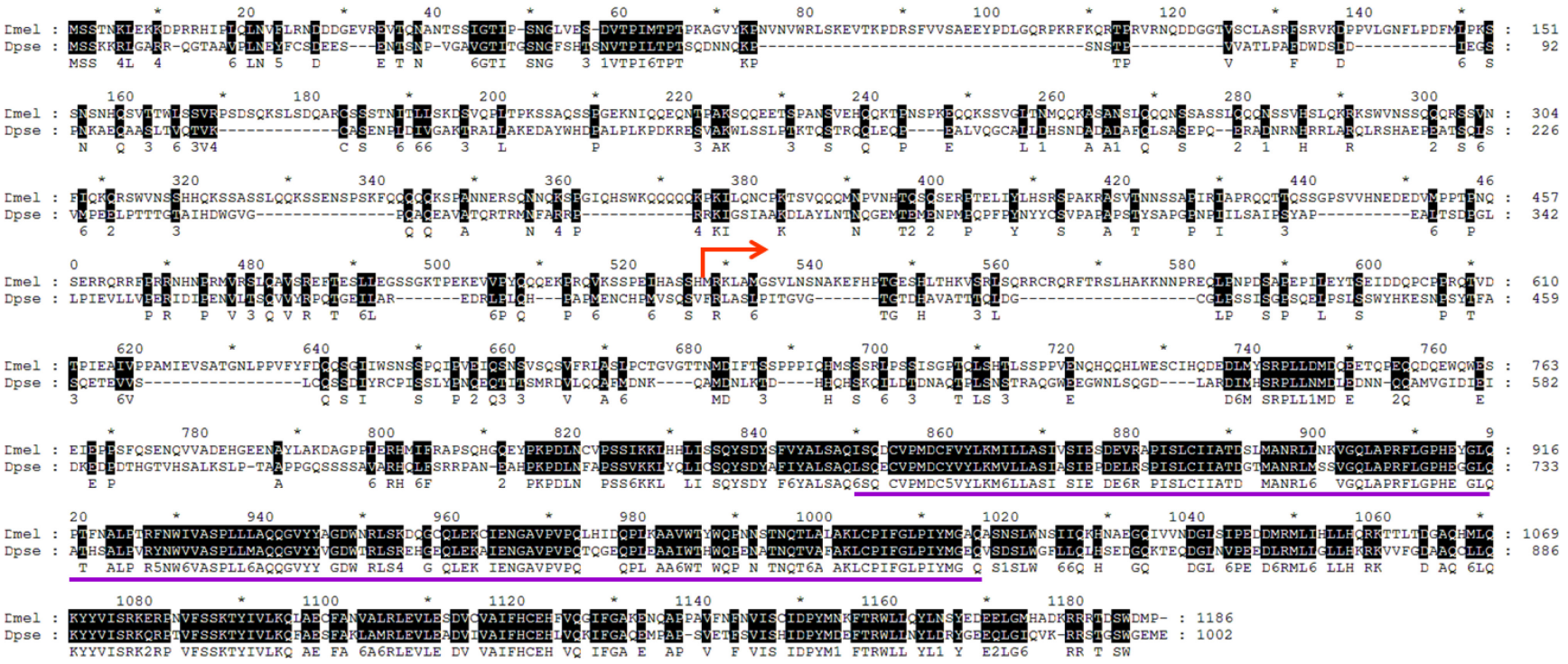

Figure 17. MEI-218 protein alignment. *D. melanogaster* and *D. pseudoobscura* MEI-218 protein sequence alignment. Positions that have identical or conserved residues in both proteins have a black background. Orange arrowhead marks start of "mini-MEI" protein. *D. melanogaster* MEI-218 AAA ATPase domain is indicated with a purple underline.

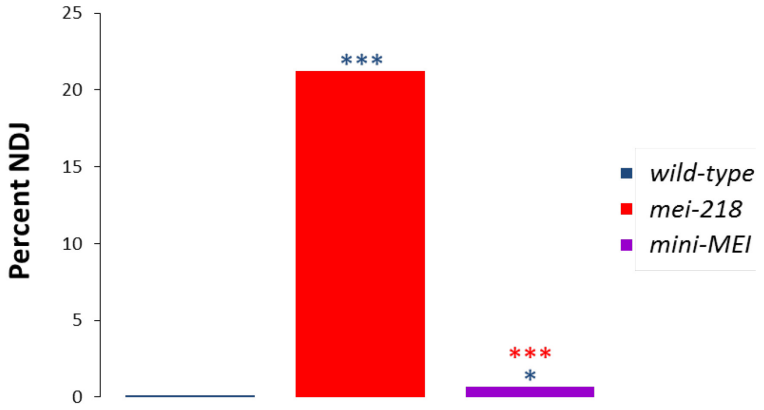

Figure 18. *mini-MEI* transgene non-disjunction. Percent non-disjunction (NDJ) was scored in the indicated genotypes. Over 1200 individuals were scored for each genotype. Color of asterisks indicates genotypes statistically compared. ***p<0.0001, *p=0.0202.

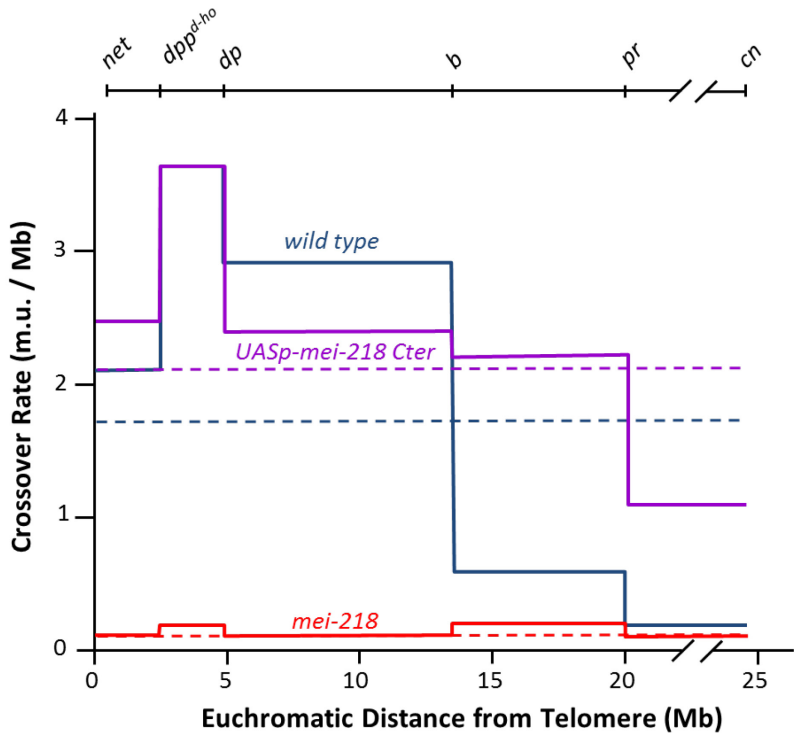

Figure 19. *mini-MEI* transgene crossover distribution. Crossover (CO) distribution across five intervals on chromosome *2L* and proximal *2R* is shown. The markers used in mapping are shown above the graph. Hash marks between *pr* and *cn* indicate the position of the centromere. Solid lines depict the number of map units (m.u.) per megabase pair (Mb) in each interval for more than 1700 individuals for each genotype.

increase in SCOs, multiple COs, or both (Table 6). I found that the number of SCOs in the *mini-MEI* allele was not statistically different from wild-type, but that this allele did have a highly significant increase in DCOs compared to wild-type. To determine if the increased CO rate was obscuring an altered CO distribution, I calculated the ratio of crossing-over in the centromere-proximal region to crossing-over across the entire chromosome arm (Table 7). Interestingly, the *mini-MEI* allele showed a ratio greater than one (3.8). Using the definition of precondition proteins of Blanton *et al*. (Blanton et al., 2005), this results suggests that like the *mei-218* null, the *mini-MEI* allele exhibited a precondition distribution of COs. However, the title "precondition mutant" has historically described flies which have a reduction in COs (Carpenter and Sandler, 1974; Sandler et al., 1968), which is clearly not the case for the *mini-MEI* allele.

	N	SCO	DCO	TCO
wild-type	2320	952	44	1
mei-218	1744	51^{*}	0^{*}	0^{NS}
mini-MEI	1819	731^{NS}	142^{*}	4^{NS}

Table 6. *mini-MEI* transgene crossover number. Number of single crossover (SCO), double crossover (DCO), and triple crossover (TCO) progeny observed in each genotype out of the total number of progeny (N) scored. $^{*}p<0.0001$, as compared to *wild-type*. ^{NS}not statistically significant, as compared to *wild-type.*

	net-dpp $^{d\text{-}ho}$	*dpp* $^{d\text{-}ho}$ *-dp*	*dp-b*	*b-pr*	*pr-cn*	total *net-cn*	ratio *pr-cn* / total*
wild-type	5.09	7.54	27.33	3.49	1.51	44.96	1.0
mei-218	0.23 (4.5)	0.34 (4.5)	0.92 (3.4)	1.03 (29.5)	0.4 (26.5)	2.92 (6.5)	4.1
mini-MEI	5.94 (117)	7.64 (101)	21.99 (80.5)	13.63 (391)	7.26 (480)	56.46 (126)	3.8

Table 7. *mini-MEI* transgene recombination frequency. Recombination frequency is expressed as map units across the intervals shown. Numbers in parentheses denote the percentage of wild-type recombination frequency. *The ratio of the percentage of wild-type recombination frequency across the centromere-proximal interval (*pr-cn*) compared to the percentage of wild-type frequency across the entire chromosome arm.

Discussion

The results from the Walker A and Walker B mutant *rec* alleles (Table 8) are best analyzed in light of other MCM ATPase mutant analyses conducted previously. Firstly, the oligomeric nature of MCM proteins is crucial to the complex's ability to hydrolyze ATP since the active sites are formed *in trans* using the Walker A and Walker B motifs of one subunit and the conserved arginine finger from a neighboring subunit (Davey et al., 2003). Of the several models for AAA+ protein ATP hydrolysis ("probabilistic" (Martin et al., 2005), "sequential" (Stitt and Xu, 1998), and "concerted" (Gai et al., 2004)), only one has been suggested for an MCM protein. A study of the archaeal *Sulfolobus solfataricus* MCM complex found that helicase activity was maintained even when multiple ATP binding sites were inactive, suggesting that MCM ATP hydrolysis is "probabilistic" (Moreau et al., 2007). Unlike archaeal MCM complexes, which are most often homomultimers, the replicative MCM2-7 complex is comprised of six non-redundant subunits. It has been shown that the ATP active sites in the MCM2-7 complex are functionally distinct and that mutations within the different subunits' Walker A and Walker B motifs have varying effects on viability and ATPase activity (Bochman et al., 2008; Gomez et al., 2002).

Despite being unable to bind ATP, the Walker A *rec* mutant was not inhibited in physically forming COs nor in localizing them properly (Figure 20). Thus, this result suggests that REC functions as part of a larger complex such that another active site was able to rescue the mutation of REC's active site. While we have previously shown that REC is a component of the mei-MCM complex along with MEI-217 and MEI-218 (Kohl et al., 2012), this data suggests at least one additional MCM protein is part of the

	NDJ	CO number	CO distribution
rec* or *mei-218	↑	↓	precondition
UAS-REC^{WT}	–	–	normal
UAS-REC^{KA}	–	↑	normal
UAS-REC^{DA}	↑	↓	~normal
mini-MEI	–	↑	precondition

Table 8. *mei-MCM* transgene phenotypes. Phenotypes for the various *mei-MCM* transgenes and *mei-MCM* (*rec* and *mei*-218) null mutants are summarized. For non-disjunction (NDJ) and crossover (CO) number, "↑" indicates increased levels as compared to wild-type, "↓" indicates decreased levels as compared to wild-type, and "–" indicates a level comparable to wild-type. For CO distribution, "precondition" denotes a precondition mutant distribution of COs, whereas "normal" denotes a wild-type distribution of COs and "~normal" denotes an approximately wild-type distribution of COs.

complex, since MEI-217 and MEI-218 lack a Walker A motif and therefore would have been unable to provide this compensation (Kohl et al., 2012). A separation-of-function allele in *Mcm5* shares the same meiotic phenotypes of the mei-MCMs (Lake et al., 2007), suggesting MCM5 is an additional member of the complex. It is unknown whether additional replicative MCMs are components of the mei-MCM complex, since four of the six *DmMCM2-7* have been genetically characterized, and null mutations in each are pupal lethal (Feger et al., 1995; Lake et al., 2007; Schwed et al., 2002; Treisman et al., 1995). It is likely that all MCM2-7 are essential for viability in *Drosophila,* as they are in yeast (Tye, 1999), and thus without separation-of-functional alleles, like the *Mcm5^{A7}* allele, we cannot ascertain the proteins' roles in meiosis.

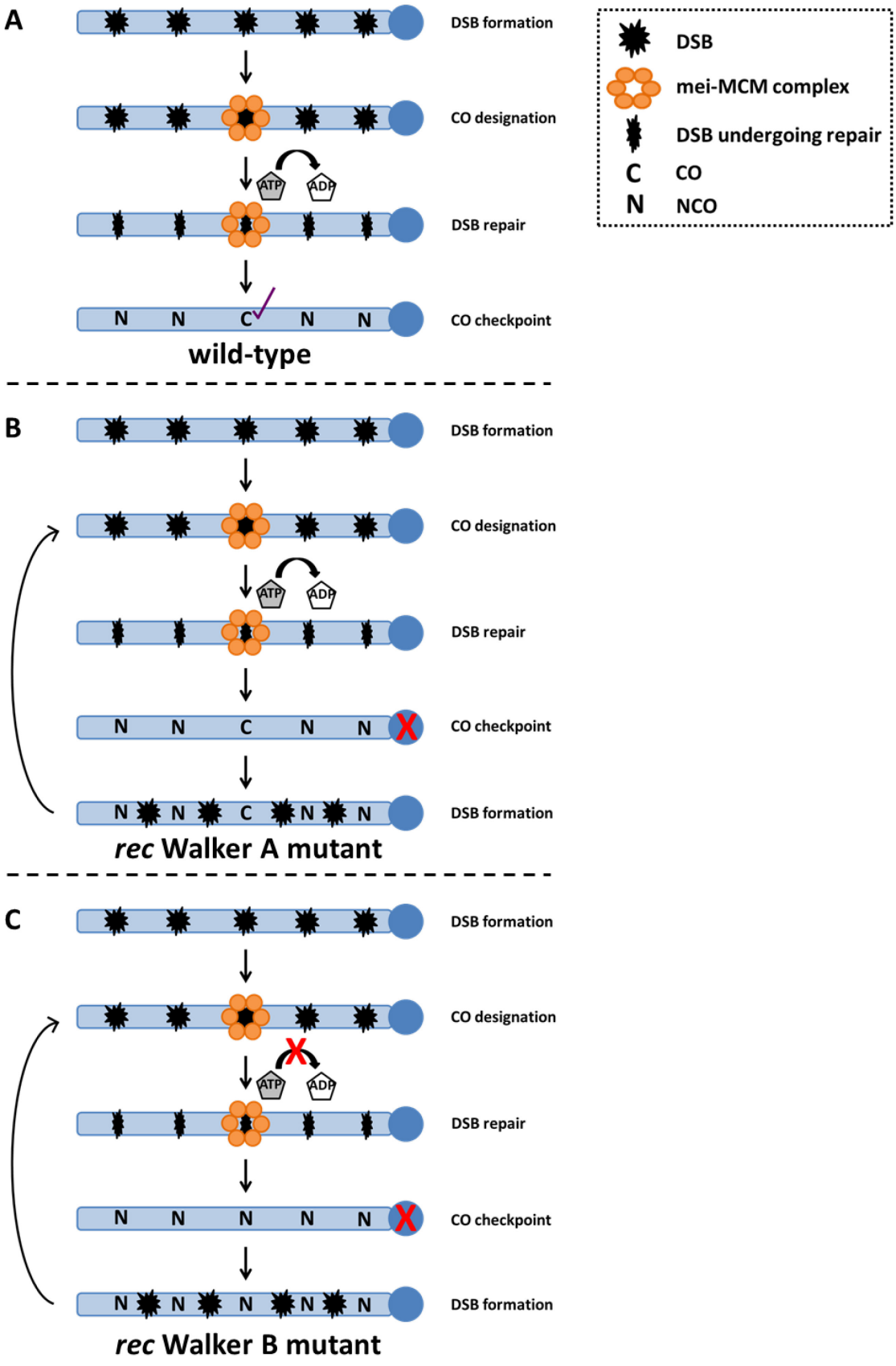
A
DSB formation
CO designation
ATP
ADP
DSB repair
N N C N N
CO checkpoint
wild-type
B
DSB formation
CO designation
ATP
ADP
DSB repair
N N C N N
CO checkpoint
N N C N N
DSB formation
rec Walker A mutant
C
DSB formation
CO designation
ATP
ADP
DSB repair
N N N N N
CO checkpoint
N N N N N
DSB formation
rec Walker B mutant
DSB
mei-MCM complex
DSB undergoing repair
C CO
N NCO

Figure 20. *rec* ATPase mutant model. (A) In wild-type, double-strand breaks (DSBs) are formed across a chromosome. The mei-MCM complex is recruited to a DSB site, thereby designating that DSB as a future crossover (CO) in an ATP hydrolysis-independent reaction. The chosen DSB occupies a central location on the chromosome arm. During DSB repair, the mei-MCM complex hydrolyzes ATP to facilitate CO formation. Once all DSBs are repaired, a CO checkpoint verifies that at least one CO was formed per chromosome. (B) In the *rec* Walker A mutant background, DSB formation, CO designation and DSB repair occur as in wild-type, resulting in CO formation. The CO checkpoint does not recognize the CO, however, triggering the formation of additional DSBs. (C) In the *rec* Walker B mutant, DSB formation and CO designation occur as in wild-type. The mei-MCM complex is unable to hydrolyze ATP during DSB repair, however, preventing CO formation. The CO checkpoint senses the lack of COs and triggers the formation of additional DSBs. This model depicts one potential explanation for the phenotypes observed, although other scenarios are possible (see Discussion). Relative timing of these events may also vary.

Furthermore, the "hyperrecombination" phenotype seen in the *rec* Walker A mutant suggests that when REC is unable to bind ATP, a CO regulation mechanism is disrupted such that more DCOs are made than normal. This could arise if increased DSBs were formed in this mutant, such that more NCOs and COs were produced than normal. This defect could arise early, such that the increased DSBs are formed with normal timing. Alternatively, a feedback mechanism that senses a CO-competent intermediate may be disrupted – either because the Walker A mutant creates these intermediates but they are unrecognized by the machinery or because the mutant cannot create these intermediates – and thus signals that more DSBs are necessary (Figure 20). Perhaps a CO-designation mechanism could be disrupted, such that more DSBs than normal are being "marked" as sites of future COs, thus reducing the number of NCOs formed while the number of DSBs are maintained at wild-type levels. Additionally, with the increase in DCOs, it will be necessary to determine whether interference is operating normally. It may be that the additional COs are formed via an alternative pathway, such as the non-interfering CO pathway that normally only produces a subset of *Drosophila* meiotic COs.

By using the *rec* Walker B mutant, I was able to uncouple the early and late roles for REC in meiotic recombination. Standard null alleles of *rec* result in ~95% reduction in COs and an abnormal, precondition distribution of residual COs (Blanton et al., 2005). This suggests that REC is required to make a majority of meiotic COs and that REC has a role in CO distribution. In a NDJ assay, the Walker B *rec* mutant also behaves like these null alleles of *rec* – both exhibit very high NDJ. Interestingly, while this phenotype appears to result from a strong reduction in crossing over in both cases, the Walker B mutant has a different effect on CO distribution than other *rec* null alleles. *rec* mutants show a polar reduction in crossing over but the Walker B mutant did not have this precondition distribution. This suggests that when REC was prevented from hydrolyzing bound ATP because of a mutated Walker B motif, REC was able to localize to sites of future COs properly but was unable to complete some function – one that presumably requires ATP hydrolysis – to physically form COs (Figure 20). This hypothesis that the mei-MCMs function as a pre-CO complex to mark sites of future COs is reminiscent of the pre-RC role of the replicative MCMs.

Interestingly, the *mini-MEI* allele rescued the high NDJ of *mei-218* null mutants (Table 8), suggesting that the N-terminus of MEI-218 is not necessary for the protein's role in female meiosis. There was, however, a slight but statistically significant increase in NDJ in the *mini-MEI* allele as compared to wild-type. Perhaps this slight defect in chromosome disjunction results from the abnormal, precondition distribution of COs seen in the *mini-MEI* mutant, as it is well-known that improperly-placed COs can result in NDJ (Hassold and Hunt, 2007).

Like the *rec* Walker A mutant, the *mini-MEI* mutant had a hyperrecombination phenotype with increased DCOs as compared to wild-type. As discussed above for the *rec* Walker A mutant, this phenotype could arise from an increase in DSBs, a change in defining the sites of future COs, a change in the CO-sensing pathway, or a combination of these possibilities. It is noteworthy that I have identified mutant versions of two mei-MCM proteins that show a significant increase in the number of DCOs but retain normal meiotic chromosome disjunction. It should be noted that we have also observed the hyperrecombination phenotype previously, in the meiotic *mus309 rec* double mutants (Kohl et al., 2012). In both the *mini-MEI* and *mus309 rec* mutants, the distribution of COs did not follow a wild-type pattern, but instead showed a more even distribution across the chromosome, reminiscent of the *mus309* and *rec* single mutant distributions. The *rec* Walker A mutant, on the other hand, showed a wild-type distribution of COs. Despite these differences, the shared hyperrecombination phenotypes in these three cases suggests that the mei-MCM complex is necessary for some mechanism of CO regulation – whether this mechanism involves designating future COs, sensing COs, or interfering with neighboring COs remains to be seen.

Finally, if the N-terminus of MEI-218 is not essential for female meiosis, what then is the function of this region? Perhaps it is necessary for MEI-218's as-yet-unknown role in the testis, where the protein is expressed (Chintapalli et al., 2007). If the region were under strong selective pressure, as is often the case with *Drosophila* testes-expressed genes (Haerty et al., 2007), this could explain the highly divergent nature of the N-terminus.

Materials and Methods

Protein sequence alignments

Protein sequences were aligned using the "Complete Alignment" setting on ClustalX (Larkin et al., 2007), using all default settings. Alignments were then viewed using the GeneDoc program.

Generating mei-MCM transgenic flies

The *rec* cDNA was cloned into the p{attBUASpW} vector downstream of the UASp germline expression promoter (Rørth, 1998) using Gateway technology (Invitrogen, Carlsbad, CA). The vector also contains a *mini-white* gene and PhiC31 attB site. In addition to the wild-type (unchanged) version of *rec,* two additional vectors were created using QuikChange (Agilent Technologies, Inc., Santa Clara, CA) to insert the Walker A mutation (K479A) and Walker B mutation (D537A). Each transgene was injected using standard PhiC31 transformation procedures (Best Gene Inc., Chino Hills, CA) into the *99F8* genomic location, creating *{UASp-rec^{WT}}*, *{UASp-rec^{KA}},* and *{UASp-rec^{DA}},* respectively.

The region of the *mei-218* cDNA corresponding to amino acids 526-1186 was cloned into p{attBUASpW} using Gateway technology. This transgene was injected using standard PhiC31 transformation procedures (Best Gene Inc.) into the *2A* genomic location, creating the "*mini-MEI*" allele.

Non-disjunction assay

Flies were maintained on standard medium at 25˚C. For *{UASp-rec*}* assay, flies were heteroallelic for null mutations of *rec* (*rec*^{1} and *rec*^{2}; (Blanton et al., 2005)), in addition to carrying one copy of the transgene and one copy of the *P{GAL4::VP16-nos.UTR}CG6325*^{MVD1} driver (referred to herein as "*nanos-GAL4*") or one copy of the *P{tubP-GAL4}LL7* driver (herein referred to as "*tubulin-GAL4*"). For the *mini-MEI* assay, flies were heteroallelic for null mutations of *mei-218* (*mei-218*^{1} *and mei-218*^{6}; (Baker and Carpenter, 1972; McKim et al., 1996)), in addition to carrying one copy of the transgene and one copy of the *nanos-GAL4* driver. Non-disjunction was scored by crossing virgin mutant females to *y cv v f / T(1:Y)B*^{S} males. The number of exceptional progeny indicative of non-disjunction (Bar-eyed females and wild-type-eyed males) was multiplied by two to account for triplo-X and nullo-X progeny, which do not survive to adulthood. This number was divided by the total number of progeny (which included the additional exceptional progeny) and expressed as a percentage. P values were calculated via a Fisher's exact test using GraphPad online software (GraphPad, Inc., La Jolla, CA).

Crossover assay

Flies were maintained on standard medium at 25˚C. The same heteroallelic gene combinations were used as in the non-disjunction assay for both *rec* and *mei-218*, in addition to one copy of the transgene of interest, and one copy of the *nanos-GAL4* driver. Crossovers were scored by crossing *net dpp*$^{d\text{-}ho}$ *dp b pr cn / +* virgin females of these genetic backgrounds to *net dpp*$^{d\text{-}ho}$ *dp b pr cn* males. Recombination frequency was calculated as the total number of crossover flies divided by the total number of flies

scored. Recombination frequency was expressed in map units – 1 map unit is equal to a recombination frequency of 1%. P values were calculated via a Fisher's exact test using GraphPad online software (GraphPad, Inc., La Jolla, CA).

CHAPTER 4

ADDITIONAL GENETIC AND MOLECULAR INVESTIGATIONS OF *rec*[2]

Introduction

Meiotic recombination initiates with a programmed double-strand break (DSB), and this break can be repaired into either a crossover (CO) or a non-crossover (NCO). In the current model for the repair of this DSB (Figure 21), COs arise through resolution of a double-Holliday junction (dHJ) intermediate (Szostak et al., 1983), while NCOs are hypothesized to arise through synthesis-dependent strand annealing (SDSA) (Allers and Lichten, 2001) or through either resolution (Szostak et al., 1983) or dissolution (Wu and Hickson, 2003) of a dHJ intermediate. Although the creation of heteroduplex DNA (hDNA), DNA in which each strand of the duplex is derived from a different parental chromosome, is a central aspect of these models, the models differ in the placement of hDNA. hDNA is typically repaired by the mismatch repair (MMR) system, potentially resulting in gene conversion (GC). If the heterologies within hDNA fail to be repaired, post-meiotic segregation (PMS) may occur, where the parental alleles segregate from each other during the first post-meiotic division (Borts et al., 2000).

[2] Susan McMahan Cheek helped conduct the *Msh6 rec* gene conversion assay. She assisted with the experiment's virgin collection, fly crossing, purine selection and scoring.

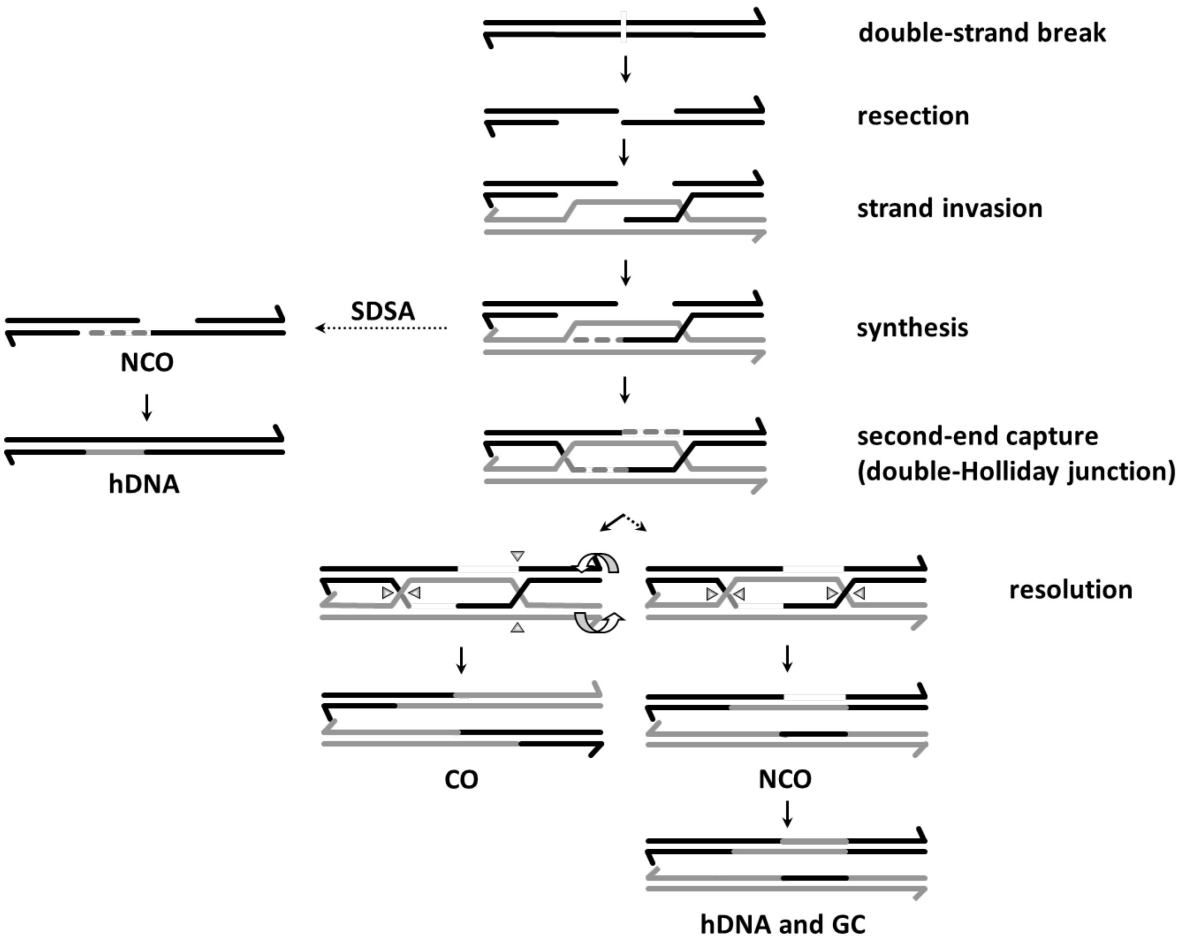

Figure 21. Double-strand break repair model. Model for the repair of the programmed double-strand break (DSB) that initiates meiotic recombination. In this model, resection occurs on either side of the DSB, leaving 3' single-stranded overhangs, one of which invades the homologous chromosome. Synthesis occurs along the homologous template, displacing one strand of the template chromosome to form a D-loop structure. If sufficient synthesis occurs, this displaced strand can be captured by the non-invading 3' overhang. Following synthesis along the D-loop structure, a double-Holliday junction (dHJ) intermediate is formed. Finally, depending on which combination of strands is cleaved, the dHJ is resolved to form either a CO (primarily) or a NCO. Not shown is dHJ dissolution, wherein a helicase branch migrates the two Holliday junctions together, creating a structure that is acted upon by a topoisomerase, creating a NCO product. Alternately, synthesis-dependent strand annealing (SDSA) can occur. In SDSA, following some synthesis along the homologous template, the D-loop is disrupted as the invading strand dissociates from the template and anneals to the opposite side of the DSB, resulting in a NCO product. Heteroduplex DNA (hDNA) arising from the two NCO pathways is depicted. NCOs arising through dHJ resolution can contain regions of hDNA adjacent to a region of gene conversion (GC), whereas NCOs arising through the SDSA pathway lack an adjacent region of GC. Each line represents one strand of DNA with partial arrowhead indicating 3' end of DNA. Black and gray lines differentiate two homologous chromosomes. Dashed lines denote newly synthesized DNA. Arrowheads indicate sites of endonuclease cleavage.

Previous research into the *Drosophila melanogaster recombination defective* (*rec*) gene found that *rec* mutants had reduced COs but nearly two-fold increased NCOs as compared to wild-type (Blanton et al., 2005). Also in this study, it was shown that *rec* mutants had shorter GC tracts than wild-type flies and epistasis experiments placed *rec* at an intermediate step in the recombination pathway. These findings, coupled with REC's paralogy to the replicative mini-chromosome maintenance (MCM) proteins, which have a known role in DNA replication, led to the hypothesis that REC is involved in the repair synthesis step of meiotic recombination. This hypothesis suggested that REC promotes repair synthesis, such that in its absence, a dHJ intermediate cannot form and DSBs are instead repaired via SDSA. By undertaking a gene conversion assay in a MMR-defective *rec* mutant background, I sought to test this hypothesis, since NCOs arising through a dHJ versus SDSA are predicted to produce different patterns of hDNA. NCOs arising through dHJ resolution can contain regions of hDNA adjacent to a region of GC, whereas NCOs arising through the SDSA pathway lack an adjacent region of GC.

Furthermore, since MCM proteins in both archaeabacteria and eukaryotes function in hexameric complexes with other MCM proteins (Bochman and Schwacha, 2009), we hypothesized that REC, as the *Drosophila* ortholog of MCM8 (Blanton et al., 2005), also functions in a hexameric complex with other MCM proteins. Thus, to gain further insight into REC's role in meiotic recombination and to identify proteins REC interacted with, I sought to use various molecular biological techniques to study REC *in vivo*.

Results and Discussion

Msh6 rec gene conversion assay

It has previously been hypothesized that in the absence of REC, NCOs arise through the SDSA pathway rather than through a dHJ intermediate (Blanton et al., 2005). To test this model, we utilized a previously-developed system to screen for intragenic recombination at the *rosy* (*ry*) locus (Chovnick et al., 1970; Chovnick et al., 1971). Briefly, the *ry* gene encodes xanthine dehydrogenase, an enzyme required for purine metabolism. After crossing females heteroallelic for two *ry* missense mutations, ry^{606} and ry^{531}, to males homozygous for a deletion of most of the *ry* locus, rare ry^{+} recombinants are selected by treating the larvae with purine, as all ry^{-} larvae die and only the rare ry^{+} recombinants, each representing a recombination event which converted one of the missense mutations into a functional wild-type allele, will survive (Figure 22). COs and NCOs can be distinguished by the presence (or absence) of flanking markers associated with each *ry* allele. For each recombination event recovered, 33 heterologies within and adjacent to the *ry* locus are utilized to map the hDNA and GC tracts by sequencing PCR products of the recombinant chromosome.

Previously, Radford *et al.* recovered hDNA in a *ry* gene conversion assay by using two deletion alleles of *Msh6,* one of two MutS homologs in *Drosophila* (Sekelsky et al., 2000), to knock out MMR (Radford et al., 2007b). As expected, PMS was observed, indicating the persistence of unrepaired hDNA. However, unexpectedly, the GC and hDNA tracts were discontinuous, perhaps resulting from a short-patch repair system that functions in the absence of canonical MMR. Thus, to recover hDNA tracts in

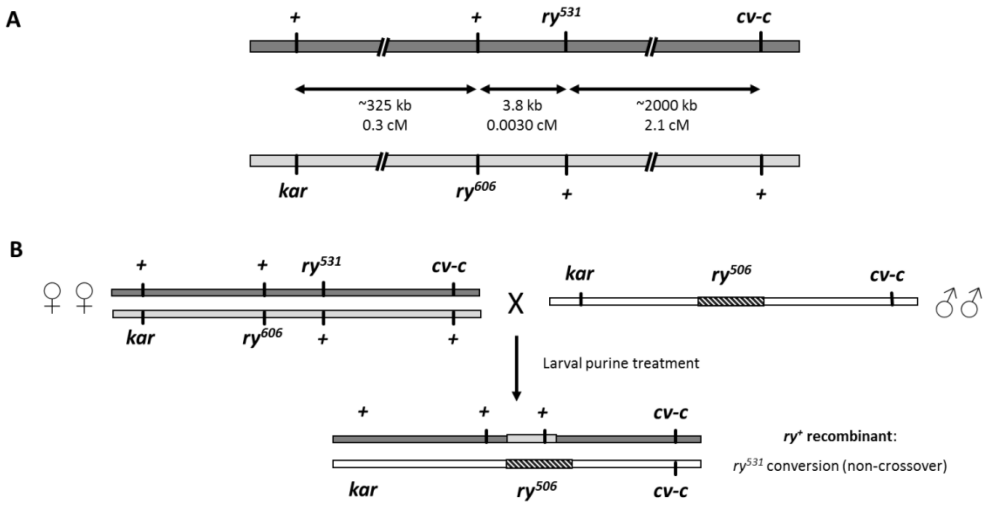

Figure 22. *rosy* gene conversion assay. (A) Schematic of the two "female" chromosomes utilized in the *rosy* (*ry*) gene conversion assay. Distances between the *ry* missense mutations (ry^{606} and ry^{531}) and the flanking markers (*kar* and *cv-c*) are indicated in kilobases (kb) and centiMorgans (cM). (B) Cross to screen for recombination events within the *ry* locus. Females heteroallelic for the two *ry* mutations are crossed to males homozygous for both flanking markers and a deletion of *ry* (ry^{506}). Larval progeny of this cross are treated with purine, and only ry^{+} recombinants survive to adulthood. One potential class of ry^{+} recombinant progeny is represented as a ry^{531} non-crossover fly, as indicated by the presence of the flanking marker *cv-c*.

rec mutant NCOs, I created *Msh6 rec* double mutants. To facilitate collecting the large number of virgin females (~145,000) necessary for this experiment, I incorporated a self-virgining scheme into the recombinant chromosomes, such that only females of the desired genotype survive the first cross to generate the experimental females (Figure 23).

After screening over 1.7 million progeny of *Msh6 rec* mutant females, we recovered 17 ry^{606} conversions, 10 ry^{531} conversions and 1 CO. *rec* mutants were previously found to have a strong reduction in CO frequency as compared to wild-type while the frequency of NCOs was nearly two-fold higher than wild-type (Blanton et al., 2005). It was hypothesized that since DSBs are not effectively processed into COs in *rec* mutants, additional DSBs are made in an attempt to produce more COs, resulting in the

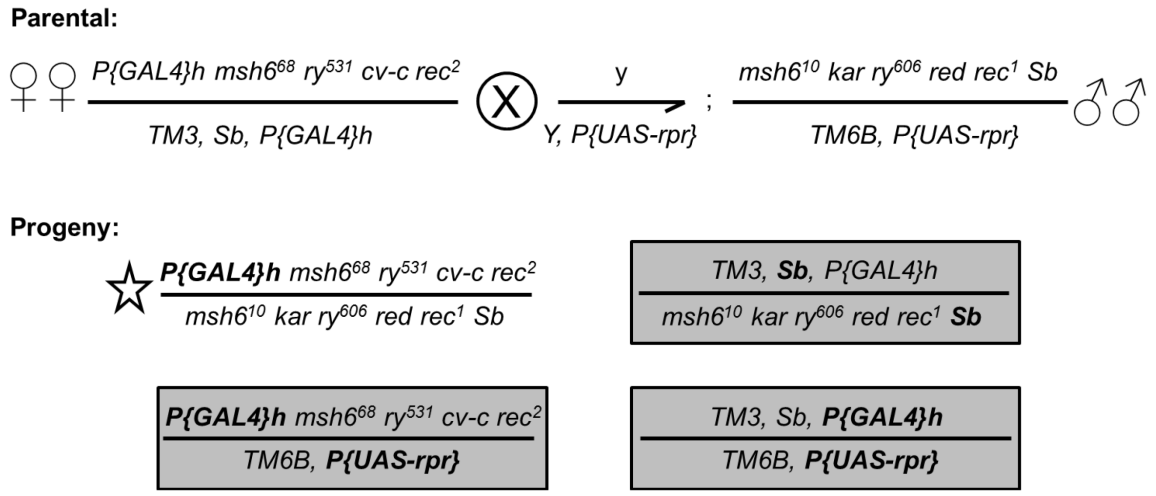

Figure 23. Self-virgining cross scheme for *Msh6 rec* gene conversion assay. Females and males of the indicated genotypes are crossed together. The only surviving progeny are females of the desired genotype, marked with a star. The other progeny classes which do not survive are marked with gray boxes. Bold font emphasizes the reason each genotype does not survive (*GAL4* driving expression of *UAS-reaper* (*UAS-rpr*), a cell death gene, or two copies of *Stubble* (*Sb*), which is homozygous lethal). Not shown in the progeny class is the male class which does not survive because of the *P{UAS-rpr}* gene on the *Y* chromosome.

increased NCOs observed as compared to wild-type. It was also shown previously that *Msh6* mutants exhibited increased COs and NCOs as compared to wild-type (Radford et al., 2007b). This result can be readily explained since eliminating MMR prevents hDNA from being randomly restored to the mutant *ry* allele, as occurs in wild-type, thus increasing the number of events recovered. I found that like in the *rec* mutant, COs remained very low in the *Msh6 rec* double mutant (2% of the wild-type level versus 8% in the *rec* single mutant) (Table 9). The difference between these percentages is not likely biologically significant, as they represent very few CO flies recovered (2 in *rec* versus 1 in *Msh6 rec*). Using the CO data, I thus conclude that *rec* is epistatic to *Msh6,* as the double mutants had the *rec* null level of COs. Interestingly, the *Msh6 rec* double mutant had near wild-type levels of NCOs (110% of wild-type versus 184% of wild-type in *rec*). It is difficult to interpret this finding. It could be that Msh6 is necessary for the

formation of a subset of the NCOs that form in the *rec* mutant and thus in the double mutant only the Msh6-independent NCOs can be produced. Alternatively, these results could indicate that NCO formation is sensitive to background effects. The *rec* and *Msh6 rec* experiments were conducted with the same *rec* alleles, but the mutations were placed into otherwise different genetic backgrounds. Perhaps the mutant chromosomes should be placed into an otherwise isogenic background in the future to eliminate as much variation as possible from the experiment.

	wild-type ^	***Msh6*** #	***rec*** *	***Msh6 rec***
CO	1 / 33,000	1 / 26,500 (124)	1 / 368,000 (8)	1 / 1,723,000 (2)
NCO	1 / 70,000	1/ 42,000 (166)	1 / 41,000 (184)	1 / 64,000 (110)

Table 9. Intragenic recombination at the *rosy* locus. Frequency of crossovers (COs) and non-crossovers (NCOs) observed in the indicated genetic backgrounds. Numbers in parentheses denote percentage of wild-type frequency. ^Data from (Radford et al., 2007a) and (Blanton et al., 2005). #Data from (Radford et al., 2007b). *Data from (Blanton et al., 2005).

I next sought to map the *Msh6 rec* NCO tracts to determine whether these NCOs arose through SDSA or via a dHJ intermediate, as each pathway is predicted to produce a different pattern of hDNA (Figure 21). Eight of the ry^{606} conversion tracts were successfully mapped using the multiple polymorphisms between the two parental chromosomes (Figure 24). Four of the tracts converted only the ry^{606} site. The recovery of such short tracts was not unexpected, as *rec* mutant GCs were shorter than wild-type (Blanton et al., 2005). Of the remaining tracts, three of the four contained one unconverted polymorphism within a stretch of otherwise converted DNA. Similar results were seen in the *Msh6* mutant assay, and are likely the result of a short-patch repair

system (Radford et al., 2007b). One of these tracts also contained hDNA, indicating that the *Msh6* mutation did eliminate at least some MMR. In this case, the hDNA incorporated one polymorphism at each end of the converted tract, with the hDNA being *in trans* (i.e., the ry^{606}-chromosome-derived polymorphism at one hDNA site was not on the same DNA strand as the other ry^{606}-chromosome-derived polymorphism at the opposite hDNA site). It is impossible to glean any information regarding recombination mechanisms from this data, with so few mapped conversion events (only one of which contained hDNA) and with the short-patch repair system potentially obscuring other conversion tracts.

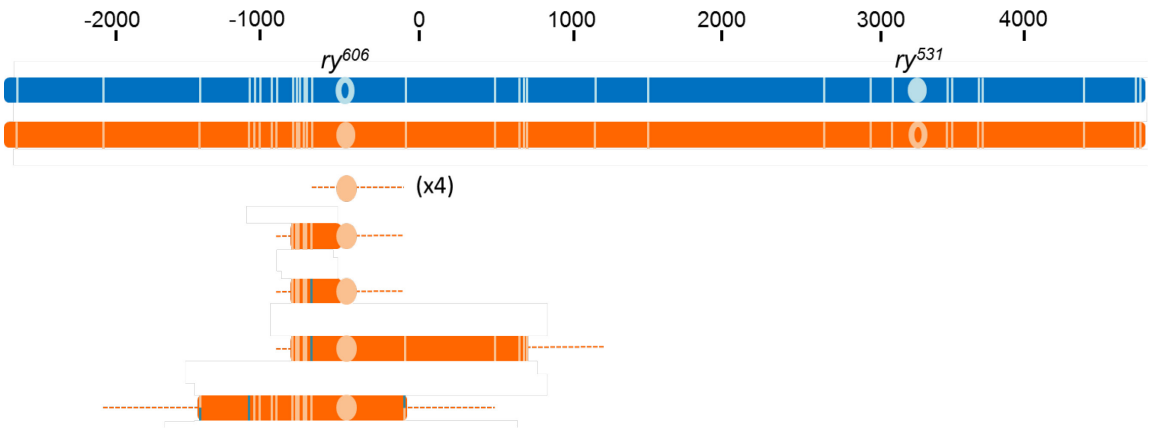

Figure 24. Non-crossover events in *Msh6 rec* mutants. Bars at top represent the two maternal chromosomes: ry^{606} chromosome (blue) and ry^{531} chromosome (orange). Mapped ry^{606} conversion tracts are depicted below the maternal chromosomes. Number in parentheses denotes number of times that tract was observed. Open ovals represent the mutant *ry* allele, while filled circles represent the wild-type allele. Vertical lines indicate polymorphisms between the two maternal chromosomes. In mapped tracts, color denotes chromosome of origin, with vertical lines indicating converted sites. Vertical lines of two colors denote heteroduplex DNA (hDNA) derived from both maternal chromosomes and the phase of this hDNA. Dotted lines extend to the next unconverted polymorphism, indicating the maximum possible tract length. Scale is in base pairs, using the coordinate system of (Bender et al., 1983).

Mapping the remaining tracts proved difficult, as many of the fly preps did not produce a PCR product with any primer combination. Furthermore, analysis of *mus210; Msh6* double mutant NCO tracts indicated that removing both the canonical MMR machinery (with the *Msh6* mutation) and the nucleotide-excision repair pathway (with the *mus210* (*DmXPC*) mutation) was necessary to eliminate the short-patch repair system (N. Crown, unpublished). Since short-patch MMR was possibly obscuring the hDNA tracts in the *Msh6 rec* mutant, and since *rec* mutant GC tracts do not span as many SNPs as in wild-type (thus decreasing the likelihood that the conversion tracts would span multiple polymorphisms to aid mapping), I conclude that mapping additional tracts would not be a time beneficial endeavor.

MCM yeast two-hybrid assay

I hypothesized that as a member of the MCM family, REC would interact with other MCM proteins. To this end, I conducted a yeast two-hybrid assay in which I tested every MCM domain-containing protein in *Drosophila* (MCM2-7, REC, MEI-217 and MEI-218) for interaction with itself and every other *Drosophila* MCM protein (Figure 25). I was able to recapitulate some of the known MCM2-7 interactions (Bochman et al., 2008), including MCM2:MCM6 and MCM3:MCM7, thus showing that the system can detect interactions between MCM proteins. I also identified some other replicative MCM interactions, including MCM3:MCM6 and a self-interaction between MCM6 subunits. These additional interactions could represent other MCM sub-complexes within the cell, as it is known that many more MCM proteins are present in a cell than are necessary for DNA replication (the "MCM paradox") (Laskey and Madine, 2003) and it is thus likely

that subsets of MCM proteins conduct other cellular processes as well. Alternatively, these interactions could be artifacts of our artificial overexpression system. To confirm if these interactions are biologically relevant, immunoprecipitation studies of the *in vivo* MCM proteins could be conducted.

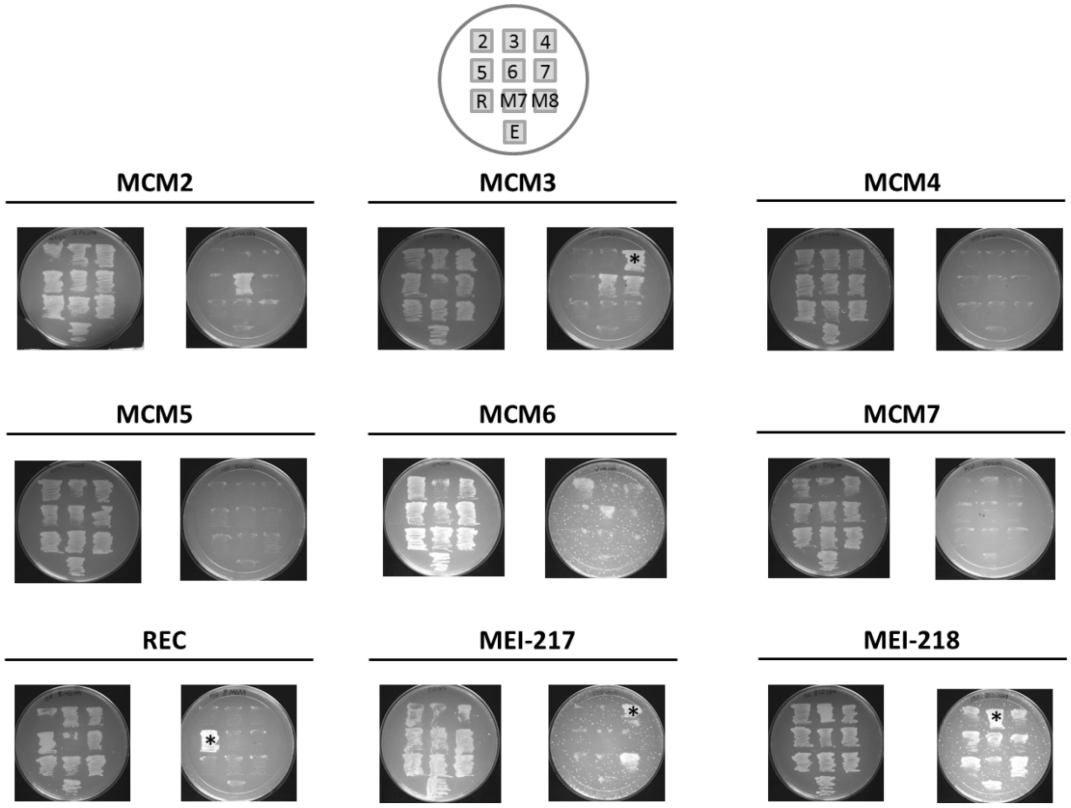

Figure 25. MCM yeast two-hybrid assay. Pairwise yeast two-hybrid assay testing for physical interaction between MCM proteins. The protein listed above each pair of plates is the protein fused to the GAL4-binding domain (BD). This protein is tested for interaction with all other MCM proteins fused to the GAL4-activating domain (AD), according to the legend above the plates, with abbreviations as follows: 2-7 represent MCM2-7, respectively; R, REC; M7, MEI-217; M8, MEI-218; E, empty AD. For each pair of plates, the plate on the left is –trp –leu. Growth on this plate indicates the presence of both AD and BD plasmids within the yeast. The plate on the right is –trp –leu –his. Growth on this plate indicates an interaction between the two tested proteins. Contaminating yeast colonies that do not represent a real interaction are marked with an asterisk.

I did not recapitulate many of the known interactions between MCM2-7 subunits. I did not expect to recover an interaction between MCM2 and MCM5, as these two

subunits are believed to form a "gate" in the heterohexamer (Bochman and Schwacha, 2010). The failure to detect an interaction between the remaining subunits could have arisen for several reasons. Some of the MCM proteins may not have expressed in our system. This is likely the case for MCM4, MCM5, MCM7 and REC in the binding domain, as these four proteins did not interact with any other subunit. Since MCM2-7 are essential proteins, expressing some *Drosophila* MCM proteins in *Saccharomyces cerevisiae* may poison yeast MCM complexes; thus, yeast which fail to express the fly MCM proteins could be selected for in this system. Furthermore, fusing the GAL4 domains to the MCM proteins could have disrupted some protein interactions.

I also found that MEI-217 interacted with MEI-218. As MEI-217 and MEI-218 are encoded on one dicistronic mRNA (Liu et al., 2000), and the proteins contain MCM N- and C-terminal domains, respectively (Kohl et al., 2012), I believe this interaction is biologically relevant. However, this interaction could not be confirmed in the reverse (with MEI-218 in the binding domain and MEI-217 in the activating domain (AD)) since MEI-218 self-activated, as shown by its interaction with every MCM in the AD, including the empty vector. Thus, future experiments with MEI-218 will require the protein to be fused to the AD. Alternatively, the MEI-218 protein may be truncated to determine the region of self-activation.

Immunoprecipitation of REC

In addition to conducting yeast two-hybrid analysis, interaction between proteins can also be identified by immunoprecipitating the protein(s) of interest. This technique has several advantages over yeast two-hybrid, including the ability to detect endogenous

interactions in *Drosophila* tissue and the ability to detect unpredicted interactions – i.e., by pulling down the protein of interest, new proteins may be identified that otherwise might not have been tested using a candidate gene approach in a yeast two-hybrid assay. To this end, I created three antibodies to REC: an affinity-purified polyclonal antibody raised against amino acids (aa) 324-423, another affinity-purified polyclonal antibody (aa 875-885), and a polyclonal antibody (aa 737-842) (Table 10). These antibodies were tested on various *Drosophila* samples, including whole adult flies (females and males), whole larvae, ovaries and testes but an unambiguous REC band was never observed on western blots (data not shown). Since *Drosophila* create ~6 COs per developing oocyte (reviewed in (McKim et al., 2002)), and each female fly has ~30 ovarioles, each containing one germarium – the anterior region of the ovariole wherein early oocyte differentiation and meiotic recombination takes place – with cells undergoing meiotic recombination (reviewed in (Lake and Hawley, 2012)), it may be that very few REC proteins exist in flies (if REC is necessary only to produce meiotic COs), and this number may be below the level of detection via western blot. Alternatively, all of the antibodies could be unable to recognize REC. To determine if the antibodies were capable of detecting REC, I tested the antibodies on a western blot against recombinant REC protein expressed in insect cells using the baculovirus system. Each antibody was able to detect REC, as evidenced by the bands in the REC samples and absence of bands in the non-REC samples (Figure 26).

		Detect REC in…	
Antibody	**A.A.**	**Flies**	**Overexpression**
α-REC-mid	324-423	No	Yes
α-REC-756	737-842	No	Yes
α-REC-C	875-885	No	Yes
α-DYKDDDK	DYKDDDK (FLAG tag)	No	Yes

Table 10. REC antibodies. Antibodies to REC and to the FLAG tag are compared for the amino acids (A.A.) they recognize and their ability to detect REC in *Drosophila* tissue ("flies") and in an overexpression system ("overexpression").

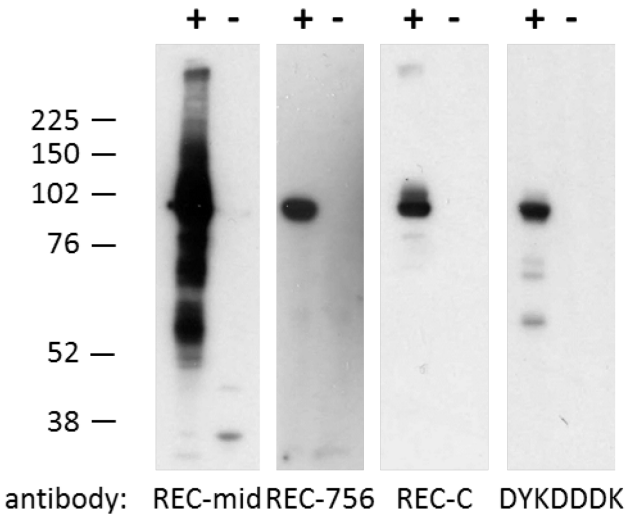

Figure 26. REC antibodies. Recombinant protein samples from baculovirus-infected insect cells were western blotted and probed with indicated antibodies. All samples were run on the same SDS-PAGE gel. +, sample contains ^{FLAG}REC. -, sample does not contain ^{FLAG}REC. Predicted molecular weight of ^{FLAG}REC is ~99 kDa.

Since the REC antibodies were not sensitive enough to detect endogenous REC, I created an N-terminal FLAG-tagged *rec* transgene so that I could utilize a commercially available FLAG antibody to probe for REC. This $P\{^{FLAG}REC\}$ transgene was tested in a non-disjunction (NDJ) assay to determine if it rescued the high NDJ phenotype

characteristic of *rec* null mutants (Grell, 1984) (Figure 27). Since the NDJ in the $P\{^{FLAG}REC\}$ transgene was not statistically significantly different from wild-type (p=0.0873), I conclude that the transgene successfully expresses REC, presumably with an N-terminal FLAG tag.

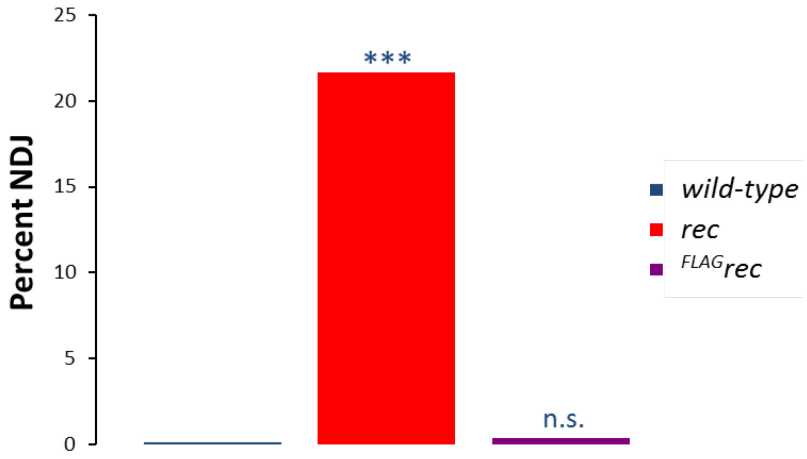

Figure 27. $P\{^{FLAG}REC\}$ non-disjunction. Percent non-disjunction (NDJ) was scored in the indicated genotypes. ^{FLAG}rec data from insertion line #14-25, on *2*. Over 1100 individuals were scored for each genotype. ***p<0.0001, as compared to *wild-type*. n.s., not statistically significant as compared to *wild-type*.

I next tested several samples from this $P\{^{FLAG}REC\}$ line, including both dissected ovaries and whole flies, via western blot with a commercial monoclonal FLAG antibody. However, as seen with the antibodies to REC, ^{FLAG}REC signal was not detectable (data not shown). To increase the likelihood of detecting REC, we next attempted to immunoprecipitate REC using commercial anti-FLAG affinity agarose beads. REC was still undetectable following immunoprecipitation, even after trichloroacetic acid precipitation to concentrate the sample. The FLAG antibody was functional, however, as

I was able to detect another FLAG-tagged protein, MEI-9, using similar protein extraction and western blotting procedures (data not shown).

Therefore, I have been unable to immunoprecipitate REC. However, as these attempts were cursory and used un-optimized protocols, it may still be possible to immunoprecipitate endogenous REC. In the future, researchers will need to weigh this experiment's potential costs and benefits before deciding whether to repeat it. While the possibility of identifying endogenous proteins interacting with REC is a tantalizing goal, the difficulties inherent with working with a low-abundance protein temper the enthusiasm for repeating this experiment.

Immunofluorescence of REC

Since I was unable to identify proteins interacting with REC via yeast two-hybrid or immunoprecipitation, I next turned to using the antibodies described above in immunofluorescence assays. By co-staining germaria with these anti-REC antibodies and antibodies against other candidate proteins, I hoped to determine whether the proteins co-localize, suggesting that the proteins function either in the same complex or in the same process. Initially, to verify that REC could be visualized by confocal microscopy using these antibodies, I co-stained germaria from *P{^{FLAG}REC}* females with one antibody to REC (either anti-REC-mid, anti-REC-756, or anti-REC-C) and another to FLAG. Unfortunately, co-localization of these signals was never observed, and instead only varied background staining was seen (data not shown). Thus, I was unable to detect REC via immunofluorescence using confocal microscopy. Furthermore, I also co-stained *P{^{FLAG}MEI-218}* germaria (stock obtained from Kim McKim, Rutgers University) with

anti-REC-C and anti-FLAG, but failed to see a convincing signal from either of these proteins (data not shown). However, other proteins in germaria, including C(3)G, a component of the synaptonemal complex (Page and Hawley, 2001) (Figure 28), and Orb, an RNA-binding protein expressed in germline cells during oogenesis (Lantz et al., 1992) (data not shown), were able to be visualized, suggesting that the dissection, fixing, staining and imaging protocols were functional.

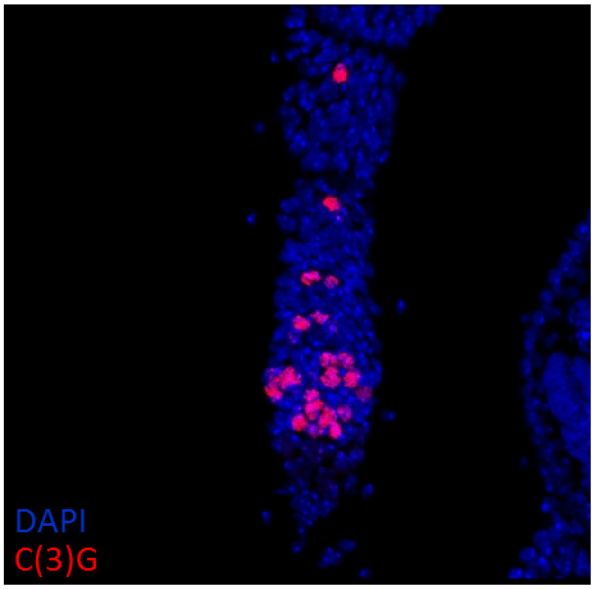

Figure 28. C(3)G staining. *w1118* ovariole stained to visualize DNA and C(3)G. Anterior end of germarium is located at the bottom. Image is a maximum projection of Z-stacks through the ovariole at 40X magnification.

Since REC is presumed to be a low-abundance protein, future immunofluorescence experiments looking to visualize REC should seek to increase the fluorescent signal from the protein. This could possibly be achieved by creating a multiply-epitope-tagged *rec* transgene. From the aforementioned experiments, I believe that REC with one FLAG tag is not sufficient to be visualized via confocal microscopy.

Perhaps increasing the number of tags would increase the signal above the threshold necessary for visualization. However, increasing the size of the tag could impede REC from conducting its normal cellular functions. To test this possibility, it will be necessary to assay CO formation in the transgenic fly. Alternatively, a "signal amplification kit" could be used to increase the fluorescent signal from the antibodies.

MCM RNA *in situ* hybridization

As my various attempts to study REC protein were unsuccessful, I next sought to visualize *rec* mRNA via *in situ* hybridization. By localizing *rec* mRNA in germaria, I hoped to gain additional insight into REC's role in meiotic recombination. Furthermore, by conducting similar RNA *in situ* hybridizations for all of the *Drosophila* MCM domain-containing proteins, I hoped to uncover evidence of shared functions between REC and the other MCM proteins. After conducting *in situs* on ovarioles for *Mcm2-7, rec, mei-217* and *mei-218*, I found that each showed seemingly random foci throughout the germaria (Figure 29). As the *in situs* were only conducted a few times each (at most), this staining could represent non-specific background. However, I believe the staining was real, and its localization fits with our hypothesis that REC, MEI-217 and MEI-218 are involved in meiotic recombination, which occurs in the germarium. Further, it is not surprising to find transcripts of MCM2-7 in germaria, as these essential proteins are necessary for DNA replication, which occurs in cells throughout the ovariole – including prior to the first meiotic division and in the endocycling nurse cells and follicle cells during later stages of oogenesis.

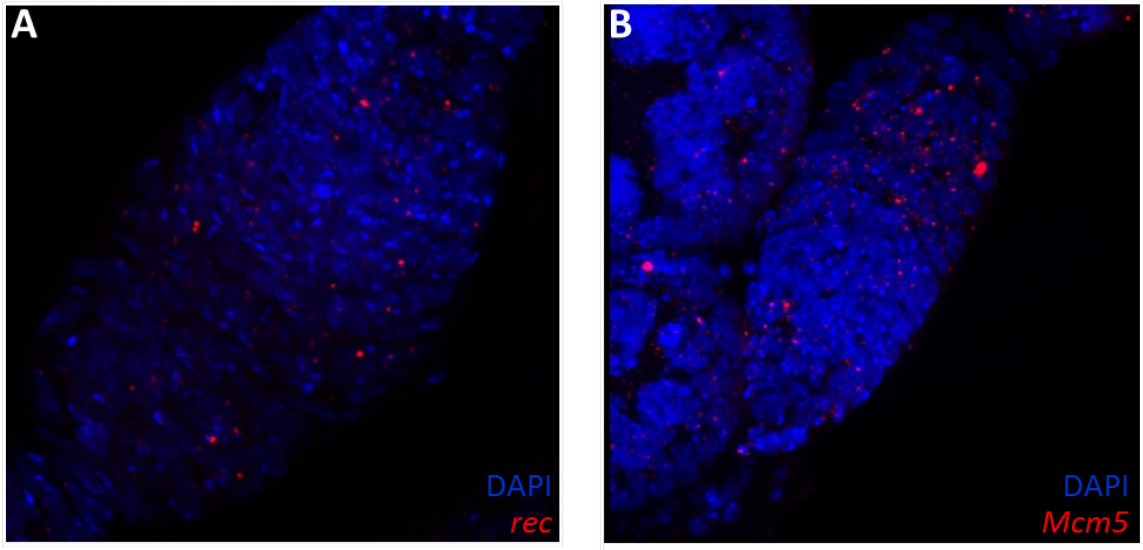

Figure 29. RNA *in situ* hybridization. Germaria stained to visualize DNA (with DAPI, blue) and (A) *rec* mRNA or (B) *Mcm5* mRNA (with Cy3, red). Anterior end of germaria are in the lower left corner. Each image is a maximum projection of Z-stacks through the germarium at 40X magnification. Other replicative *Mcm, mei-217* and *mei-218* images appeared similar (data not shown).

Interestingly, I also saw distinct *rec* foci on nurse cell nuclei in stage ~10 oocytes (Figure 30). mRNA transcribed in nurse cells is deposited into the adjacent developing oocyte for use from fertilization until the initiation of zygotic transcription. Discovering that *rec* mRNA was being transcribed in nurse cells was unexpected since *rec* null mutants have no obvious developmental defects that would suggest a role for REC in early development. Similar staining was only observed for *Mcm5* mRNA. The absence of nurse cell foci for the other *Mcm2-7* mRNAs is likely the result of experimental error due to an un-optimized hybridization protocol. We predict that *Mcm2-7* mRNA is highly transcribed in nurse cells, since numerous replicative MCM2-7 complexes are essential for DNA replication occurring prior to zygotic transcription. Alternatively, the staining observed for *Mcm5* may represent higher-than-normal levels of transcription (i.e., higher

than the other *Mcm2-7* mRNAs), suggesting an additional role for MCM5 outside of the replicative MCM2-7 complex. However, neither hypothesis explains the finding that *rec* mRNA was being transcribed in nurse cells – a finding that suggests REC plays a role in early embryonic development. It would be of interest to discover this additional function of REC. Perhaps REC acts with a subset of the replicative MCMs to assist the rapid rounds of DNA replication in the early embryo. If MCM5 were a component of this sub-complex, this could explain the high levels of *Mcm5* mRNA observed in nurse cell nuclei. As *rec* null flies are viable, it is clear that the function of REC in the early embryo is not essential.

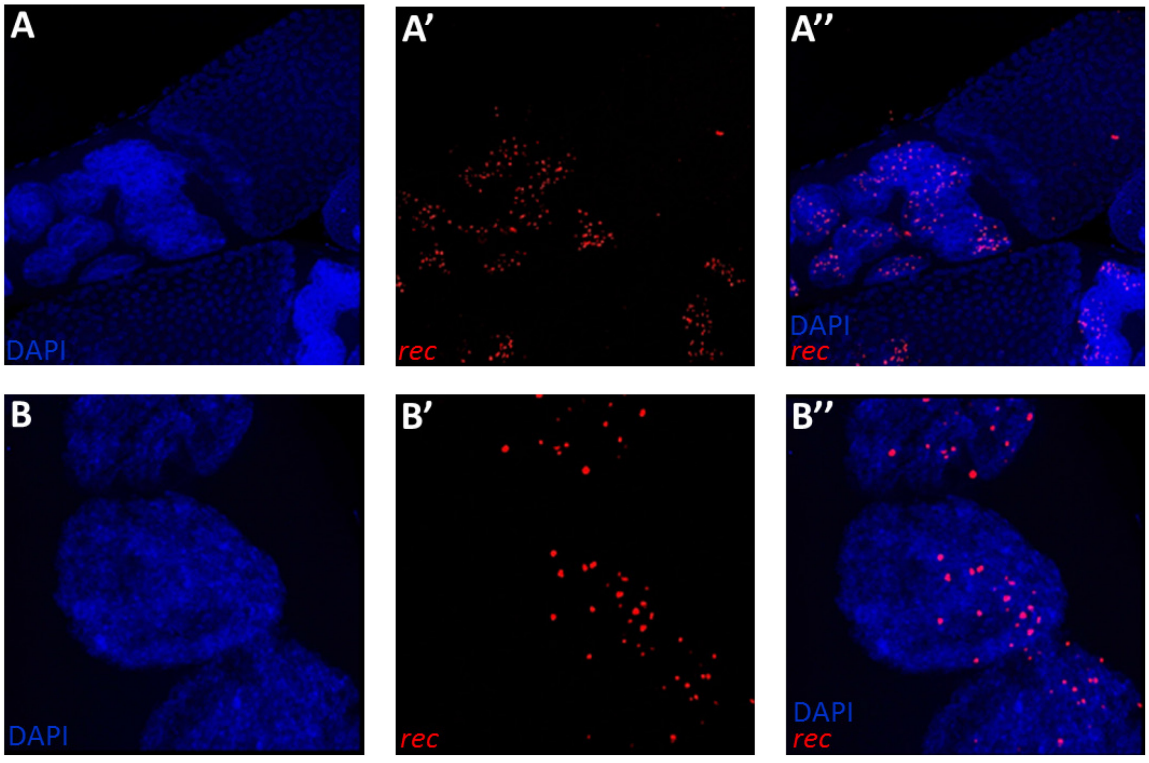

Figure 30. *rec* RNA *in situ* hybridization. *Drosophila* ovariole stained to visualize DNA (with DAPI, blue) and *rec* mRNA (with Cy3, red). (A) ~Stage 10 oocyte at 40X zoom. (B) Three nuclei from same oocyte as in (A) at 63X. Both images are maximum projections of Z-stacks through the oocyte.

Thus, I initiated these genetic and immunochemical experiments hoping to better understand the role of REC in meiotic recombination. Instead, I found evidence that REC is likely a low-abundance protein in *Drosophila,* making these experiments more technically challenging than anticipated. However, I was able to show an interaction between MEI-217 and MEI-218 via yeast two-hybrid – an initial discovery that led to additional experiments discussed in Kohl *et al.* (Kohl et al., 2012). I also made a potentially useful tool by creating *P{^{FLAG}REC},* an epitope-tagged *rec* transgene that fully rescues the high NDJ phenotype of *rec* null mutants. Finally, I discovered an abundance of *rec* mRNA in nurse cells of the *Drosophila* oocyte, suggesting a potential role for REC in early embryonic development.

Materials and Methods

Msh6 rec gene conversion assay

Flies were maintained on standard medium at 25˚C. 40 virgin females of the genotype *P{GawB}h^{1J3} msh6^{68} ry^{531} cv-c rec^{2} / TM3, P{w^{+mC}=GAL4-twi.G}2.3, P{UAS-2xEGFP}AH2.3*, *Sb, Ser* were crossed to 15 males of the genotype *Y, P{w^{+c}=UAS-rpr.Y}; msh6^{10} kar ry^{606} red rec^{1} Sb / TM6B, P{w^{+mC}=UAS-rpr.C}, Tb, Hu* per bottle. *rec* mutations (Blanton et al., 2005) and *Msh6* mutations *(Radford et al., 2007b)* have been described previously. From this self-virgining scheme, 100 virgin females of the genotype *P{GawB}h^{1J3} msh6^{68} ry^{531} cv-c rec^{2} / msh6^{10} kar ry^{606} red rec^{1} Sb* were collected and crossed to 20 males of the genotype *kar ry^{506} cv-c* per bottle. Gene conversion assay was conducted as in Radford *et al.* (Radford et al., 2007b). Surviving *ry^{+}* recombinants were homogenized in buffer containing proteinase K, as in Gloor *et al.*

(Gloor et al., 1993). Conversion tracts were amplified using one primer anchored in the ry^{506} deletion to select for the recombinant, maternally-derived chromosome, using iProof polymerase (Bio-Rad, Hercules, CA). PCR product was excised from an agarose gel which was then melted using QG buffer (Qiagen, Valencia, CA) and purified with a PCR purification kit (Fermentas, Burlington, ON). From this clean DNA, smaller, nested PCR reactions were run, agarose-gel-excised, purified and sequenced using the UNC Genome Analysis Facility to finely map conversion tracts. Phasing of the hDNA tract was determined using allele-specific PCR primers to one of the hDNA polymorphisms.

Yeast two-hybrid assay

Drosophila MCM2-7, REC, MEI-217 (aa 52-279) and MEI-218 were cloned using the Gateway system (Life Technologies, Carlsbad, CA) into pGBD-DEST, a Gateway-compatible derivative of pGBD-C1 (James et al., 1996) constructed with the Gateway Vector Conversion System (Life Technologies) and into pACT2.2gtwy (Addgene plasmid 11346 deposited by Guy Caldwell), a Gateway-compatible derivative of pACT2.2. Constructs were transformed into *S. cerevisiae* strain PJ69-4A (James et al., 1996). Co-transformants were selected on plates of SD minimal medium containing dropout supplements lacking leucine (-leu) and tryptophan (-trp) for 3 days at 30˚C. Single colonies were streaked onto fresh –trp –leu plates and grown for 3 days at 30˚. Colonies were then streaked onto –trp –leu –histidine plates containing 3mM 3AT. Interaction between proteins was scored 3 days later. Plates were left at 4˚C for several weeks to check for abnormal growth indicative of false-positive interactions.

Western blotting

Insoluble protein pellets containing either ^{FLAG}REC or ^{HA}MEI-217 and $^{Strep\text{-}II}$MEI-218 expressed in High Five cells were boiled in SDS-PAGE sample buffer. Samples were run on a 7.5% SDS-PAGE gel, transferred to PVDF membrane, and probed with the following antibodies at 1:20,000: anti-REC-mid (raised in rabbit to aa 324-423 (Strategic Diagnostics, Inc., Newark, DE), anti-REC-756 (raised in rabbit to aa 737-842; Covance, Denver, PA), anti-REC-C (raised in rabbit to aa 875-885; Pacific Immunology, San Diego, CA), anti-DYKDDDK (FLAG) monoclonal mouse antibody (Millipore, Billerica, MA), and HRP-conjugated anti-rabbit or anti-mouse secondary (Santa Cruz Biotechnology, Santa Cruz, CA) 1:21,000. SuperSignal West Pico Chemiluminescent Substrate (Pierce) was used to detect proteins.

^{FLAG}REC transgene

The 5'UTR of *rec* and the *rec* cDNA with an N-terminal FLAG tag were cloned into the P{CaSpeR4} vector. Construct was then injected via standard P-element transformation procedures (Rainbow Transgenics, Thousand Oaks, CA) to create *P{^{FLAG}REC}*.

Non-disjunction

Flies were maintained on standard medium at 25˚C. For *{^{FLAG}rec}* assay, flies were heteroallelic for null mutations of *rec* (*rec^{1}* and *rec^{2}*; (Blanton et al., 2005)), in addition to carrying one copy of the transgene. Non-disjunction was scored by crossing virgin females to *y cv v f / T(1:Y)B^{S}* males. The number of exceptional progeny indicative

of non-disjunction (Bar-eyed females and wild-type-eyed males) was multiplied by two to account for triplo-X and nullo-X progeny, which do not survive to adulthood. This number was divided by the total number of progeny (which included the additional exceptional progeny) and expressed as a percentage. P values were calculated via a Fisher's exact test using GraphPad online software (GraphPad, Inc., La Jolla, CA).

Immunofluorescence

Females of the indicated genotypes were fattened overnight on yeast paste prior to dissection of the ovaries in *Drosophila* Ringer's solution (182mM KCl, 46mM NaCl, 3mM CaCl2, 10mM Tris, pH 7.2). Ovaries were fixed and stained using the Buffer A protocol as in McKim *et al.* (McKim et al., 2009). Primary antibodies included: rabbit anti-REC-C used at 1:300, rabbit anti-REC-mid used at 1:300, rabbit anti-REC-756 used at 1:300, mouse anti-FLAG used at 1:300 (Millipore), rabbit anti-FLAG used at 1:300 (Sigma), mouse anti-C(3)G antibody used at 1:500 (Page and Hawley, 2001) and a combination of two mouse anti-ORB antibodies (4H8 and 6H4) used at 1:100 (Lantz et al., 1994). Secondary antibodies were Alexa-Fluor goat anti-mouse 555 and Alexa-Fluor goat anti-rabbit 488 used at 1:1000 (Life Technologies). DAPI staining was conducted for 1min using 1:1000 of 1mg/ml DAPI solution. Ovaries were mounted in Fluoromount G (Southern Biotech, Birmingham, AL). Slides were visualized using a Leica SP5 confocal microscope.

RNA *in situ* hybridization

Forward primers were designed with the T7 RNA polymerase binding sequence followed by a gene-specific sequence, while reverse primers were designed with the T3 RNA polymerase binding sequence prior to a gene-specific sequence. Primers were spaced ~500 bp apart for each gene. Following amplification of the DNA template using *Taq* polymerase, PCR products were excised from the agarose gel, melted in QG buffer (Qiagen), purified using a GeneJET PCR purification column (Fermentas), and eluted in 50ul DEPC H_2O. Transcription reactions were as follows: 0.5ul RNasin (Promega, Madison, WI), 10ul purified PCR product, 2ul 10X transcription buffer, 4ul DEPC H_2O, 2ul T3 (or T7) RNA polymerase (Roche, Indianapolis, IN). Reactions were placed at 37˚C for 2.5h prior to adding 1ul RQ1 DNase (Promega) and 1ul RNasin, after which reactions were returned to 37˚C for 30min.

w^{1118} females were fattened overnight on yeast paste prior to ovary dissection. Ovaries were fixed in 500ul fixation buffer (PBS, 0.05M EGTA, 9% formaldehyde) and 500ul heptane for 25min. Fixation buffer was removed and 750ul MeOH was added and immediately removed. Two 1.5ml 100% EtOH washes and six PBT (PBS, Tween-20) washes followed. 500ul hybridization buffer (50% deionized formamide, 5X SSC, 100ug/ml sonicated denatured salmon sperm, 100ug/ml *E. coli* tRNA (Sigma), 50ug/ml heparin, 0.1% Tween-20, pH4.5) was added for 1h. Probe was diluted 1:1000 in hybridization buffer containing 5% dextran sulfate prior to heating at 85˚C for 5min, cooling on ice 2min and heating again at 55˚C 2min. Hybridization buffer was removed from ovaries and the warmed probe was added. Reaction incubated overnight at 55˚C. Ovaries were washed twice for several minutes with wash buffer (125ml formamide,

25ml 20X SSC, 100ml DEPC H2O, 25ul Tween-20) at 55˚C. Then ovaries were washed in wash buffer eight times for 30min each at 55˚C, and left overnight in wash buffer at 55˚C. Ovaries were rinsed in PBT for 30min and then blocked for 30min in blocking solution (0.5% blocking reagent in PBS). Ovaries were rocked with anti-digoxigenin-POD, Fab fragments (Roche) diluted 1:200 in blocking solution for 30min, washed three times for 5min with PBT, then rocked with tyramide amplification reagent working solution (6ul tyramide reagent Cy3, 294ul amplification solution) (Perkin-Elmer, Waltham, MA). Ovaries were washed three times for 5min with PBT prior to staining for 1min with 1:1000 1mg/ml DAPI diluted in PBT. After one final 15min PBT wash ovaries were mounted in Fluoromount G (Southern Biotech). Slides were imaged using a Leica SP5 confocal microscope.

CHAPTER 5

DISCUSSION AND FUTURE DIRECTIONS

Through the research detailed in this dissertation, I have sought to understand the genetic and molecular mechanisms by which meiotic recombination occurs and the pathways involved in regulating this recombination. This research is important on many levels. At its narrowest definition, this research incorporated genetic, biochemical and evolutionary analyses to increase our knowledge about the meiotic recombination pathway in *Drosophila melanogaster.* I believe the importance of this research extends beyond *Drosophila,* however. Our findings allowed us to see a connection between the meiotic and mitotic crossover (CO) pathways and to update a decade-old meiotic CO paradigm. Furthermore, these studies have proven interesting from an evolutionary standpoint. We found a strong signature of positive selection in the history of one recombination protein and were able to couple this finding with a convincing hypothesis for the source of this strong selection. In another intriguing evolutionary finding, we showed that two recombination proteins are descendant from one ancestral protein, and in doing so, discovered a new member of a well-conserved protein family. Here I summarize the key findings of this dissertation and look to the future of the meiotic recombination field by discussing the questions that arose from these new results.

Highlighted Findings

I began this work with the hypothesis that the *Drosophila* precondition proteins (REC, MEI-217, MEI-218 and MCM5) shared similar meiotic mutant phenotypes (Baker et al., 1976; Baker and Carpenter, 1972; Blanton et al., 2005; Carpenter, 1979; Grell, 1984; Lake et al., 2007; Liu et al., 2000) because they worked together to accomplish some task necessary for meiotic CO formation. However, I had no data to support this hypothesis beyond the shared phenotype and a possible connection that some, but certainly not all, of the proteins resembled mini-chromosome maintenance (MCM) family proteins (Blanton et al., 2005; Lake et al., 2007). By utilizing a secondary structure prediction program, we discovered that MEI-217, formerly considered an orphan protein, structurally resembled the N-terminus of MCM proteins. MEI-218, encoded on the same transcript as MEI-217, structurally resembled the C-terminus of MCM proteins, suggesting that MEI-217 and MEI-218 together represented one divergent MCM protein (Chapter 2). Thus, the precondition proteins were indeed members of the MCM family. Additionally, we were able to identify the homolog of MEI-218 in other organisms, including humans, and in doing so discover a previously unrecognized MCM protein. Interestingly, according to the Mouse Transcriptome Project, the mouse MEI-218 protein is expressed in the ovary and testis, suggesting that this protein may have a role in meiosis in other organisms as well (Barrett et al., 2009).

At the conclusion of this work, I now know that the meiotic mutant phenotype shared by *rec, mei-217* and *mei-218* mutants is a result of the encoded proteins working together as a complex (mei-MCMs) (Chapter 2). I further hypothesize that MCM5 is a component of this complex as well, not simply because of its shared mutant phenotype

and membership in the MCM family, but also in light of the *rec* ATPase mutant analyses I conducted. These analyses suggested that another member of the complex existed in addition to REC – a member that was capable of binding and hydrolyzing ATP (Chapter 3).

We found that the mei-MCMs function as pro-CO proteins by antagonizing the *Drosophila* BLM ortholog, DmBLM (Chapter 2). This finding was particularly significant, as it explained how flies were able to form interfering meiotic COs without Msh4 and Msh5, two proteins necessary for interfering CO formation in other organisms (Berchowitz and Copenhaver, 2010). Our results suggested that the strong positive selection observed for *rec* prior to the split of fruit flies from tsetse flies was a result of MCM8/REC evolving to fill the functional niche left open by the loss of Msh4 and Msh5 (Chapter 2). By showing that flies replaced one pro-CO complex (Msh4-Msh5) with another (mei-MCMs), we were able to place *Drosophila* into the two-pathway paradigm for meiotic CO formation. This finding, coupled with recent research in a number of other labs (Crismani et al., 2012; De Muyt et al., 2012; Zakharyevich et al., 2012), allowed us to present a revised, more universal interpretation of the two-pathway paradigm that noted the meiotic novelties of the Class I interfering CO pathway and also the similarities between the Class II non-interfering CO pathway and the mitotic recombination pathway (Chapter 1).

Additionally, several experiments provided evidence that the mei-MCMs play a role in regulating CO formation and CO distribution. The first evidence came from the ATPase mutant analyses which showed that the *rec* Walker B mutant had a wild-type CO distribution, in contrast to the *rec* null precondition distribution, despite being unable to

form a normal number of meiotic COs (Chapter 3). This suggested that the mei-MCMs functioned early in meiotic recombination to affect the distribution of meiotic COs. Furthermore, I found three genetic backgrounds that induced a hyperrecombination phenotype. One of these, the *rec* Walker A mutant, retained a wild-type distribution of COs, whereas the other two, the *mini-MEI* MEI-218 truncation mutant and the meiotic *mus309 rec* double mutant, showed a random CO distribution (Chapters 2 and 3). These findings are important, as the mechanisms involved in regulating CO distribution are not understood in any organism. In particular, the hyperrecombination phenotype hints at a possible role for the mei-MCMs in the interference pathway. If so, these mutants will be invaluable in studying this pathway, as I am unaware of any other mutants in any organism that affect only the interference pathway but do not reduce the number of COs formed.

Future Directions

While the work in this dissertation answered several long-standing questions in the *Drosophila* meiotic recombination field, it also raised new questions to be the subject of future studies. The first of these questions asks, what is the source of the increased double COs (DCOs) in the three hyperrecombination genotypes we discovered? Perhaps the mei-MCM complex is involved in CO interference. To determine whether this is the case, COs need to be scored again in these genotypes using a different marked chromosome than the one originally used. This new marked chromosome requires the markers to be more equally-spaced so that an appropriate comparison can be made between the number of COs in each interval and how this number is affected when a CO

occurs in an adjacent interval. If the hyperrecombination in these genetic backgrounds is a result of an alteration to the interference pathway, I would expect to see an increased incidence of DCOs in adjacent intervals as compared to wild-type. If, however, the mei-MCMs do not play a role in CO interference, I would expect that the DCOs would be widely-spaced across the chromosome arm, as is normally the case when interference is functioning.

If the hyperrecombination phenotype is not a result of an aberrant interference pathway, then perhaps there is an increase in the formation of double-strand breaks (DSBs) in these genetic backgrounds. To assay this possibility, DSBs can be visualized using an antibody to γH2Av, a marker of DSBs (Madigan et al., 2002). By staining both wild-type and mutant germaria, the anterior region of the ovariole wherein early oocyte differentiation and meiotic recombination takes place, with this antibody we can compare the number of DSBs that form. An absence of an increase in DSBs in these genetic backgrounds could suggest that the CO/non-crossover (NCO) decision had been disrupted – i.e., COs were being formed at the expense of NCOs. Additionally, the hyperrecombination phenotype begs the question as to whether the additional COs arise from canonical programmed DSBs? For this experiment, the hyperrecombination genotypes can be placed into a *mei-P22* mutant background. MEI-P22 is required for programmed meiotic DSB formation in *Drosophila* (Liu et al., 2002). Thus, if the additional COs in these genotypes arise from programmed DSBs, then the level of crossing over should approach zero in the *mei-P22* mutant background. Alternatively, the DSBs could arise as a result of DNA damage, in which case the increase in COs would not be affected by the *mei-P22* mutant background. To this end, I have created

mei-P22^{103} *mus309*^{N1} *rec*^{2} *P{UASp-mus309} / mei-P22*^{103} *mus309*^{D2} *rec*^{1} *matα-GAL4* female flies and found that these flies are highly infertile (i.e., from ~890 virgin females only 162 progeny were recovered). This result suggests that the increased COs seen in the *mus309 rec* double mutants are a result of canonical programmed DSBs. However, the low fertility does preclude measuring COs in this background.

Looking in a *mei-P22* mutant background is one way of assaying whether the extra COs are "normal" meiotic COs – i.e., arise from the normal meiotic CO pathway. Another way of assaying this is to determine whether the additional COs are dependent upon MEI-9. MEI-9 is required for ~90% of *Drosophila* meiotic COs (Baker and Carpenter, 1972; Sekelsky et al., 1995) and is the *Drosophila* Class I CO pathway resolvase. In this experiment we would place the hyperrecombination mutants into a *mei-9* mutant background and assay crossing over as before. If the additional COs are formed through the Class I pathway, then in the absence of *mei-9* we would see a drastic reduction in CO formation. If, however, the additional COs arise from an alternative CO pathway, then we would still see many COs being formed in the *mei-9* mutant background.

Finally, recombination is exceedingly rare on the fourth chromosome – with most historical recombination events being attributed to gene conversion not COs (Arguello et al., 2010). With this in mind, we need to ascertain whether COs are forming on the fourth chromosomes of the hyperrecombination mutants. This would suggest that the normal methods of regulating recombination have been disrupted in these genotypes. To accomplish this, fourth chromosome phenotypic markers will need to be placed into both wild-type and mutant backgrounds. Then crossing over can be scored as in the original

CO assays I conducted. If no fourth chromosome COs are seen in the hyperrecombination mutants, then we will know that the pathway suppressing recombination on the fourth chromosome is still intact.

The next major question to arise from the research detailed in this dissertation is, what are the biochemical properties of the mei-MCM complex? This question will be difficult to answer until all of the subunits within this complex have been identified. I know that REC, MEI-217 and MEI-218 are components of the complex, and I hypothesize that MCM5 is as well. To verify that MCM5 is a component of the complex, the baculovirus system can be utilized to express epitope-tagged MCM5 with the other mei-MCMs. To this end, I have found that baculovirus-infected insect cells are unable to co-express full-length epitope-tagged REC, MEI-217, MEI-218 and MCM5 (data not shown). To circumvent this problem, I attempted to reduce the strain on the cells by expressing the truncated form of MEI-218 (mini-MEI) – since this protein rescues the meiotic non-disjunction (NDJ) defects of *mei-218* null mutants (Chapter 3) – in addition to REC, MEI-217 and MCM5. I found that under these conditions, the insect cells were able to express all four proteins (data not shown). Thus, by conducting immunoprecipitation experiments similar to the ones used to identify an interaction between REC and MEI-217 (Chapter 2), we may be able to determine if MCM5 is a mei-MCM. If it can be successfully shown that MCM5 is a component of the mei-MCM complex, the next logical experiment would be to repeat the interaction assay with the $MCM5^{A7}$ mutant version of the protein. This experiment would allow us to determine if

the MCM5^{A7} missense mutation prevents MCM5 from binding to the complex, thereby explaining the meiotic recombination mutant phenotype.

Like MCM5, I do not know whether any of the other replicative MCM2-7 are components of the mei-MCM complex. Unlike MCM5, however, I do not have the luxury of separation-of-function alleles of these genes – alleles that produce viable flies with a meiotic recombination mutant phenotype. Transgenic point mutants of the replicative MCMs (similar to the ones used in Chapter 3) could be created if we could hypothesize mutations that would create such separation-of-function alleles. A more likely source of these mutations would be in a genetic screen for meiotic mutants, like the screen which gave rise to the *Mcm5^{A7}* allele (Lake et al., 2007; Page et al., 2007). As it is now believed that the *X* chromosome has now been saturated for meiotic alleles (Collins et al., 2012), I hypothesize that either MCM3 and MCM6, both encoded on the *X* chromosome, are not involved in meiotic recombination or that it is highly unlikely that such screens will hit upon an equally fortuitous mutation as was found in *Mcm5*. Alternatively, we could turn to immunoprecipitation of the mei-MCM complex from *Drosophila* in an attempt to identify any missing components. However, as the mei-MCMs appear to be in low abundance *in vivo* (Chapter 4), this technique would most likely be technically unfeasible. Immunoprecipitation of the complex could also be attempted from the *Drosophila* S2 cell line, as this procedure could be easily scalable. However, as cells in culture are not undergoing a meiotic program, it is unlikely that the mei-MCM complex would be regulated properly. To this end, REC, MEI-217 and MEI-218 are only expressed at low levels in the S2 cell line (Roy et al., 2010).

There are several biochemical assays that would help us better understand the mei-MCM complex. First, as a control for the Walker A and Walker B *rec* mutant analyses I conducted (Chapter 3), ATPase activity should be measured using a wild-type complex along with Walker A and Walker B mutant REC versions of the complex. Since I made well-characterized mutations in REC, I expect that the wild-type complex will be able to hydrolyze ATP, while the Walker B version will not. I expect that a complex consisting solely of Walker A mutant REC would be unable to hydrolyze ATP, while a full mei-MCM complex that includes Walker A mutant REC would be able to hydrolyze ATP, based on the *in vivo* phenotypes I observed (Chapter 3). Additionally, it would be informative to conduct a helicase assay using the mei-MCM complex. The replicative MCM2-7 complex has helicase activity (Bochman and Schwacha, 2008), and since the mei-MCM complex is also comprised of MCM proteins, it stands to reason that the mei-MCM complex may also be able to unwind DNA. In this assay we could present the complex with various structures resembling recombination intermediates (for example, a 5' flap mimics a structure seen during repair synthesis) to determine when during recombination the mei-MCM helicase acts. Perhaps the mei-MCM complex does not have helicase activity. In this case, it would still be enlightening to incubate the mei-MCM complex with various DNA structures, again mimicking recombination intermediates, to use in an electrophoretic mobility shift assay to see if the complex binds to DNA during certain steps of the recombination process. Similarly, if the mei-MCM complex is found to bind to Holliday junctions (HJs), the DNA-protein complex could be visualized by electron microscopy to visualize how the mei-MCMs are bound (i.e., do they encircle the entire HJ, does more than one complex bind to one HJ, etc.).

Another question remaining after this dissertation research is, what is the relationship between other *Drosophila* meiotic recombination proteins and the two meiotic CO pathways? We have hypothesized that the mei-MCMs function in the Class I CO pathway in a role reminiscent of Msh4-Msh5 in other organisms (Chapter 2). Further tests of this hypothesis can be conducted, including making double mutants with the mei-MCMs and the Class II resolvases such as Gen or Mus81 to determine if there is an increase in NDJ and/or reduction in COs, as would be expected if both CO pathways are removed simultaneously. If the Class II resolvases are redundant, as they are in *Saccharomyces cerevisiae* (De Muyt et al., 2012; Zakharyevich et al., 2012), then we may need to remove all of the resolves in the *mei-MCM* mutant background before we see a noticeable effect. To this end, I have created *mus81; rec* double mutants and *Gen rec* double mutants and assayed NDJ in both genotypes. In support of our hypothesis that the mei-MCMs function in the Class I CO pathway while Mus81 functions in the Class II pathway, *mus81; rec* double mutants had significantly higher NDJ levels than either *mus81* or *rec* single mutants (Figure 31), as would be expected if two CO pathways were being disrupted. Contrary to our hypothesis, however, the *Gen rec* double mutants had significantly lower NDJ levels than the *rec* single mutants. Before this result can be properly interpreted, COs should be measured in both the *Gen* and *Gen rec* mutants. Perhaps Gen is a non-crossover specific resolvase, and in its absence more COs are formed than in wild-type, thus partially rescuing the low level of COs observed in *rec* mutants.

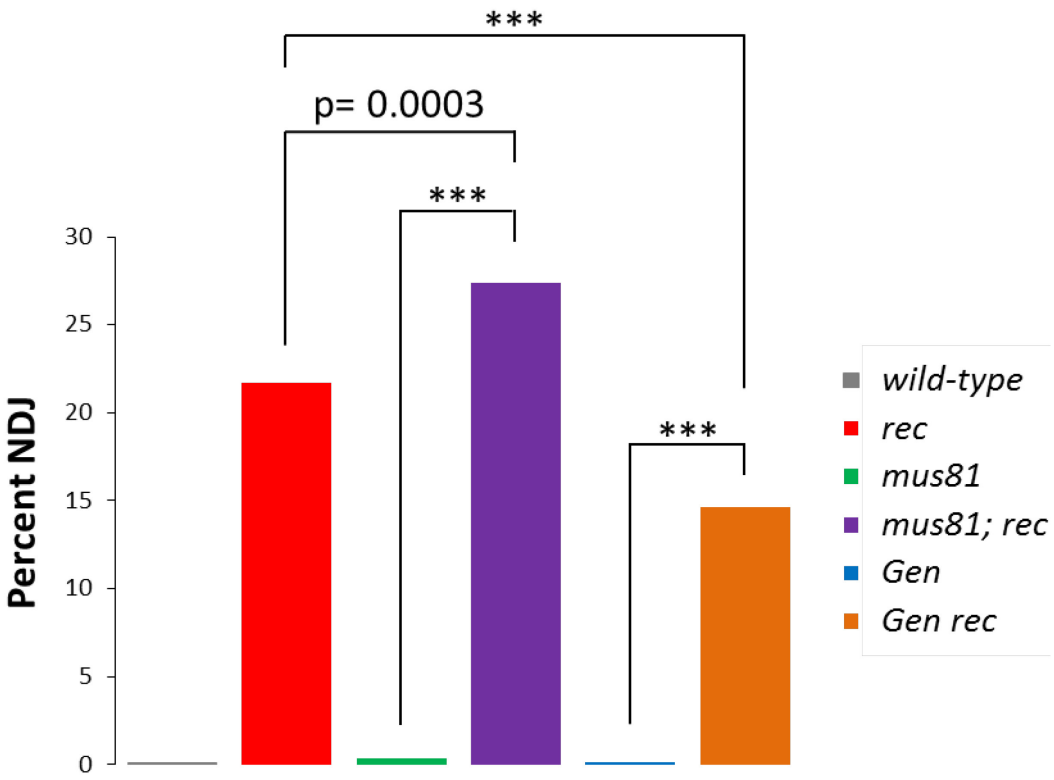

Figure 31. Class I and Class II crossover mutant non-disjunction. Percent non-disjunction (NDJ) was scored in the indicated genotypes. Over 1300 individuals were scored for each genotype. ***p<0.0001, as compared between paired genotypes.

Additionally, removal of Sgs1, the *S. cerevisiae* BLM ortholog, creates a requirement for the Class II resolvases in meiotic CO formation (De Muyt et al., 2012; Zakharyevich et al., 2012). To determine the universality of the two meiotic CO pathway paradigm presented in Chapter 1, we should determine if mutation of *mus309*, the gene encoding the *Drosophila* BLM ortholog, creates a similar requirement in flies. This experiment is very technically challenging, however. The first of these challenges – that *mus309* mutant females produce few viable progeny due to a requirement for DmBLM in the early embryo (McVey et al., 2007) – was overcome by the *mus309* meiotic mutant null I created (Chapter 2), wherein DmBLM is expressed after meiotic recombination has

taken place using the *matα4-GAL4* driver. However, even more challenging is that *mus309* mutants are synthetically lethal with mutations in any of the Class II resolvases (Andersen et al., 2011; Trowbridge et al., 2007). Perhaps this challenge can be overcome by creating Class II resolvase transgenes, similar to the *mus309* transgene, such that the *mus309 resolvase* double mutants would lack DmBLM and the chosen resolvase during meiotic recombination, but would express all genes after recombination is completed. However, since it is believed that some of the synthetic lethality is due to replication and proliferation defects (Andersen et al., 2011), the double mutants created in this manner may not be able to produce functional ovarioles, preventing such experiments from being conducted.

While creating mutants lacking both DmBLM and the Class II resolvases is technically challenging, I have tested the hypothesis that removal of DmBLM creates a requirement for the Class II pathway in an alternative way. In this experiment, I removed the *Drosophila* Class I resolvase, MEI-9, in a *mus309* mutant background. Strikingly, the high NDJ phenotype of *mei-9* mutants was rescued in *mei-9; mus309* double mutants (Figure 32). This result suggests that in the absence of DmBLM, the Class I pathway (and its resolvase MEI-9) are not utilized, thus implicating the Class II pathway in the formation of meiotic COs in the absence of DmBLM.

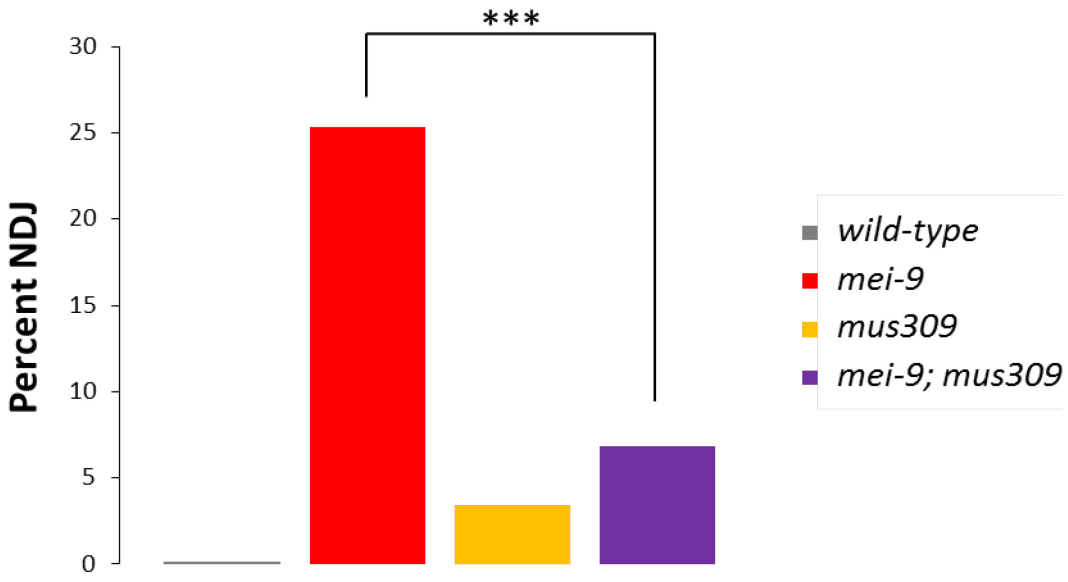

Figure 32. *mei-9; mus309* non-disjunction. Percent non-disjunction (NDJ) was scored in the indicated genotypes. Over 1100 individuals were scored for each genotype. ***p<0.0001.

Finally, the ability of the *rec* Walker B mutant to have a normal CO distribution despite being unable to physically form COs raises the question, do the mei-MCMs have a role in CO licensing? In this CO licensing role, reminiscent of the replication licensing role of the replicative MCMs, I envision the mei-MCMs marking sites of future COs. Immunofluorescence assays can be utilized to test this hypothesis. Firstly, by staining germaria for the mei-MCM complex, perhaps using an antibody to a multiply-epitope-tagged protein since our current REC antibodies were unsuccessful in initial immunofluorescence assays (Chapter 4), we can determine how many mei-MCM complexes are present. Since there is a ~3:1 ratio of NCOs to COs in *Drosophila* (Mehrotra and McKim, 2006), knowing how many mei-MCM complexes form will tell us whether mei-MCM complexes form at all sites of DSBs or whether they localize only to sites of future COs. Furthermore, by conducting this same assay in a DSB-defective mutant, such as a *mei-P22* mutant background, we will be able to determine whether the

mei-MCM complex marks future DSB sites. If in a *mei-P22* background we still see mei-MCM foci in the same number as in the original immunofluorescence assay, we will know that the complex marks sites prior to DSB formation. Alternately, if mei-MCM foci are absent, we will know that the complex is only recruited to sites following DSB formation.

In short, through the work described in this dissertation, I have made great advances in our understanding of *Drosophila* meiotic recombination and have uncovered new avenues for future research – research that will provide clues into the mechanisms of meiotic CO formation and CO regulation.

REFERENCES

Adams, M.D., Celniker, S.E., Holt, R.A., Evans, C.A., Gocayne, J.D., Amanatides, P.G., Scherer, S.E., Li, P.W., Hoskins, R.A., Galle, R.F*., et al.* (2000). The genome sequence of *Drosophila melanogaster*. Science *287*, 2185-2196.

Adams, M.D., McVey, M., and Sekelsky, J. (2003). Drosophila BLM in double-strand break repair by synthesis-dependent strand annealing. Science *299*, 265-267.

Allers, T., and Lichten, M. (2001). Differential timing and control of noncrossover and crossover recombination during meiosis. Cell *106*, 47-57.

Andersen, S.L., Kuo, H.K., Savukoski, D., Brodsky, M.H., and Sekelsky, J. (2011). Three structure-selective endonucleases are essential in the absence of BLM helicase in *Drosophila*. PLoS Genet *7*, e1002315.

Andersen, S.L., and Sekelsky, J. (2010). Meiotic versus mitotic recombination: two different routes for double-strand break repair: the different functions of meiotic versus mitotic DSB repair are reflected in different pathway usage and different outcomes. Bioessays *32*, 1058-1066.

Arguello, J.R., Zhang, Y., Kado, T., Fan, C., Zhao, R., Innan, H., Wang, W., and Long, M. (2010). Recombination yet inefficient selection along the Drosophila melanogaster subgroup's fourth chromosome. Mol Biol Evol *27*, 848-861.

Argueso, J.L., Wanat, J., Gemici, Z., and Alani, E. (2004). Competing crossover pathways act during meiosis in *Saccharomyces cerevisiae*. Genetics *168*, 1805-1816.

Ashburner, M. (1989). Drosophila: A laboratory handbook (Cold Spring Harbor, N.Y., Cold Spring Harbor Laboratory).

Baker, B.S., Boyd, J.B., Carpenter, A.T.C., Green, M.M., Nguyen, T.D., Ripoll, P., and Smith, P.D. (1976). Genetic controls of meiotic recombination and somatic DNA metabolism in *Drosophila melanogaster*. Proc Natl Acad Sci U S A *73*, 4140-4144.

Baker, B.S., and Carpenter, A.T.C. (1972). Genetic analysis of sex chromosomal meiotic mutants in *Drosophila melanogaster*. Genetics *71*, 255-286.

Barrett, T., Troup, D.B., Wilhite, S.E., Ledoux, P., Rudnev, D., Evangelista, C., Kim, I.F., Soboleva, A., Tomashevsky, M., Marshall, K.A*., et al.* (2009). NCBI GEO: archive for high-throughput functional genomic data. Nucleic Acids Res *37*, D885-890.

Bell, S.P., and Dutta, A. (2002). DNA replication in eukaryotic cells. Annu Rev Biochem *71*, 333-374.

Bender, W., Spierer, P., and Hogness, D.S. (1983). Chromosomal walking and jumping to isolate DNA from the *Ace* and *rosy* loci and the bithorax complex in *Drosophila melanogaster*. J Mol Biol *168*, 17-33.

Berchowitz, L.E., and Copenhaver, G.P. (2010). Genetic interference: don't stand so close to me. Curr Genomics *11*, 91-102.

Berchowitz, L.E., Francis, K.E., Bey, A.L., and Copenhaver, G.P. (2007). The role of AtMUS81 in interference-insensitive crossovers in *A. thaliana*. PLoS Genet *3*, e132.

Bishop, D.K., and Zickler, D. (2004). Early decision; meiotic crossover interference prior to stable strand exchange and synapsis. Cell *117*, 9-15.

Blanton, H.L., Radford, S.J., McMahan, S., Kearney, H.M., Ibrahim, J.G., and Sekelsky, J. (2005). REC, *Drosophila* MCM8, drives formation of meiotic crossovers. PLoS Genet *1*, 343-353.

Bochman, M.L., Bell, S.P., and Schwacha, A. (2008). Subunit organization of Mcm2-7 and the unequal role of active sites in ATP hydrolysis and viability. Mol Cell Biol *28*, 5865-5873.

Bochman, M.L., and Schwacha, A. (2008). The Mcm2-7 complex has in vitro helicase activity. Mol Cell *31*, 287-293.

Bochman, M.L., and Schwacha, A. (2009). The Mcm complex: unwinding the mechanism of a replicative helicase. Microbiol Mol Biol Rev *73*, 652-683.

Bochman, M.L., and Schwacha, A. (2010). The Saccharomyces cerevisiae Mcm6/2 and Mcm5/3 ATPase active sites contribute to the function of the putative Mcm2-7 'gate'. Nucleic Acids Res *38*, 6078-6088.

Boddy, M.N., Gaillard, P.H., McDonald, W.H., Shanahan, P., Yates, J.R., 3rd, and Russell, P. (2001). Mus81-Eme1 are essential components of a Holliday junction resolvase. Cell *107*, 537-548.

Borner, G.V., Kleckner, N., and Hunter, N. (2004). Crossover/noncrossover differentiation, synaptonemal complex formation, and regulatory surveillance at the leptotene/zygotene transition of meiosis. Cell *117*, 29-45.

Borts, R.H., Chambers, S.R., and Abdullah, M.F. (2000). The many faces of mismatch repair in meiosis. Mutat Res *451*, 129-150.

Boyd, J.B., Golino, M.D., Shaw, K.E.S., Osgood, C.J., and Green, M.M. (1981). Third-chromosome mutagen-sensitive mutants of *Drosophila melanogaster*. Genetics *97*, 607-623.

Burns, C., Stajich, J.E., Rechtsteiner, A., Casselton, L., Hanlon, S.E., Wilke, S.K., Savytskyy, O.P., Gathman, A.C., Lilly, W.W., Lieb, J.D*., et al.* (2010). Analysis of the Basidiomycete *Coprinopsis cinerea* reveals conservation of the core meiotic expression program over half a billion years of evolution. PLoS Genet *6*.

Carpenter, A.T.C. (1979). Recombination nodules and synaptonemal complex in recombination-defective females of *Drosophila melanogaster*. Chromosoma *75*, 259-292.

Carpenter, A.T.C., and Sandler, L. (1974). On recombination-defective meiotic mutants in *Drosophila melanogaster*. Genetics *76*, 453-475.

Cavalier-Smith, T. (1981). The origin and early evolution of the eukaryotic cell. In Molecular and Cellular Aspects of Microbial Evolution, M.J. Carlile, J. F. Collins, and B.E.B Moseley, ed. (Cambridge, UK, Cambridge University Press), pp. 33-84.

Chintapalli, V.R., Wang, J., and Dow, J.A. (2007). Using FlyAtlas to identify better Drosophila melanogaster models of human disease. Nat Genet *39*, 715-720.

Chovnick, A., Ballantyne, G.H., Baillie, D.L., and Holm, D.G. (1970). Gene conversion in higher organisms: half-tetrad analysis of recombination within the rosy cistron of *Drosophila melanogaster*. Genetics *66*, 315-329.

Chovnick, A., Ballantyne, G.H., and Holm, D.G. (1971). Studies on gene conversion and its relationship to linked exchange in *Drosophila melanogaster*. Genetics *69*, 179-209.

Chu, W.K., and Hickson, I.D. (2009). RecQ helicases: multifunctional genome caretakers. Nat Rev Cancer *9*, 644-654.

Cole, F., Keeney, S., and Jasin, M. (2012). Preaching about the converted: how meiotic gene conversion influences genomic diversity. Ann N Y Acad Sci *1267*, 95-102.

Collin, R., and Cipriani, R. (2003). Dollo's law and the re-evolution of shell coiling. Proceedings Biological sciences / The Royal Society *270*, 2551-2555.

Collin, R., and Miglietta, M.P. (2008). Reversing opinions on Dollo's Law. Trends Ecol Evol *23*, 602-609.

Collins, I., and Newlon, C.S. (1994). Meiosis-specific formation of joint DNA molecules containing sequences from homologous chromosomes. Cell *76*, 65-75.

Collins, K.A., Callicoat, J.G., Lake, C.M., McClurken, C.M., Kohl, K.P., and Hawley, R.S. (2012). A germline clone screen on the *X* chromosome reveals novel meiotic mutants in *Drosophila melanogaster*. G3 (Bethesda) *2*, 1369-1377.

Copenhaver, G.P., Housworth, E.A., and Stahl, F.W. (2002). Crossover interference in Arabidopsis. Genetics *160*, 1631-1639.

Crismani, W., Girard, C., Froger, N., Pradillo, M., Santos, J.L., Chelysheva, L., Copenhaver, G.P., Horlow, C., and Mercier, R. (2012). FANCM limits meiotic crossovers. Science *336*, 1588-1590.

Davey, M.J., Indiani, C., and O'Donnell, M. (2003). Reconstitution of the Mcm2-7p heterohexamer, subunit arrangement, and ATP site architecture. J Biol Chem *278*, 4491-4499.

de Boer, E., and Heyting, C. (2006). The diverse roles of transverse filaments of synaptonemal complexes in meiosis. Chromosoma *115*, 220-234.

de los Santos, T., Hunter, N., Lee, C., Larkin, B., Loidl, J., and Hollingsworth, N.M. (2003). The Mus81/Mms4 endonuclease acts independently of double-Holliday junction resolution to promote a distinct subset of crossovers during meiosis in budding yeast. Genetics *164*, 81-94.

de los Santos, T., Loidl, J., Larkin, B., and Hollingsworth, N.M. (2001). A role for MMS4 in the processing of recombination intermediates during meiosis in Saccharomyces cerevisiae. Genetics *159*.

De Muyt, A., Jessop, L., Kolar, E., Sourirajan, A., Chen, J., Dayani, Y., and Lichten, M. (2012). BLM helicase ortholog Sgs1 is a central regulator of meiotic recombination intermediate metabolism. Mol Cell *46*, 43-53.

Edgar, R.C. (2004). MUSCLE: multiple sequence alignment with high accuracy and high throughput. Nucleic Acids Res *32*, 1792-1797.

Feger, G., Vaessin, H., Su, T.T., Wolff, E., Jan, L.Y., and Jan, Y.N. (1995). dpa, a member of the MCM family, is required for mitotic DNA replication but not endoreplication in Drosophila. Embo J *14*, 5387-5398.

Fekairi, S., Scaglione, S., Chahwan, C., Taylor, E.R., Tissier, A., Coulon, S., Dong, M.Q., Ruse, C., Yates, J.R., 3rd, Russell, P.*, et al.* (2009). Human SLX4 is a Holliday junction resolvase subunit that binds multiple DNA repair/recombination endonucleases. Cell *138*, 78-89.

Fogel, S., and Hurst, D.D. (1967). Meiotic gene conversion in yeast tetrads and the theory of recombination. Genetics *57*, 455-481.

Forsburg, S.L. (2004). Eukaryotic MCM proteins: beyond replication initiation. Microbiol Mol Biol Rev *68*, 109-131.

Foss, E., Lande, R., Stahl, F.W., and Steinberg, C.M. (1993). Chiasma interference as a function of genetic distance. Genetics *133*, 681-691.

Gai, D., Zhao, R., Li, D., Finkielstein, C.V., and Chen, X.S. (2004). Mechanisms of conformational change for a replicative hexameric helicase of SV40 large tumor antigen. Cell *119*, 47-60.

Gilchrist, B.M., and Haldane, J.B.S. (1947). Sex linkage and sex determination in a mosquito, *Culex molestus*. Hereditas *33*, 175-190.

Gloor, G.B., Preston, C.R., Johnson-Schlitz, D.M., Nassif, N.A., Phillis, R.W., Benz, W.K., Robertson, H.M., and Engels, W.R. (1993). Type I repressors of P element mobility. Genetics *135*, 81-95.

Goldman, N., and Yang, Z. (1994). A codon-based model of nucleotide substitution for protein-coding DNA sequences. Mol Biol Evol *11*, 725-736.

Gomez, E.B., Catlett, M.G., and Forsburg, S.L. (2002). Different phenotypes in vivo are associated with ATPase motif mutations in Schizosaccharomyces pombe minichromosome maintenance proteins. Genetics *160*, 1305-1318.

Gooding, R.H., and Rolseth, B.M. (1995). Genetics of *Glossina palpalis palpalis*: designation of linkage groups and the mapping of eight biochemical and visible marker genes. Genome *38*, 833-837.

Gozuacik, D., Chami, M., Lagorce, D., Faivre, J., Murakami, Y., Poch, O., Biermann, E., Knippers, R., Brechot, C., and Paterlini-Brechot, P. (2003). Identification and functional characterization of a new member of the human Mcm protein family: hMcm8. Nucleic Acids Res *31*, 570-579.

Grell, R.F. (1984). Time of recombination in the *Drosophila melanogaster* oocyte. III. Selection and characterization of temperature-sensitive and -insensitive, recombination-defecient alleles in Drosophila. Genetics *108*, 425-443.

Grimaldi, D.A., and Engel, M.S. (2005). Evolution of the Insects (Cambridge University Press).

Haerty, W., Jagadeeshan, S., Kulathinal, R.J., Wong, A., Ravi Ram, K., Sirot, L.K., Levesque, L., Artieri, C.G., Wolfner, M.F., Civetta, A.*, et al.* (2007). Evolution in the fast lane: rapidly evolving sex-related genes in Drosophila. Genetics *177*, 1321-1335.

Hanson, P.I., and Whiteheart, S.W. (2005). AAA+ proteins: have engine, will work. Nat Rev Mol Cell Biol *6*, 519-529.

Hassold, T., and Hunt, P. (2007). Rescuing distal crossovers. Nat Genet *39*, 1187-1188.

Hawley, R.S. (1993). Meiosis as an "M" thing: twenty-five years of meiotic mutants in Drosophila. Genetics *135*, 613-618.

Higgins, J.D., Armstrong, S.J., Franklin, F.C., and Jones, G.H. (2004). The Arabidopsis MutS homolog AtMSH4 functions at an early step in recombination: evidence for two classes of recombination in Arabidopsis. Genes Dev *18*, 2557-2570.

Hilliker, A.J., Clark, S.H., and Chovnick, A. (1991). The effect of DNA sequence polymorphisms on intragenic recombination in the *rosy* locus of *Drosophila melanogaster*. Genetics *129*, 779-781.

Ho, C.K., Mazon, G., Lam, A.F., and Symington, L.S. (2010). Mus81 and Yen1 promote reciprocal exchange during mitotic recombination to maintain genome integrity in budding yeast. Mol Cell *40*, 988-1000.

Holliday, R. (1964). A mechanism for gene conversion in fungi. Genetical research *78*, 282-304.

Hollingsworth, N.M., Ponte, L., and Halsey, C. (1995). *MSH5*, a novel MutS homolog, facilitates meiotic reciprocal recombination between homologs in *Saccharomyces cerevisiae* but not mismatch repair. Genes Dev *9*, 1728-1739.

Ip, S.C., Rass, U., Blanco, M.G., Flynn, H.R., Skehel, J.M., and West, S.C. (2008). Identification of Holliday junction resolvases from humans and yeast. Nature *456*, 357-361.

James, P., Halladay, J., and Craig, E.A. (1996). Genomic libraries and a host strain designed for highly efficient two-hybrid selection in yeast. Genetics *144*, 1425-1436.

Jessop, L., Rockmill, B., Roeder, G.S., and Lichten, M. (2006). Meiotic chromosome synapsis-promoting proteins antagonize the anti-crossover activity of sgs1. PLoS Genet *2*, e155.

Johnson, E.M., Kinoshita, Y., and Daniel, D.C. (2003). A new member of the MCM protein family encoded by the human MCM8 gene, located contrapodal to GCD10 at chromosome band 20p12.3-13. Nucleic Acids Res *31*, 2915-2925.

Jones, G.H. (1984). The control of chiasma distribution. Symp Soc Exp Biol *38*, 293-320.

Joyce, E.F., and McKim, K.S. (2009). Drosophila PCH2 is required for a pachytene checkpoint that monitors double-strand-break-independent events leading to meiotic crossover formation. Genetics *181*, 39-51.

Joyce, E.F., Tanneti, S.N., and McKim, K.S. (2009). Drosophila hold'em is required for a subset of meiotic crossovers and interacts with the dna repair endonuclease complex subunits MEI-9 and ERCC1. Genetics *181*, 335-340.

Keeney, S., Giroux, C.N., and Kleckner, N. (1997). Meiosis-specific DNA double-strand breaks are catalyzed by Spo11, a member of a widely conserved protein family. Cell *88*, 375-384.

Kelley, L.A., and Sternberg, M.J. (2009). Protein structure prediction on the Web: a case study using the Phyre server. Nat Protoc *4*, 363-371.

Kelly, K.O., Dernburg, A.F., Stanfield, G.M., and Villeneuve, A.M. (2000). Caenorhabditis elegans msh-5 is required for both normal and radiation-induced meiotic crossing over but not for completion of meiosis. Genetics *156*, 617-630.

King, J.S., and Mortimer, R.K. (1990). A polymerization model of chiasma interference and corresponding computer simulation. Genetics *126*, 1127-1138.

Knoll, A., Higgins, J.D., Seeliger, K., Reha, S.J., Dangel, N.J., Bauknecht, M., Schropfer, S., Franklin, F.C., and Puchta, H. (2012). The Fanconi Anemia ortholog FANCM ensures ordered homologous recombination in both somatic and meiotic cells in *Arabidopsis*. Plant Cell.

Kohl, K.P., Jones, C.D., and Sekelsky, J. (2012). Evolution of an MCM complex in flies that promotes meiotic crossovers by blocking BLM helicase. Science *338*, 1363-1365.

Koonin, E.V. (1993). A common set of conserved motifs in a vast variety of putative nucleic acid-dependent ATPases including MCM proteins involved in the initiation of eukaryotic DNA replication. Nucleic Acids Res *21*, 2541-2547.

Lake, C.M., and Hawley, R.S. (2012). The molecular control of meiotic chromosomal behavior: events in early meiotic prophase in Drosophila oocytes. Annu Rev Physiol *74*, 425-451.

Lake, C.M., Teeter, K., Page, S.L., Nielsen, R., and Hawley, R.S. (2007). A genetic analysis of the Drosophila *mcm5* gene defines a domain specifically required for meiotic recombination. Genetics *176*, 2151-2163.

Lantz, V., Ambrosio, L., and Schedl, P. (1992). The Drosophila orb gene is predicted to encode sex-specific germline RNA-binding proteins and has localized transcripts in ovaries and early embryos. Development *115*, 75-88.

Lantz, V., Chang, J.S., Horabin, J.I., Bopp, D., and Schedl, P. (1994). The Drosophila orb RNA-binding protein is required for the formation of the egg chamber and establishment of polarity. Genes Dev *8*, 598-613.

Larkin, M.A., Blackshields, G., Brown, N.P., Chenna, R., McGettigan, P.A., McWilliam, H., Valentin, F., Wallace, I.M., Wilm, A., Lopez, R.*, et al.* (2007). Clustal W and Clustal X version 2.0. Bioinformatics *23*, 2947-2948.

Laskey, R.A., and Madine, M.A. (2003). A rotary pumping model for helicase function of MCM proteins at a distance from replication forks. EMBO Rep *4*, 26-30.

Lee, T., and Luo, L. (1999). Mosaic analysis with a repressible cell marker for studies of gene function in neuronal morphogenesis. Neuron *22*, 451-461.

Lindegren, C.C. (1955). Non-Mendelian segregation in a single tetrad of Saccharomyces ascribed to gene conversion. Science *121*, 605-607.

Liu, H., Jang, J.K., Graham, J., Nycz, K., and McKim, K.S. (2000). Two genes required for meiotic recombination in Drosophila are expressed from a dicistronic message. Genetics *154*, 1735-1746.

Liu, H., Jang, J.K., Kato, N., and McKim, K.S. (2002). mei-P22 encodes a chromosome-associated protein required for the initiation of meiotic recombination in Drosophila melanogaster. Genetics *162*, 245-258.

Liu, Y., Richards, T.A., and Aves, S.J. (2009). Ancient diversification of eukaryotic MCM DNA replication proteins. BMC Evol Biol *9*, 60.

Lu, X., Liu, X., An, L., Zhang, W., Sun, J., Pei, H., Meng, H., Fan, Y., and Zhang, C. (2008). The Arabidopsis MutS homolog AtMSH5 is required for normal meiosis. Cell Res *18*, 589-599.

Lutzmann, M., Grey, C., Traver, S., Ganier, O., Maya-Mendoza, A., Ranisavljevic, N., Bernex, F., Nishiyama, A., Montel, N., Gavois, E.*, et al.* (2012). MCM8- and MCM9-deficient mice reveal gametogenesis defects and genome instability due to impaired homologous recombination. Mol Cell *47*, 523-534.

Madigan, J.P., Chotkowski, H.L., and Glaser, R.L. (2002). DNA double-strand break-induced phosphorylation of Drosophila histone variant H2Av helps prevent radiation-induced apoptosis. Nucleic Acids Res *30*, 3698-3705.

Maiorano, D., Cuvier, O., Danis, E., and Mechali, M. (2005). MCM8 is an MCM2-7-related protein that functions as a DNA helicase during replication elongation and not initiation. Cell *120*, 315.

Malik, S.B., Pightling, A.W., Stefaniak, L.M., Schurko, A.M., and Logsdon, J.M., Jr. (2008). An expanded inventory of conserved meiotic genes provides evidence for sex in *Trichomonas vaginalis*. PLoS One *3*, e2879.

Manheim, E.A., Jang, J.K., Dominic, D., and McKim, K.S. (2002). Cytoplasmic localization and evolutionary conservation of MEI-218, a protein required for meiotic crossing-over in Drosophila. Mol Biol Cell *13*, 84-95.

Marchler-Bauer, A., Lu, S., Anderson, J.B., Chitsaz, F., Derbyshire, M.K., DeWeese-Scott, C., Fong, J.H., Geer, L.Y., Geer, R.C., Gonzales, N.R., *et al.* (2011). CDD: a Conserved Domain Database for the functional annotation of proteins. Nucleic Acids Res *39*, D225-229.

Marcon, E., and Moens, P.B. (2005). The evolution of meiosis: recruitment and modification of somatic DNA-repair proteins. Bioessays *27*, 795-808.

Martin, A., Baker, T.A., and Sauer, R.T. (2005). Rebuilt AAA + motors reveal operating principles for ATP-fuelled machines. Nature *437*, 1115-1120.

Martini, E., Diaz, R.L., Hunter, N., and Keeney, S. (2006). Crossover homeostasis in yeast meiosis. Cell *126*, 285-295.

McClelland, G.A. (1966). Sex-linkage at two loci affecting eye pigment in the mosquito *Aedes aegypti* (diptera: culicidae). Canadian journal of genetics and cytology Journal canadien de genetique et de cytologie *8*, 192-198.

McGaugh, S.E., and Noor, M.A. (2012). Genomic impacts of chromosomal inversions in parapatric Drosophila species. Philos Trans R Soc Lond B Biol Sci *367*, 422-429.

McKim, K.S., Dahmus, J.B., and Hawley, R.S. (1996). Cloning of the *Drosophila melanogaster* meiotic recombination gene *mei-218*: a genetic and molecular analysis of interval 15E. Genetics *144*, 215-228.

McKim, K.S., Jang, J.K., and Manheim, E.A. (2002). Meiotic recombination and chromosome segregation in Drosophila females. Annu Rev Genet *36*, 205-232.

McKim, K.S., Joyce, E.F., and Jang, J.K. (2009). Cytological analysis of meiosis in fixed Drosophila ovaries. Methods Mol Biol *558*, 197-216.

McVey, M., Andersen, S.L., Broze, Y., and Sekelsky, J. (2007). Multiple functions of Drosophila BLM helicase in maintenance of genome stability. Genetics *176*, 1979-1992.

McVey, M., Larocque, J.R., Adams, M.D., and Sekelsky, J.J. (2004). Formation of deletions during double-strand break repair in *Drosophila* DmBlm mutants occurs after strand invasion. Proc Natl Acad Sci U S A *101*, 15694-15699.

Mehrotra, S., and McKim, K.S. (2006). Temporal analysis of meiotic DNA double-strand break formation and repair in Drosophila females. PLoS Genet *2*, e200.

Meneely, P.M., Farago, A.F., and Kauffman, T.M. (2002). Crossover distribution and high interference for both the X chromosome and an autosome during oogenesis and spermatogenesis in Caenorhabditis elegans. Genetics *162,* 1169-1177.

Moreau, M.J., McGeoch, A.T., Lowe, A.R., Itzhaki, L.S., and Bell, S.D. (2007). ATPase site architecture and helicase mechanism of an archaeal MCM. Mol Cell *28*, 304-314.

Morgan, T.H. (1911). Random segregation versus coupling in mendelian inheritance. Science *34*, 384.

Morgan, T.H. (1912). Complete linkage in the second chromosome of the male of *Drosophila*. Science *36*, 719-720.

Munz, P. (1994). An analysis of interference in the fission yeast *Schizosaccharomyces pombe*. Genetics *137*, 701-707.

Neale, M.J., and Keeney, S. (2006). Clarifying the mechanics of DNA strand exchange in meiotic recombination. Nature *442*, 153-158.

Nishant, K.T., Plys, A.J., and Alani, E. (2008). A mutation in the putative MLH3 endonuclease domain confers a defect in both mismatch repair and meiosis in *Saccharomyces cerevisiae*. Genetics *179*, 747-755.

Nishimura, K., Ishiai, M., Horikawa, K., Fukagawa, T., Takata, M., Takisawa, H., and Kanemaki, M.T. (2012). Mcm8 and Mcm9 form a complex that functions in homologous recombination repair induced by DNA interstrand crosslinks. Mol Cell *47*, 511-522.

Novak, J.E., Ross-Macdonald, P.B., and Roeder, G.S. (2001). The budding yeast Msh4 protein functions in chromosome synapsis and the regulation of crossover distribution. Genetics *158*, 1013-1025.

Oh, S.D., Lao, J.P., Hwang, P.Y., Taylor, A.F., Smith, G.R., and Hunter, N. (2007). BLM ortholog, Sgs1, prevents aberrant crossing-over by suppressing formation of multichromatid joint molecules. Cell *130*, 259-272.

Page, S.L., and Hawley, R.S. (2001). *c(3)G* encodes a *Drosophila* synaptonemal complex protein. Genes Dev *15*, 3130-3143.

Page, S.L., Nielsen, R.J., Teeter, K., Lake, C.M., Ong, S., Wright, K.R., Dean, K.L., Agne, D., Gilliland, W.D., and Hawley, R.S. (2007). A germline clone screen for meiotic mutants in *Drosophila melanogaster*. Fly (Austin) *1*, 172-181.

Pâques, F., and Haber, J.E. (1999). Multiple pathways of recombination induced by double-strand breaks in *Saccharomyces cerevisiae*. Microbiol Mol Biol Rev *63*, 349-404.

Pochart, P., Woltering, D., and Hollingsworth, N.M. (1997). Conserved properties between functionally distinct MutS homologs in yeast. J Biol Chem *272*, 30345-30349.

Radford, S.J., Goley, E., Baxter, K., McMahan, S., and Sekelsky, J. (2005). Drosophila ERCC1 is required for a subset of MEI-9-dependent meiotic crossovers. Genetics *170*, 1737-1745.

Radford, S.J., McMahan, S., Blanton, H.L., and Sekelsky, J. (2007a). Heteroduplex DNA in meiotic recombination in Drosophila *mei-9* mutants. Genetics *176*, 63-72.

Radford, S.J., Sabourin, M.M., McMahan, S., and Sekelsky, J. (2007b). Meiotic recombination in Drosophila *Msh6* mutants yields discontinuous gene conversion tracts. Genetics *176*, 53-62.

Remus, D., Beuron, F., Tolun, G., Griffith, J.D., Morris, E.P., and Diffley, J.F. (2009). Concerted loading of Mcm2-7 double hexamers around DNA during DNA replication origin licensing. Cell *139*, 719-730.

Rockmill, B., Fung, J.C., Branda, S.S., and Roeder, G.S. (2003). The Sgs1 helicase regulates chromosome synapsis and meiotic crossing over. Curr Biol *13*, 1954-1962.

Rørth, P. (1998). Gal4 in the Drosophila female germline. Mech Dev *78*, 113-118.

Ross-Macdonald, P., and Roeder, G.S. (1994). Mutation of a meiosis-specific MutS homolog decreases crossing over but not mismatch correction. Cell *79*, 1069-1080.

Roy, S., Ernst, J., Kharchenko, P.V., Kheradpour, P., Negre, N., Eaton, M.L., Landolin, J.M., Bristow, C.A., Ma, L., Lin, M.F*., et al.* (2010). Identification of functional elements and regulatory circuits by Drosophila modENCODE. Science *330*, 1787-1797.

Sandler, L., Lindsley, D.L., Nicoletti, B., and Trippa, G. (1968). Mutants affecting meiosis in natural populations of *Drosophila melanogaster*. Genetics *60*, 525-558.

Schulz, G. (1992). Binding of nucleotides by proteins. Curr Opin Struct Biol, 61-67.

Schwacha, A., and Kleckner, N. (1994). Identification of joint molecules that form frequently between homologs but rarely between sister chromatids during yeast meiosis. Cell *76*, 51-63.

Schwacha, A., and Kleckner, N. (1995). Identification of double Holliday junctions as intermediates in meiotic recombination. Cell *83*, 783-791.

Schwed, G., May, N., Pechersky, Y., and Calvi, B.R. (2002). Drosophila minichromosome maintenance 6 is required for chorion gene amplification and genomic replication. Mol Biol Cell *13*, 607-620.

Sekelsky, J., Brodsky, M.H., and Burtis, K.C. (2000). DNA Repair in Drosophila. Insights from the Drosophila genome sequence. J Cell Biol *150*, F31-F36.

Sekelsky, J., McKim, K.S., Chin, G.M., and Hawley, R.S. (1995). The Drosophila meiotic recombination gene *mei-9* encodes a homologue of the yeast excision repair protein Rad1. Genetics *141*, 619-627.

Smith, G.R., Boddy, M.N., Shanahan, P., and Russell, P. (2003). Fission yeast Mus81.Eme1 Holliday junction resolvase is required for meiotic crossing over but not for gene conversion. Genetics *165*, 2289-2293.

Snowden, T., Acharya, S., Butz, C., Berardini, M., and Fishel, R. (2004). hMSH4-hMSH5 recognizes Holliday Junctions and forms a meiosis-specific sliding clamp that embraces homologous chromosomes. Mol Cell *15*, 437-451.

Stahl, F.W. (1994). The Holliday junction on its thirtieth anniversary. Genetics *138*, 241-246.

Stitt, B.L., and Xu, Y. (1998). Sequential hydrolysis of ATP molecules bound in interacting catalytic sites of Escherichia coli transcription termination protein Rho. J Biol Chem *273*, 26477-26486.

Sturtevant, A.H. (1913). The linear arrangement of six sex-linked factors in *Drosophila*, as shown by their mode of association. J Exp Biol *14*, 43-59.

Szostak, J.W., Orr-Weaver, T.L., Rothstein, R.J., and Stahl, F.W. (1983). The double-strand-break repair model for recombination. Cell *33*, 25-35.

Tamura, K., Peterson, D., Peterson, N., Stecher, G., Nei, M., and Kumar, S. (2011). MEGA5: molecular evolutionary genetics analysis using maximum likelihood, evolutionary distance, and maximum parsimony methods. Mol Biol Evol *28*, 2731-2739.

Treisman, J.E., Follette, P.J., O'Farrell, P.H., and Rubin, G.M. (1995). Cell proliferation and DNA replication defects in a Drosophila MCM2 mutant. Genes Dev *9*, 1709-1715.

Trowbridge, K., McKim, K.S., Brill, S., and Sekelsky, J. (2007). Synthetic lethality in the absence of the Drosophila MUS81 endonuclease and the DmBlm helicase is associated with elevated apoptosis. Genetics *176*, 1993-2001.

Tye, B.K. (1999). MCM proteins in DNA replication. Annu Rev Biochem *68*, 649-686.

Villeneuve, A.M., and Hillers, K.J. (2001). Whence meiosis? Cell *106*, 647-650.

Volkening, M., and Hoffmann, I. (2005). Involvement of human MCM8 in prereplication complex assembly by recruiting hcdc6 to chromatin. Mol Cell Biol *25*, 1560-1568.

Walker, J.E., Saraste, M., Runswick, M.J., and Gay, N.J. (1982). Distantly related sequences in the alpha- and beta-subunits of ATP synthase, myosin, kinases and other ATP-requiring enzymes and a common nucleotide binding fold. EMBO J *1*, 945-951.

Whelan, S., and Goldman, N. (2001). A general empirical model of protein evolution derived from multiple protein families using a maximum-likelihood approach. Mol Biol Evol *18*, 691-699.

Wiegmann, B.M., Trautwein, M.D., Winkler, I.S., Barr, N.B., Kim, J.W., Lambkin, C., Bertone, M.A., Cassel, B.K., Bayless, K.M., Heimberg, A.M.*, et al.* (2011). Episodic radiations in the fly tree of life. Proc Natl Acad Sci U S A *108*, 5690-5695.

Wilkins, A.S., and Holliday, R. (2009). The evolution of meiosis from mitosis. Genetics *181*, 3-12.

Wu, L., and Hickson, I.D. (2003). The Bloom's syndrome helicase suppresses crossing over during homologous recombination. Nature *426*, 870-874.

Wu, X., Sandhu, S., and Ding, H. (2007). Establishment of conditional knockout alleles for the gene encoding the regulator of telomere length (RTEL). Genesis *45*, 788-792.

Yang, Z. (1997). PAML: a program package for phylogenetic analysis by maximum likelihood. Comput Appl Biosci *13*, 555-556.

Yang, Z. (2007). PAML 4: phylogenetic analysis by maximum likelihood. Mol Biol Evol *24*, 1586-1591.

Yildiz, Ö., Majumder, S., Kramer, B.C., and Sekelsky, J. (2002). Drosophila MUS312 interacts with the nucleotide excision repair endonuclease MEI-9 to generate meiotic crossovers. Mol Cell *10*, 1503-1509.

Ying, C.Y., and Gautier, J. (2005). The ATPase activity of MCM2-7 is dispensable for pre-RC assembly but is required for DNA unwinding. EMBO J *24*, 4334-4344.

Youds, J.L., Mets, D.G., McIlwraith, M.J., Martin, J.S., Ward, J.D., NJ, O.N., Rose, A.M., West, S.C., Meyer, B.J., and Boulton, S.J. (2010). RTEL-1 enforces meiotic crossover interference and homeostasis. Science *327*, 1254-1258.

Zakharyevich, K., Ma, Y., Tang, S., Hwang, P.Y., Boiteux, S., and Hunter, N. (2010). Temporally and biochemically distinct activities of Exo1 during meiosis: double-strand break resection and resolution of double Holliday junctions. Mol Cell *40*, 1001-1015.

Zakharyevich, K., Tang, S., Ma, Y., and Hunter, N. (2012). Delineation of joint molecule resolution pathways in meiosis identifies a crossover-specific resolvase. Cell *149*, 334-347.

Zalevsky, J., MacQueen, A.J., Duffy, J.B., Kemphues, K.J., and Villeneuve, A.M. (1999). Crossing over during *Caenorhabditis elegans* meiosis requires a conserved MutS-based pathway that is partially dispensable in budding yeast. Genetics *153*, 1271-1283.

Zheng, L., Benedict, M.Q., Cornel, A.J., Collins, F.H., and Kafatos, F.C. (1996). An integrated genetic map of the African human malaria vector mosquito, *Anopheles gambiae*. Genetics *143*, 941-952.

Zickler, D., and Kleckner, N. (1999). Meiotic chromosomes: integrating structure and function. Annu Rev Genet *33*, 603-754.